



SAPIENZA
UNIVERSITÀ DI ROMA

On the role of visceral physiological signals in corporeal awareness

International Ph.D. Program in Cognitive, Social and Affective Neuroscience
Dottorato di Ricerca in Psicologia e Neuroscienze Sociali – XXXII Ciclo

Candidate

Alessandro Monti

ID number 1757249

Thesis Advisor

Prof. Salvatore Maria Aglioti

A thesis submitted in partial fulfillment of the requirements
for the degree of Doctor of Philosophy in Psychology and Social Neuroscience

2019

Thesis defended on 27 February 2020

in front of a Board of Examiners composed by:

Prof. Camillo Regalia, Università Cattolica del Sacro Cuore, Milano (chairman)

Prof. Andrea Serino, Centre hospitalier universitaire vaudois, Lausanne

Prof. Sarah Garfinkel, University of Sussex, Brighton

Dr. Giorgio Arcara, Ospedale San Camillo, Venezia

On the role of visceral physiological signals in corporeal awareness

Ph.D. thesis. Sapienza – University of Rome

© 2019 Alessandro Monti. All rights reserved

This thesis has been typeset by L^AT_EX and the Sapthesis class.

Author's email: alessandro.monti@uniroma1.it

Suspiciendo despicio, despiciendo suspicio.
Tycho

Acknowledgements

Few things are more visceral, physiological, and corporeal than the gratitude I feel after completing this Ph.D. thesis. Perhaps I should have reported this feeling as additional evidence to strengthen the conclusions in the final chapter, but I suppose it is more fitting to describe it in this section.

I am deeply grateful to my supervisor, Professor Salvatore Maria Aglioti. Thank you for convincing me to swap London for Rome with a single phone call, and making me happy about that choice every single day of my PhD.

The outstanding quality of a supervisor is also measured by the post-docs they choose to support a doctoral student. I was exceptionally blessed with the most supportive post-doc one could ever ask for: Giuseppina Porciello. Thank you for showering me with a constant outpouring of warmth, competence, and enthusiasm. I am deeply indebted also to Gaetano Tieri and Maria Serena Panasiti, who helped me with their invaluable technical support and inspired me with their passionate dedication.

It was my pleasure and my joy to make this journey together with many talented and hilarious fellow PhD students. Matteo Marucci generously shared with me his deep knowledge of virtual reality in countless occasions. Michael Schepisi proved to be a delightful debater, and a true friend. Martina Fanghella bore witness to the astonishing fact that one could be a scientist, a Jungian, and a marvellous human being at the same time.

Each and every experiment I performed would not have been possible without the joint effort of many other collaborators. I would especially like to extend my gratitude to Maria Teresa di Giorgio, Luca Occhigrossi, Maurizio Molisso, Michele Scandola, Andrea Famà, Danila Cosenza, and Michela La Padula. Fr. Mauro Oliva and Professor Tonino Cantelmi helped me solve a difficult ethical issue. Enea Francesco Pavone provided me with his selfless assistance when he was here, and the example he set keeps resonating in my mind now that he is not with us anymore.

Professor Carsten Bönnemann, Reghan Foley, Ana Paz, Dimah Saade, Eleni Frangos, Alex Chesler, and Andy Gravunder allowed me to spend a productive period at the National Institutes of Health in Bethesda, Maryland. Gail, a wonderful NIH nurse, rescued me in a difficult situation. Special thanks to Patient A and to all my participants for their time and bravery in taking part in the experiments.

I also had the privilege to discuss the content of the thesis with many researchers from other universities and institutes. In particular, I greatly benefited from the perceptive feedback given by Cosimo Urgesi, Laura Crucianelli, Laura Barca, Daniele Di Lernia, and Aikaterini Fotopoulou. I look forward to continuing this fruitful exchange of ideas in the months to come.

And finally, let me mention the veritable pillars not just of my PhD, but of my whole life - my parents. There is indeed something far more visceral than this thesis, and I cannot express it but in my native tongue: *mamma, papà, vi amo*.

Contents

Acknowledgements	ii
List of Tables	vii
List of Figures	ix
1 Introduction	1
1.1 State of the art	1
1.2 Objectives and structure of the project	3
2 The ‘pneumoception’ test: development and validation	6
2.1 Introduction	6
2.2 Materials and methods	7
2.3 Results	9
2.4 Discussion	11
3 Experiment I: the ‘embreathment’ illusion	13
3.1 Introduction	13
3.2 Materials and methods	14
3.3 Results	23
3.4 Discussion	30
4 Experiment II: gastric embodiment	39
4.1 Introduction	39
4.2 Materials and methods	41
4.3 Results	45
4.4 Discussion	48
5 Experiment III: gastric emotional awareness	50
5.1 Introduction	50
5.2 Materials and methods	51
5.3 Results	54
5.4 Discussion	60
6 Experiment IV: gastric moral awareness	64
6.1 Introduction	64
6.2 Materials and methods	65
6.3 Results	68
6.4 Discussion	79

7	Experiment V: interoception in a PIEZO2 patient	83
7.1	Introduction	83
7.2	Materials and methods	85
7.3	Results	87
7.4	Discussion	87
8	General discussion and conclusions	89
8.1	Summary and discussion of key findings	89
8.2	Future perspectives	92
	Bibliography	94

List of Tables

2.1	Descriptive statistics of breathing recordings used as ‘self’ stimuli in the pneumoception task. Smoke (cigs./day): participants’ daily number of cigarettes. Sport (hrs./wk.): participants’ weekly hours devoted to sports. Frequency (cy./min.): participants’ respiratory frequency (breaths per minute). Amplitude (db): participants’ respiratory amplitude (decibels). Freq gap (cy./min.): absolute deviation between self- and non-self frequencies. Ampl gap (db): absolute deviation between self- and non-self amplitudes.	11
3.1	Visual analogue scale (VAS) questionnaire on corporeal awareness (translated from Italian; adapted from Longo et al., 2008). P.: perceived. b.: body. VR: virtual.	18
3.2	List of experimental conditions and relative manipulations. 1PP: first-person perspective. 3PP: third-person perspective.	19
3.3	Respiratory rates, respiratory depths and their correlation at baseline and in each condition. Frequency: participants’ respiratory rate (breaths per minute). Amplitude: participants’ respiratory depth (millimetres). Correlation: Pearson’s product-moment correlation (r) between respiratory rate and depth at baseline and in each condition.	30
5.1	Visual analogue scale (VAS) questionnaire on emotions and feelings perceived in each sequence of video clips (abridged translation from Italian). Please note that questionnaire instructions specifically asked the participant to rate emotions and feelings that were aroused by that sequence in particular. it.: item. resp: respiratory. f.: feelings. GI: gastrointestinal.	52
6.1	Summary of scripts used as stimuli in experiment IV. 1PP: first-person perspective (the main character who acts throughout the script is the subject himself). sc.: script. persp.: perspective. 3PP: third-person perspective (the main character who acts throughout the script is a third party).	66
6.2	Visual analogue scale (VAS) questionnaire on emotions and feelings perceived while listening to each audio track (abridged translation from Italian). it.: item. resp: respiratory. f.: feelings. GI: gastrointestinal.	66

7.1	WLT-II questionnaire on gastric sensations. Responses were provided through a 7-point Likert scale ranging from 1 (not at all) to 7 (very much).	86
7.2	WLT-II test data for patient A. vs the normative values measured in a healthy female sample (cf. van Dyck et al., 2016).	87

List of Figures

2.1	Pneumoception test procedure	9
2.2	Pneumoception task results. Large dots: proportion of correct responses for each participant, ranked from the worst to the best performance. Small dots: metacognitive judgement of each participant (each dot is vertically aligned with the proportion correct dot of each subject). The line interpolates participants' A sensitivity values.	10
3.1	Embreathtment experimental set-up. Top: experimental apparatus, consisting of a head-mounted display and a breathing belt sensor (A), used to map the real breathing pattern of a participant onto a virtual body (avatar) in an immersive virtual reality environment (B). The mapping produced an 'embreathtment' illusion which made the avatar breathe in or out of synchrony with the participant (see Video 3.2). Bottom: Besides mapping breathing in a synchronous or asynchronous fashion, the apparatus allowed also to manipulate the visual appearance and the spatial perspective of the avatar, yielding four possible combinations – an avatar with a 'human-like' (C) or 'wooden' (D) appearance seen from a first-person perspective (1PP), and a 'human-like' (E) or 'wooden' (F) avatar seen from a third-person perspective (3PP).	15
3.2	Timeline of experiment I. MAIA: Multidimensional Assessment of Interoceptive Awareness. VR: Virtual Reality experience. HCT: Heartbeat Counting Task. PNEU: pneumoception task. HCT and PNEU were counterbalanced across participants but always placed after VR to avoid increasing salience of interoceptive cues.	20
3.3	Congruency between real and virtual bodily signals impacts on feelings of body ownership (A-B), location (C-D) and agency (E-F). Left panels: boxplots of perceived ownership (A), location (C), and agency (E) ratings as a function of type of congruent bodily signals: appearance (a), breathing (b), perspective (p) and their combinations. Right panels: estimated effects of each bodily signal on the ratings of perceived ownership (B), location (D), and agency (F). Effects expressed as standardised regression coefficients (slopes) of the underlying linear mixed models. The steeper the slope, the greater the relative importance of a predictor (Darlington, 1990; cf. Johnson and LeBreton, 2004), i.e. the importance of a given bodily signal.	24

3.4	The effects of both visceral and non-visceral cues on corporeal awareness depend on the ability to perceive visceral signals, as measured through self-report questionnaires (interoceptive sensibility) and objective tests (interoceptive accuracy), including a new self-breathing discrimination test (pneumoception task). Interoceptive sensibility moderates the effects of perspective on ratings of perceived body ownership (A) and location (B). Interoceptive accuracy moderates the effects of perspective (C) and breathing (D) on perceived ownership, and the effect of breathing (E) on perceived agency. Overall, participants with lower interoception scores are more susceptible to the experimental manipulations. MAIA: Multidimensional Assessment of Interoceptive Awareness. HCT: Heartbeat Counting Task.	26
3.5	Boxplots representing the amplitude of participants' real breathing waves recorded in conditions 1-8 (A); estimated effect of perspective, appearance and breathing on the amplitude of participants' breathing waves (B); interaction plots showing how appearance (congruent vs incongruent) moderates the estimated effects of breathing (C) and perspective (D) on the amplitude of breathing waves.	28
3.6	Boxplot of visual analogue scale (VAS) responses to experimental questions (yellow boxes) and control questions (grey boxes)	29
4.1	Timeline of experiment II.	42
4.2	Example of an artifact-free, bandpass-filtered electrogastrographic recording on a 120 s period.	43
4.3	Example of spectral density estimate (periodogram) of an EGG signal with its peak frequency in the normogastric range.	44
4.4	Median values for each item of the VAS embodiment questionnaire. Since the notches of the boxes of experimental items (yellow) do not overlap with the notches of the boxes of control items (grey), there is strong evidence that the median values are significantly different (Mc Gill et al., 1978; cf. Section 3.3). For numbers 1-5, cf. Table 3.1. . .	45
4.5	Predicted ratings of perceived body ownership as a function of electrogastrographic (EGG) peak frequency.	47
5.1	Timeline of experiment III. Q: inter-sequence intervals in which the VAS questionnaires relative to each preceding sequence were filled. . .	52
5.2	Estimated marginal means for disgust ratings in the five experimental conditions: disgust (1), fear (2), happiness (3), neutral (4) and sadness (5).	55
5.3	Estimated marginal means for fear ratings in the five experimental conditions: disgust (1), fear (2), happiness (3), neutral (4) and sadness (5).	56
5.4	Estimated marginal means for happiness ratings in the five experimental conditions: disgust (1), fear (2), happiness (3), neutral (4) and sadness (5).	57

5.5	Estimated marginal means for sadness ratings in the five experimental conditions: disgust (1), fear (2), happiness (3), neutral (4) and sadness (5).	58
5.6	EKG baseline X condition interaction: marginal effect of condition-specific EKG peak frequency on VAS ratings of disgust at different EKG baseline levels.	59
5.7	The three-way interaction between EKG baseline peak frequency, EKG condition-specific peak frequency and experimental condition predicts the subjective ratings of sadness.	61
5.8	The three-way interaction between EKG baseline peak frequency, EKG condition-specific peak frequency and experimental condition predicts the subjective ratings of arousal.	62
6.1	Timeline of experiment IV. Q: inter-sequence intervals in which the VAS questionnaires relative to each preceding audio track were filled.	67
6.2	Estimated marginal means for disgust ratings in the six experimental conditions: first-person physical disgust (1), third-person physical disgust (2), first-person moral disgust (3), third-person moral disgust (4), first-person neutral (5) and third-person neutral (6)	69
6.3	Estimated marginal means for immorality ratings in the six experimental conditions: first-person physical disgust (1), third-person physical disgust (2), first-person moral disgust (3), third-person moral disgust (4), first-person neutral (5) and third-person neutral (6)	70
6.4	Estimated marginal means for guilt ratings in the six experimental conditions: first-person physical disgust (1), third-person physical disgust (2), first-person moral disgust (3), third-person moral disgust (4), first-person neutral (5) and third-person neutral (6)	71
6.5	The three-way interaction between baseline EKG peak frequency, condition-specific EKG peak frequency and experimental condition predicts the judgement of immorality.	73
6.6	The two-way interaction between baseline EKG peak frequency and experimental condition predicts subjective ratings of disgust.	74
6.7	The two-way interaction between EKG peak frequency at baseline and experimental condition predicts subjective ratings of anger.	75
6.8	The two-way interaction between condition-specific EKG peak frequency and experimental condition predicts subjective ratings of anger.	76
6.9	The two-way interaction between baseline EKG peak frequency and experimental condition predicts participants' arousal ratings.	77
6.10	The three-way interaction between baseline EKG peak frequency, condition-specific EKG peak frequency and experimental condition predicts the conscious perception of cardiac activity.	78
6.11	The three-way interaction between baseline EKG peak frequency, condition-specific EKG peak frequency and experimental condition predicts participants' imageability ratings.	80

6.12	EKG peak frequency in the six experimental conditions: first-person physical disgust (1), third-person physical disgust (2), first-person moral disgust (3), third-person moral disgust (4), first-person neutral (5) and third-person neutral (6)	81
7.1	Timeline of experiment III.	86
7.2	WLT-II questionnaire data for patient A.	88

Chapter 1

Introduction

1.1 State of the art

Humans and other primates are uniquely aware of having a body, controlling its actions, and dwelling in it – a form of self-consciousness which goes under the name of corporeal awareness (Berlucchi and Aglioti, 1997, 2010; Critchley, 1979) or embodiment (Longo et al., 2008). Research on neurological disorders (Blanke and Arzy, 2005; Heydrich and Blanke, 2013) and on bodily illusions, from the rubber hand (Botvinick and Cohen, 1998) to the full body illusion (Lenggenhager et al., 2007) the body swap illusion (Petkova and Ehrsson, 2008) and the enfacement illusion (Sforza et al., 2010) imply that one becomes aware of one’s body when different cues, from the appearance of the body to the position of its parts, are aligned in space and time and integrated at the neural level.

These cues can come both from outside and from inside the body. Classical studies on corporeal awareness chiefly focused on exteroceptive signals, from touch to vision: that is, researchers investigated how various features of exteroception determined specific changes in awareness of one’s own body. Interoception, i.e. the sense of the physiological condition of the body (Craig, 2002), likely plays an important role in shaping corporeal awareness, too. However, to date, research trying to ascertain the impact of interoceptive signals on the bodily self has been

hampered by the fact that these signals are extremely diverse and difficult to record.

A series of recent experiments applied an ‘interoceptive’ twist to classical embodiment paradigms. Tsakiris and colleagues (2011) found that performance in the heartbeat counting task (Schandry, 1981) predicted the degree of susceptibility to the rubber hand illusion. At the same time, Barnsley and co-workers (2011) reported that the illusion itself could impact on histamine reactivity in the real arm. While tantalisingly pointing to a closed loop between interoception and corporeal awareness, these studies did not manipulate neither the physiological signals giving rise to interoception, nor their perceptual or symbolic representation in the minds of the participants.

Two other research groups made a step further by making a virtual rubber hand (Suzuki et al. 2013) or a full virtual body (Aspell et al. 2013) flash either in sync or out of sync with the participant’s heartbeat. Their results suggested that visuo-cardiac synchrony boosts embodiment. However, one may wonder whether cardiac signals can be considered an embodiment factor also in ordinary ecological circumstances, where heartbeats are perceived only faintly and transiently.

An elegant study by Park et al. (2016) answered the question in the affirmative. Combining electrocardiography, electroencephalography and virtual reality, they discovered that heartbeat-evoked potentials (HEPs) originating from the posterior cingulate cortex are linked to changes in corporeal awareness induced by the full body illusion. This landmark result spurred the quest for other forms of coupling between visceral signals and bodily self-consciousness, particularly focusing on the gastric domain.

Rebollo and colleagues (2018) did indeed find that also the electrical oscillations coming from the interstitial cells of Cajal in the stomach can explain a sizeable degree of fluctuation in the resting BOLD signal of a cluster of brain areas they termed the ‘gastric network’. Although the authors propose that this gastro-cerebral coupling contributes to the representation of the bodily self, further research is needed, since this study relied on a no-task, resting state paradigm and the gastric

network may simply act as a homeostatic circuit sensitive to hunger cues (Porciello et al. 2018).

Other lines of research on corporeal awareness targeted physiological signals straddling the boundary between interoception, proprioception and exteroception. Converging evidence highlights that pleasant touch mediated by C tactile (CT) afferents is more effective than purely exteroceptive touch in giving rise to the rubber hand illusion (Crucianelli et al. 2013, Lloyd et al. 2013, Van Stralen et al. 2014). By contrast, the embodying power of another multisensory cue, respiration, is far from being clear, since the very few studies which investigated the issue lead to conflicting or inconclusive findings (Adler et al., 2014; Allard et al., 2017; Czub and Kowal, 2019).

1.2 Objectives and structure of the project

Overall, the upshot of these studies is that there is still a considerable gap of knowledge about the role of visceral physiological signals in corporeal awareness beyond the cardiac domain. The research project described in the present dissertation aimed at filling this gap in the scientific literature. More precisely, its main objectives were:

O1 - to improve methods to record interoceptive signals;

O2 - to test how each interoceptive modality contributes to bodily awareness;

O3 - to assess changes in bodily awareness due to altered interoception.

Objective 1 - Improving methods to record interoceptive signals Current methods to measure interoception are marred by several limitations. Interoceptive signals come from a wide variety of sources - peripheral receptors conveying information about heart and respiration rate, gut motility, hunger, thirst, temperature, pain, itch, and sensual touch. Nevertheless, existing techniques cover a fraction of

these sources, partly due to the fact that many receptors are difficult to reach, being located inside the body rather than on its surface.

Moreover, some interoceptive signals give rise to distinct conscious sensations, while some others produce faint, transient, or individually variable feelings. The latter include heartbeats, which are particularly salient only in exceptional circumstances like panic attacks (Ehlers et al., 2000), intense physical activity, and tachycardia. Yet the most widespread interoceptive test to date, Schandry's (1981) task, requires subjects to gauge their own heart rate in a quiet laboratory setting, where heart-related perceptions would not normally occur. Many current tests for interoception outside the scope of heart signals, e.g. air load judgements (Daubenmier et al., 2013) and gastric balloon distention procedures (Geliebter, 1988; Wang et al., 2008) are often uncomfortable or downright invasive.

To tackle these issues, the research project carefully appraised existing measures of interoceptive signals, and endeavoured to find new tools for tracking multiple interoceptive signals in a non-invasive manner. In particular, as described in [Chapter 2](#), the project led to the development of a new test of respiratory interoception, or 'pneumoception'. Overall, this will hopefully allow researchers to correlate more precise, reliable and valid interoception scores to self-reported feelings of bodily awareness.

Objective 2 - Testing the contribution of each interoceptive modality to bodily awareness It is not clear how much each interoceptive signal, from heart rate to breathing to gastric feelings, contributes to the three main components of bodily awareness - the feelings of having a body (perceived body ownership), controlling its actions (perceived body agency) and dwelling in it (perceived body location), as detailed above. Assessing the relative weight of each of these signals will help to establish a hierarchy of interoceptive cues, from the least to the most relevant for bodily consciousness. In order to do so, the research project applied new experimental paradigms to trigger conflicts between interoceptive and exteroceptive

signals and see whether such conflicts alter bodily awareness.

In the last two decades, a couple of new tools proved particularly effective in revealing the neural correlates of bodily awareness: virtual reality (VR) environments and bodily illusions (Botvinick & Cohen, 1998; Leggenhager et al., 2007; Sforza et al., 2010). Building on these results, recent studies introduced new cardio-visual or respiratory-visual manipulations: these techniques allow subjects to embody avatars that flash synchronously with their heart rate or breathing rhythm (Adler et al., 2014; Aspell et al., 2013; see above).

Despite their importance, such intero-exteroceptive awareness paradigms clearly lack ecological validity. To overcome this problem, the project spawned a more ecologically plausible interoceptive bodily illusion, named ‘embreathment’, and harnessed its power to explore the links between interoception, exteroception and the bodily self, as detailed in [Chapter 3](#). A simplified version of the illusion was also coupled to electrogastrographic recordings to test the contribution of gastric signals to embodiment, as explained in [Chapter 4](#).

Finally, we hypothesised that respiratory, cardiac and gastric physiology may underpin not only corporeal, but also emotional and moral awareness, thus contributing to several facets of the self at once. [Chapter 5](#) thus reports the impact of visceral signals on the perception of emotional stimuli, while [Chapter 6](#) presents data on the visceral underpinnings of moral judgements towards oneself and others.

Objective 3 - Assessing changes in bodily awareness due to altered interoception In conjunction with virtual reality environments, it may be fruitful to probe changes in bodily awareness by observing what happens when the activity of interoception-related organs and nerves is impaired. [Chapter 7](#) contains the first data on the interoceptive sensibility of a rare patient unable to feel physical forces of tension and compression acting upon her body. The concluding remarks in [Chapter 8](#) provide the reader with a general discussion of the results obtained so far and lay down the groundwork for future studies on clinical populations.

Chapter 2

The ‘pneumoception’ test: development and validation

2.1 Introduction

Despite its pivotal role in homeostasis and its increasingly clear influence on cognition and emotion (Del Negro et al. 2018), normal, eupnoeic breathing has received a surprisingly scant attention from the research community working on interoceptive feelings. Indeed, most interoception-related respiratory research focused on altered breathing patterns, such as those occurring in breathlessness or in meditation. As a consequence, there are several available tests of air hunger, but no validated procedure for assessing normal respiratory interoception.

The respiratory load detection task (Davenport et al. 2007, Zhao et al. 2002) requires participants to detect when a resistance has been introduced into a tube through which they are breathing. While the test is reasonably short (35 trials) and taps into real-time detection of breathing signals, it requires a custom made apparatus and probes respiration far from its homeostatic equilibrium - a situation which is very different from the everyday eupnoeic breathing experience.

In a similar vein, the respiratory load *discrimination* task (Webster and Colrain, 2000) requires participants to discriminate among degrees of resistive loads introduced

into the airway, while Faull et al. (2016) asked experimental subjects to rate their own breathlessness and anxiety while breathing through a hypercapnia-inducing system. As the load detection task, these procedures actually assess the ability of participants to perceive shortness of breath rather than normal breathing.

In order to gauge the ability of healthy participants to accurately perceive their own breathing during eupnoea, we drew inspiration from the cardioception test recently developed by Azevedo and colleagues (2016). The test consists in a self-other heartbeat discrimination task: participants listen to unlabelled pre-recorded audio tracks in which each sound corresponds to a heartbeat and judge whether each track contains a record of their own heartbeat (self-tracks) or of someone else's (other-tracks). Self-tracks and other-tracks are matched for cardiac frequency.

Since the cardioception test is quick, its instructions are easy to follow, and the task explicitly focuses on the distinction between self-related and nonself-related physiological signals, we constructed an analogous 'pneumoception' test that measures how much one can discriminate one's own breathing sounds from someone else's. Of note, in our case there was no need to transform physiological signals into auditory information, as respiration produces an actual sound: thus we recorded real breathing sounds from the nostrils of the participants and used them for the procedure detailed below.

2.2 Materials and methods

Phase 1: construction of a breathing sound database. To sample the naturally occurring variety of breathing sounds, from low to high frequency and amplitude, we recruited 58 participants. Breathing sounds were recorded in Audacity 2.1.3 with a Sennheiser PC3 CHAT noise-cancelling microphone placed under the nostrils (impedance: 2kW, frequency response: 90-15000 Hz, pick-up pattern: unidirectional; Sennheiser electronic GmbH & Co. KG).

To keep breathing as spontaneous as possible, participants were just told that

experimenters ought to tape their voice before and after a relaxation period. Thus, participants pronounced two lists of words, and their naturally occurring breathing was covertly recorded in a 5' 'pause' between the two lists.

The raw breathing sound recordings were edited removing background noise and artifacts. Average frequency and amplitude values were calculated for each recording, which was then split into short tracks with a standard length of 23 s. Sound editing and splitting was performed in Praat 6.0.29 (Boersma and Weenink, 2017).

Phase 2: pneumoception test proper. A subset of 32 subjects took part in the experimental phase a few days after phase 1. A customised MATLAB script (The MathWorks, Inc.) matched the breathing tracks of a participant (self-tracks) with another's (nonself-tracks) based on their frequency and amplitude. To prevent ceiling effects, the nonself-tracks frequency and amplitude could be at most 25% higher or lower than the self-tracks'. Nonself-tracks were taken from the database collected in phase 1.

All tracks (13 self-tracks and 13 nonself-tracks) were finally played in random order on the MATLAB Psychophysics Toolbox (Brainard, 1997; Kleiner et al., 2007; Pelli, 1997) to get accuracy and reaction time data: at the end of each track, participants were asked to decide whether the sounds they heard were their own breathing or someone else's, and press a key accordingly. At the end of the test, subjects were required to provide a metacognitive assessment of their own performance (Figure 2.1).

Phase 3: data analysis. Respiratory accuracy was gauged comparing the percentage of correct responses to the chance-level threshold, as obtained from binomial distribution probabilities, and computing the non-parametric index of sensitivity A (Pollack and Norman, 1964; Zhang and Mueller, 2005).

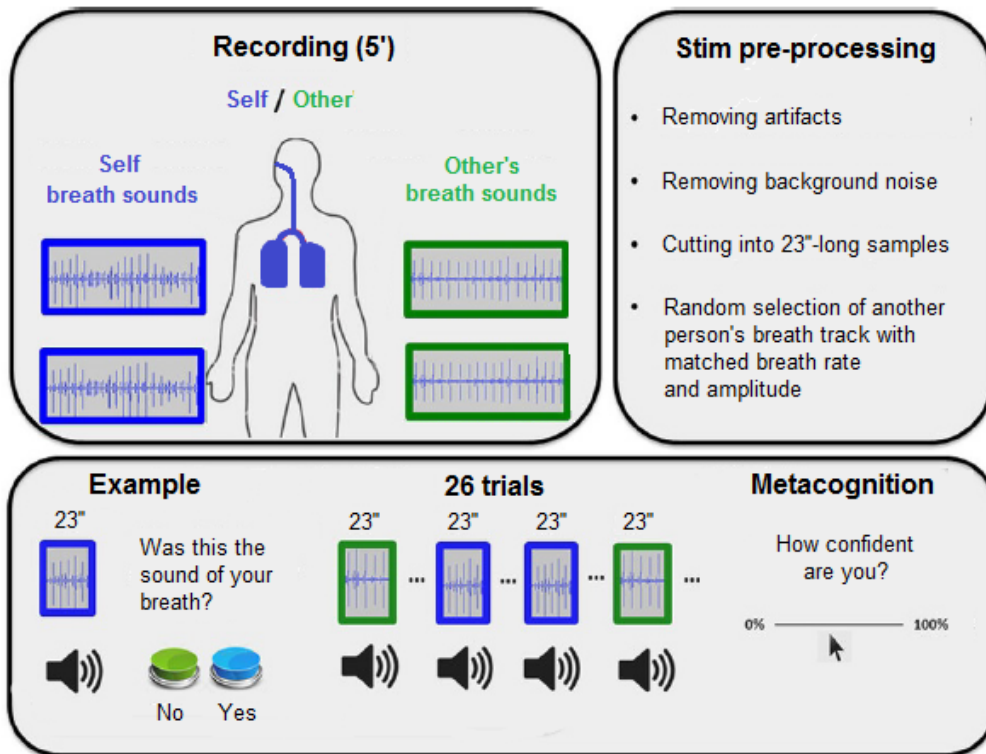


Figure 2.1. Pneumoception test procedure

2.3 Results

On average, the proportion of correct responses was 57.69% (SD = 23.61, range: 18.89%-100%). According to binomial distribution probabilities, participants who performed above chance should have a score equal to or above 69.23% (18 hits or correct rejections out of 26 trials, $p = .038$). 12 participants out of 32 (37.5%) scored above this threshold, reliably discriminating their own breathing from others'. 16 participants (50%) did not reliably discriminate their own breathing tracks from others', displaying scores which ranged from 30.76% to 69.23%. Finally, 4 participants (12.5%) mistook their own breathing for another's (proportion correct < 30.76%). Reaction times (RTs) of correct responses to 'self' breathing tracks did not significantly differ from RTs for 'non-self' tracks, $\chi^2(1, N = 467) = 0.71, p = .40$. As expected, metacognitive judgement did not correlate with actual performance. The average A sensitivity index was 0.51 (SD = 0.39, range: 0-1). Figure 2.2 depicts these results, while Table 1 summarises the descriptive statistics of the 'self' stimuli.

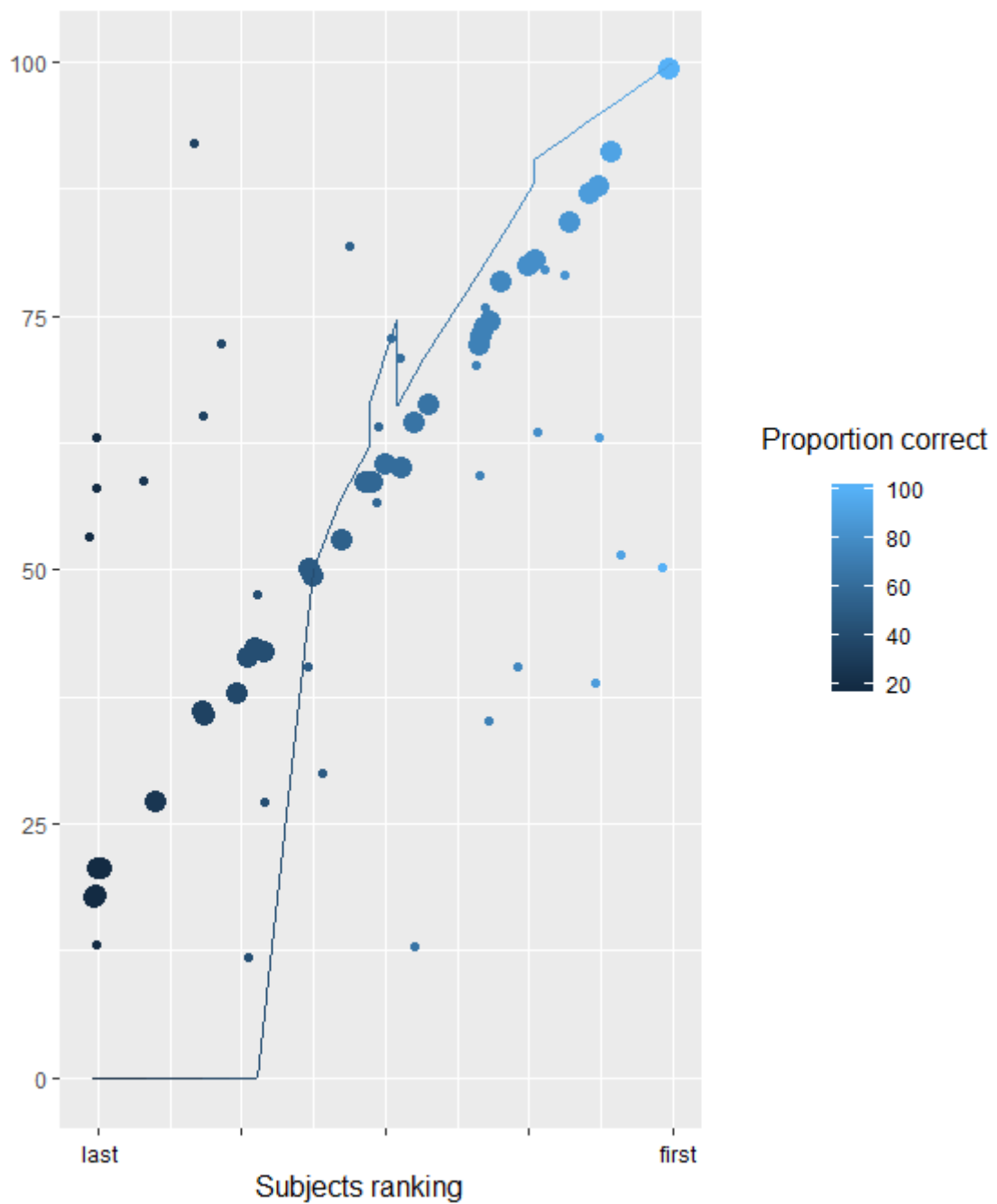


Figure 2.2. Pneumoception task results. Large dots: proportion of correct responses for each participant, ranked from the worst to the best performance. Small dots: metacognitive judgement of each participant (each dot is vertically aligned with the proportion correct dot of each subject). The line interpolates participants' A sensitivity values.

	smoke (<i>cigs./day</i>)	sport (<i>hrs./wk.</i>)	frequency (<i>cy./min.</i>)	amplitude (<i>db</i>)	freq gap (<i>cy./min.</i>)	ampl gap (<i>db</i>)
<i>mean</i>	1.83	1.44	15.45	61.55	1.72	6.68
<i>SD</i>	3.74	2.26	3.83	9.04	1.10	4.81
<i>min</i>	0.00	0.00	8.00	41.77	0.20	0.01
<i>max</i>	15.00	7.00	23.60	75.69	4.60	14.49

Table 2.1. Descriptive statistics of breathing recordings used as ‘self’ stimuli in the pneumoception task. Smoke (*cigs./day*): participants’ daily number of cigarettes. Sport (*hrs./wk.*): participants’ weekly hours devoted to sports. Frequency (*cy./min.*): participants’ respiratory frequency (breaths per minute). Amplitude (*db*): participants’ respiratory amplitude (decibels). Freq gap (*cy./min.*): absolute deviation between self- and non-self frequencies. Ampl gap (*db*): absolute deviation between self- and non-self amplitudes.

2.4 Discussion

We developed a new ‘pneumoception’ test to measure respiratory interoception of normal, eupnoeic breathing. The test was quick and easy to administer and explicitly focused on the distinction between self-related and nonself-related physiological signals. However, it also proved to be quite difficult. Results indicate that only one third of participants reliably performed above chance. We hypothesise that this is largely due to the severe constraints of the matching algorithm, as by design the amplitude and frequency of each self-breathing track was at most 25% higher or lower than the corresponding nonself-track (cf. section 2.2). Indeed, the average absolute deviation between self and non-self tracks was 1.72 breaths per minute in terms of frequency and 6.68 db in terms of amplitude (table 2.1). It remains to be ascertained whether relaxing this constraint would make the participants improve their performance.

Measuring individual sensitivity to respiratory load would arguably provide a more direct assessment of respiratory interoception; however, resistive loads elicit a breathing experience that is qualitatively very different from normal, eupnoeic resting-state breathing, involving different receptors and neural mechanisms (Davenport

and Vovk, 2009). In contrast with that, the stimuli of the pneumoception task are designed to capture the everyday experience of breathing at rest.

In principle, since stimuli are recorded before the experiment, participants could compare them with their own breathing relying not just on their interoceptive abilities, but also on their memory. However, breathing sounds are very rarely attended to in ordinary circumstances, and their memory trace should not be particularly strong. Therefore, it seems more likely that participants discriminate their own breathing sounds from others' by trying to reproduce online the sequence they hear, observing whether there is a correspondence between the sounds and the flow of air they sense through small-fibre $A\delta$ interoceptive afferents of the nasal mucosa (Sozansky and Houser, 2014; Zhao et al., 2011).

While the test constraints could be loosened in order to make it easier, we believe that the pneumoception sensitivity index A , which is computed taking into account not just hits but also misses and false alarms, could be used in conjunction with other established interoceptive measures to gauge the ability of participants to perceive their own physiological condition. The next chapter will present an application of the test to an experiment.

Chapter 3

Experiment I: the 'embreathment' illusion

3.1 Introduction

Among bodily cues, breathing has an intuitive appeal as a factor inducing a sense of embodiment. Indeed, breaths enable bodily survival and continuously provide the brain with vital information about physiology (Del Negro et al., 2018), emotion (Boiten, 1998; Boiten et al., 1994), and cognition (Huijbers et al., 2014; Perl et al., 2019; Vlemincx et al., 2011; Zelano et al., 2016). Furthermore, contrary to other bodily signals, breaths are easily accessible to consciousness and partially amenable to voluntary control. For the same reasons, though, the impact of breathing on corporeal awareness is difficult to gauge in a safe, ecological, and experimentally controlled fashion. Thus, here we sought to measure how much breaths influence the awareness of one's body through a new bodily illusion that we call 'embreathment'.

In particular, we performed a real-time mapping of the respiratory frequency and amplitude of each participant onto a virtual body (avatar), using a custom-made immersive virtual reality setup (Figure 3.1 and [Video 3.2](#)). We thus made the avatar breathe either like the real body of the participant (congruent breathing) or with an opposite, anti-phase pattern (incongruent breathing). We also manipulated the

visual appearance of the virtual body and the perspective from which the participant looked at it: thus, the avatar could resemble either a human body (congruent appearance) or a wooden mannequin (incongruent appearance) and lie either in the same position of the real body (congruent, first-person perspective) or not (incongruent, third-person perspective).

We expected that participants would feel more embodied in a ‘congruent’ avatar matching the respiratory, spatial, or visual features of their real body than in an ‘incongruent’ avatar where such a matching did not occur. Furthermore, we hypothesized that some kinds of congruent features would exert a more powerful influence on embodiment than others, thus allowing us to rank sources of corporeal awareness from the least to the most influential. Finally, we thought that the influence of bodily signals on explicit and implicit markers of embodiment would be moderated by interoceptive sensibility and accuracy (as defined by Garfinkel et al., 2015). Hence, we collected interoceptive sensibility trait measures through a validated questionnaire (Calì et al., 2015) and tested interoceptive accuracy combining the standard heartbeat counting task (Schandry, 1981) with the new ‘pneumoception’ test (see above, [Chapter 2](#)).

3.2 Materials and methods

Participants Thirty-two healthy male volunteers took part in the study ($M = 22.25$ years, $SD = 3.14$, range: 19-33). None of them had a history of neurological, psychiatric, cardiac or respiratory disorders, nor practised meditation, as assessed through a preliminary screening procedure. All participants gave their informed consent before being included in the research sample. The local ethics committee at the Fondazione Santa Lucia Research Hospital reviewed and approved the experimental protocol in accordance with the ethical standards of the Declaration of Helsinki.

Virtual reality apparatus and stimuli Our immersive virtual reality environment consisted of life-size three-dimensional characters (avatars) lying on a deck

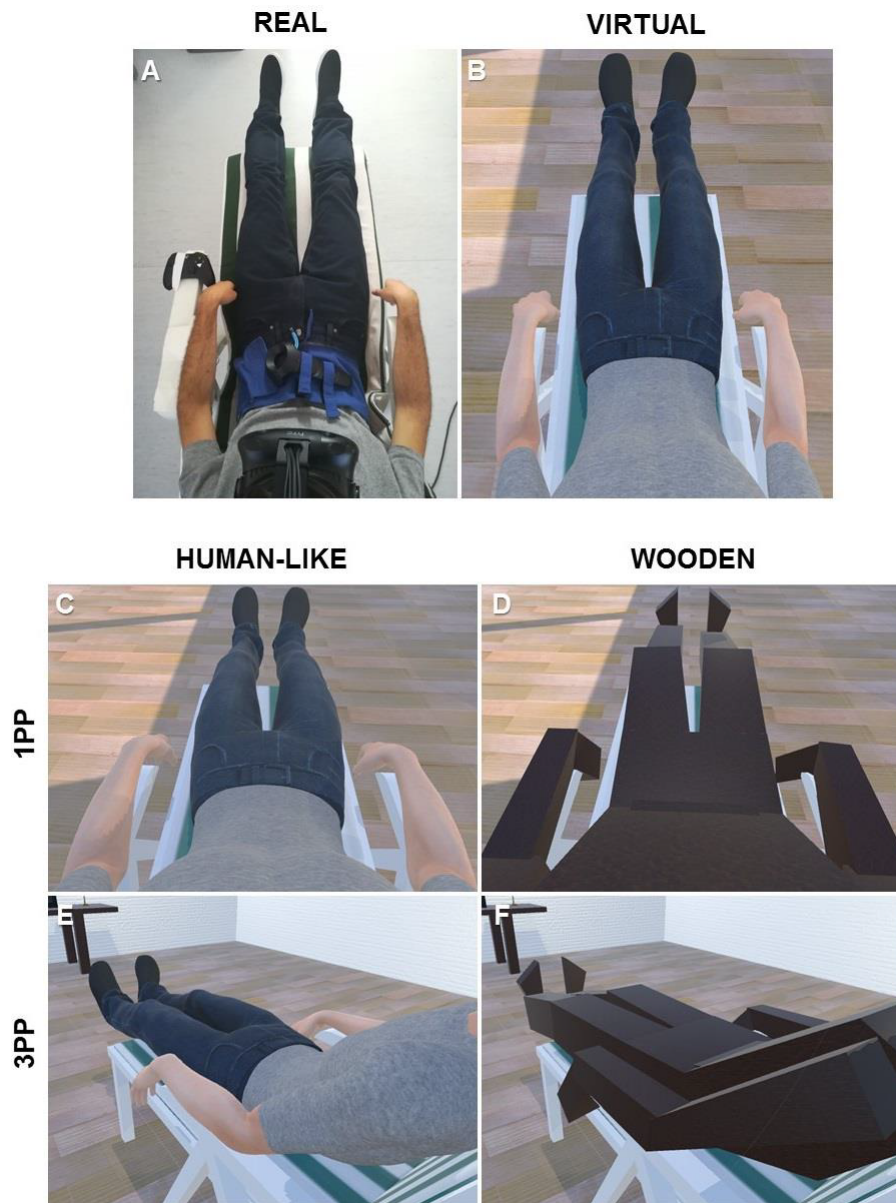


Figure 3.1. Embreathment experimental set-up. Top: experimental apparatus, consisting of a head-mounted display and a breathing belt sensor (A), used to map the real breathing pattern of a participant onto a virtual body (avatar) in an immersive virtual reality environment (B). The mapping produced an ‘embreathment’ illusion which made the avatar breathe in or out of synchrony with the participant (see [Video 3.2](#)). Bottom: Besides mapping breathing in a synchronous or asynchronous fashion, the apparatus allowed also to manipulate the visual appearance and the spatial perspective of the avatar, yielding four possible combinations – an avatar with a ‘human-like’ (C) or ‘wooden’ (D) appearance seen from a first-person perspective (1PP), and a ‘human-like’ (E) or ‘wooden’ (F) avatar seen from a third-person perspective (3PP).

chair in a living room. Avatars were designed with iClone 6 (Reallusion, Inc.) and 3DS Max 2015, and came in two flavours: ‘human-like’ and ‘wooden’ avatars. The former closely resembled a human body, while the latter were created replacing each human body part with a wooden, squared box retaining the size and length of the original part. Both human-like and wooden avatars came in twenty different sizes, allowing participants to fit the avatar to the size of their real body. The virtual deck chair was created with 3DS Max 2015 matching the physical dimensions and appearance of a real deck chair to the nearest centimetre. In addition to the chair, the virtual living room included a door, a sofa, a flat TV screen, several lamps and a door window looking out onto a balcony. Walls, floors, doors, furniture and windows were designed with Unity 2017.1.

The virtual environment was live broadcast in Unity 2017.1 on an HTC Vive head-mounted display (field of view: 110°, resolution: 2160×1200 px, resolution per eye: 1080×1200 px, aspect ratio: 9/5, refresh rate: 90 Hz; HTC Corp.). The Vive accelerometer, gyroscope, Lighthouse laser tracking system and front-facing cameras automatically detected head movements and adjusted the computer-generated image accordingly. A Vive controller was tied to a belt worn by participants in order to track their breathing and live map the corresponding belly movements onto the avatars by means of a customised Unity 2017.1 script (Figure 3.1 and [Video 3.2](#)).

Interoception tests In addition to the virtual bodily illusion, the experiment included also three interoception tests.

1. The Italian version of the Multidimensional Assessment of Interoceptive Awareness (MAIA), a 32-item questionnaire measuring how much someone is aware of their physiological condition with a 5-point Likert scale (Calì et al., 2015).
2. The heartbeat counting task (HCT; Dale & Anderson, 1978; Schandry, 1981), which requires participants to estimate the number of heartbeats in different time windows (i.e., 25s; 35s; 45s and 100s) while their cardiac activity is recorded through a standard electrocardiogram (ECG). Electrocardiographic

data were recorded with three pre-gelled, disposable Ag/AgCl 50 mm electrodes arranged in a bipolar lead II configuration and connected to a BIOPAC ECG100C/MP150 system (BIOPAC Systems, Inc.). Subjective heartbeat estimates were collected with E-Prime 2.0 (Psychology Software Tools, Inc.).

3. The pneumoception test (see above [Chapter 2](#))

Experimental procedure After reading and signing the informed consent, each participant completed the MAIA questionnaire, then fastened a belt tied to an HTC Vive controller, lay on a deck chair and wore the HTC Vive. This was followed by a calibration phase, which included two stages.

In stage 1 (*size and space calibration*) a human-like avatar was shown in a first-person perspective (1PP) to check which body size and viewpoint were deemed most natural by the participant. Importantly, during stage 1 the avatar did not breathe, as the script mapping breathing patterns to the virtual body was not activated yet.

In stage 2 (*respiratory calibration*), a virtual panel temporarily screened off the participant from the virtual room, blocking the view of the virtual body. At that point, unbeknownst to the participant, the experimenter launched the customised Unity 2017.1 script that mapped the participant's breathing pattern onto the avatar in real time; then, the experimenter observed the respiration-induced motion of both the virtual and the real belly to check that 1) the script did not produce any error, 2) there was no detectable delay between the real and the virtual movements, and 3) the moving virtual belly was seamlessly integrated in the virtual body mesh. In all 32 participants, the script successfully met conditions 1), 2) and 3). Finally, the experimenter recorded the baseline belly movements for 2 minutes while participants relaxed and stared at a fixation mark.

Since the breathing script was not activated in phase 1 and the participant did not see the breathing virtual body in phase 2, no breath-related habituation, entrainment or priming effect was subsequently carried over to the experimental phase.

item	construct	statement
1	<i>p. b. ownership</i>	I felt the VR body/object was mine
2	<i>p. b. agency</i>	I felt I controlled the movements of the VR body/object
3	<i>p. b. location</i>	I felt I was in the same place of the VR body/object
4	<i>control item</i>	I felt I had no body
5	<i>control item</i>	I felt I had more than one body

Table 3.1. Visual analogue scale (VAS) questionnaire on corporeal awareness (translated from Italian; adapted from Longo et al., 2008). P.: perceived. b.: body. VR: virtual.

Next, participants were told that they were about to see a variety of virtual scenarios, and that at the end of each scenario they had to answer a 5-item questionnaire using a visual analogue scale (VAS). All five items were statements on corporeal awareness-related feelings that could arise out of the virtual experience (Table 3.1; adapted from Longo et al., 2008). Participants indicated how much they agreed with each statement by picking a VAS ranging from 0 (“I did not have that feeling at all”) to 100 (“I perceived a strong feeling of that sort”) through a joystick-controlled cursor. A short training session helped them familiarise with the items and the response method.

After the practice session, each participant passively observed eight different experimental conditions (Table 3.2) and after each condition they completed the relative 5-item VAS questionnaires. Experimental conditions lasted two minutes each, and displayed an avatar whose physical appearance, position and breathing pattern could either be congruent or incongruent with the real-world participant. Hence, the avatar could either be a ‘human-like’ or ‘wooden’ virtual character; it could be seen either from the first- or third-person perspective (in the latter case, the avatar was displayed at distance of ~ 40 cm to the participant’s right side, and a panel covered the part above the neck); and it breathed either exactly like the participant, in real time (‘in phase’ avatar) or with an opposite pattern, i.e., it inhaled when the participant exhaled, and vice versa (‘in antiphase’ avatar).

The avatar always lay on a deck chair in a virtual living room, whose features were kept constant across conditions (see above). In condition 1, appearance, location,

no.	appearance	perspective	breathing
1	wooden	3PP	antiphase
2	wooden	3PP	phase
3	wooden	1PP	antiphase
4	wooden	1PP	phase
5	human-like	3PP	antiphase
6	human-like	3PP	phase
7	human-like	1PP	antiphase
8	human-like	1PP	phase

Table 3.2. List of experimental conditions and relative manipulations. 1PP: first-person perspective. 3PP: third-person perspective.

and breathing were all incongruent; in condition 8, participants saw an avatar which looked, lay, and breathed like their real body; and conditions 2-7 presented all possible intermediate combinations of congruent and incongruent bodily signals (Table 3.2). The order of experimental conditions was counterbalanced across participants with a Williams design, i.e., a generalised Latin square which is also balanced for the estimation of first-order carryover effects (Williams, 1949; Sailer, 2005).

Finally, participants completed the heartbeat counting and pneumoception tasks, in counterbalanced order. In the counting task, subjects counted their heartbeats during four different randomised time intervals (25 s, 35 s, 45 s, 100 s) while undergoing a bipolar lead II ECG. In the pneumoception task, each subject listened to a list of 26 random unlabelled breathing sound tracks and classified them as ‘self-tracks’ or ‘nonself-tracks’ (see above, Chapter 1). After both tasks, participants provided the experimenter with a metacognitive judgement of their own performance through a VAS. Figure 3.2 depicts the timeline of the experiment.

Data analysis: corporeal awareness ratings during the ‘embreathment’ illusion The primary goal of the study was to quantify the influence of breathing, visual appearance and spatial perspective on corporeal awareness. Hence, we used R 3.3.2 and the R lme4 package (Bates et al., 2015) to perform a linear mixed-effects analysis, modelling how much ratings of perceived body ownership, agency, and

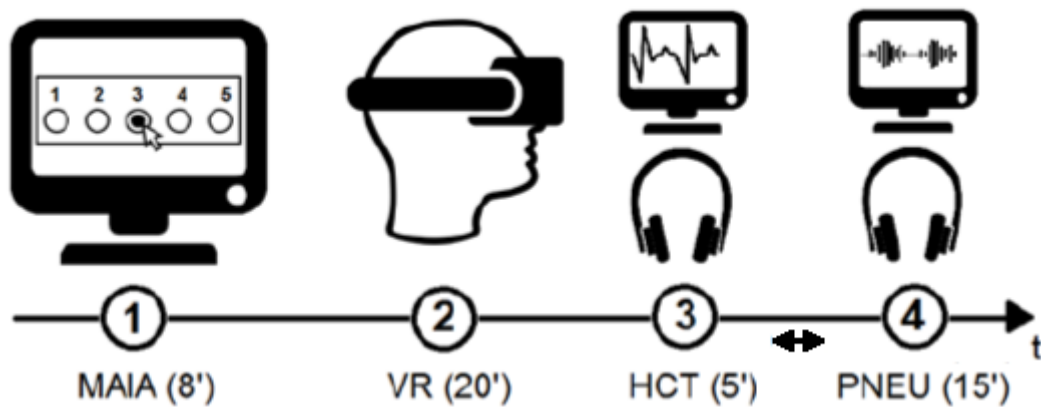


Figure 3.2. Timeline of experiment I. MAIA: Multidimensional Assessment of Interoceptive Awareness. VR: Virtual Reality experience. HCT: Heartbeat Counting Task. PNEU: pneumoception task. HCT and PNEU were counterbalanced across participants but always placed after VR to avoid increasing salience of interoceptive cues.

location changed when respiratory, visual and spatial features of the virtual body were either congruent or incongruent with those of the real body. Moreover, we tested if such rating changes were moderated by individual levels of interoceptive sensibility and accuracy.

Ratings were collected through visual analogue scales (VAS; see “Experimental procedure” above). Sensibility was assessed through three MAIA subscales of interest – noticing, attention regulation, and body listening (Mehling et al., 2012). Respiratory accuracy was gauged computing the non-parametric index of sensitivity A (Pollack and Norman, 1964; Zhang and Mueller, 2005) from the responses of the pneumoception task. Cardiac accuracy, on the other hand, was measured comparing objective and estimated heartbeat counts in the heartbeat counting task (Pollatos et al., 2008; Schandry, 1981). Individual electrocardiograms were processed on AcqKnowledge 4.4 (BIOPAC Systems, Inc.) to find QRS complexes and thus compute heart rates in each time interval.

Thus, in addition to the experimentally manipulated factors (respiratory, visual and spatial congruency), the maximal mixed-effects model should include five separate covariates, namely, the three MAIA subscales, the A index, and the IS score. However, statistical tests revealed that such a model does not converge; moreover,

one of the condition indices of the independent variables matrix is greater than 30 and is associated with more than two variables with large variance decomposition proportions ($> .50$), indicating a remarkable level of multicollinearity (Belsley et al., 1980). To overcome this issue, IS and A scores were averaged to obtain a general interoceptive accuracy score (i_{acc}) for each participant p :

$$i_{acc_p} = \frac{A_p + IS_p}{2}$$

Likewise, a general interoceptive sensibility (i_{sen}) score was obtained averaging over the three MAIA subscales of interest – noticing (*not*), attention regulation (*att*), and body listening (*lis*):

$$i_{sen_p} = \frac{MAIA_{not_p} + MAIA_{att_p} + MAIA_{lis_p}}{3}$$

Therefore, the three linear mixed models which were actually used in the data analysis were specified as follows. We built three mixed models, whose dependent variables were the VAS ratings of perceived body ownership, perceived body agency, and perceived body location, respectively. As fixed effects, all models had appearance (*app*, two levels: human-like and wooden), perspective (*persp*, two levels: first- and third-person perspective) and breathing (*breath*, two levels: phase and antiphase). These fixed effects were tested for interactions with each other, as well as with the interoceptive sensibility (i_{sen}) and accuracy (i_{acc}) scores. Finally, as random effects, the models included by-subject intercepts as well as by-subject slopes for the effects of appearance, perspective and breathing:

$$p.ownership \sim app * persp * breath * (i_{sen} + i_{acc}) + (app + persp + breath|subj)$$

$$p.agency \sim app * persp * breath * (i_{sen} + i_{acc}) + (app + persp + breath|subj)$$

$$p.location \sim app * persp * breath * (i_{sen} + i_{acc}) + (app + persp + breath|subj)$$

The relative importance of each effect was gauged comparing its standardised

regression coefficient with the others' (Darlington, 1990; Johnson & LeBreton, 2004).

Data analysis: respiratory signals during the ‘embreathment’ illusion

Breathing movements, i.e. the HTC Vive controller movements on the Y-axis, were analysed in MATLAB (The MathWorks, Inc.). Signals were downsampled to 43 Hz with a Hamming window-designed finite impulse response (FIR) anti-aliasing filter of order 30, detrended and baseline-corrected to get phase peaks, amplitudes and frequencies of each participant in each experimental condition. Values outside the median plus or minus 2.5 times the median absolute deviation were classified as outliers and subsequently excluded from further analysis (Hampel, 1974; Leys et al., 2013).

To measure how much the participants' baseline-corrected breathing amplitude varied as a function of human-avatar sensory congruency, we built a linear mixed-effects model which featured amplitude as a dependent variable; appearance (two levels: human-like and wooden), perspective (two levels: first- and third-person perspective) and breathing (two levels: phase and antiphase) as fixed effects. Interaction terms and random effects were specified as in the models above:

$$amplitude \sim app * persp * breath * (i_{sen} + i_{acc}) + (app + persp + breath|subj)$$

All models described so far were tested for linearity, absence of collinearity, homoscedasticity, normality of residuals, and absence of influential data points. p-values were computed through Type II Wald chi-square tests performed with the Anova function of the R car package (Fox & Weisberg, 2011). Marginal and conditional R^2 goodness-of-fit measures of each mixed-effects model (Johnson, 2014; Nakagawa and Schielzeth, 2013) were calculated with the R MuMIn package (Bartoń, 2018).

Supplemental Video 3.2 A video of the experimental set-up is available here:

<https://www.youtube.com/watch?v=4zBx27OoIRE&feature=youtu.be>

3.3 Results

Perspective > appearance > breathing: the hierarchy of perceived body ownership The multilevel mixed linear regression run on participants' subjective ratings of body ownership (see Section 3.2) showed three main effects: breathing, visual appearance, and spatial perspective, in ascending order of relative importance, as gauged through standardised regression coefficients (Darlington, 1990; cf. Johnson and LeBreton, 2004).

Specifically, across conditions, congruent breathing increased the ratings of body ownership by about 7.86 points (SE = 4.54) along a 0-100 visual analogue scale (VAS) relative to incongruent breathing trials, $\chi^2(1, N = 255) = 16.72, p < .001$. There was also a slightly greater effect of visual appearance, $\chi^2(1, N = 255) = 11.68, p < .001$, as congruent (human-like) appearance yielded an increase of 9.46 VAS points (SE = 4.66). Congruent perspective had an even stronger effect on perceived body ownership, $\chi^2(1, N = 255) = 151.29, p < .001$, resulting in an estimated increase of 37.55 VAS points (SE = 4.78) (Figure 3.3B).

The main effect of perspective was further qualified by an interaction with the interoceptive sensibility index (i_{sen}), $\chi^2(1, N = 255) = 12.22, p < .001$: for each 1-unit decrease in i_{sen} , the effect of perspective went up by about 11.86 points (SE = 7.97) (Figure 3.4A). A further interaction between perspective and the interoceptive accuracy index (i_{acc}), $\chi^2(1, N = 255) = 5.41, p = .02$, entailed that the effect of perspective went up by about 53.3 points (SE = 24.47) whenever i_{acc} decreased by 1-unit (Figure 3.4C). There was also an interaction between interoceptive accuracy and breathing, $\chi^2(1, N = 255) = 7.85, p = .005$ (Figure 3.4D), which produced a similar pattern: for each 1-unit decrease in i_{acc} , the effect of breathing increased by about 40.99 points (SE = 23.21).

Overall, the model had a marginal R^2 of 0.39 and a conditional R^2 of 0.75 (for details on i_{sen} and i_{acc} , see Section 3.2 above).

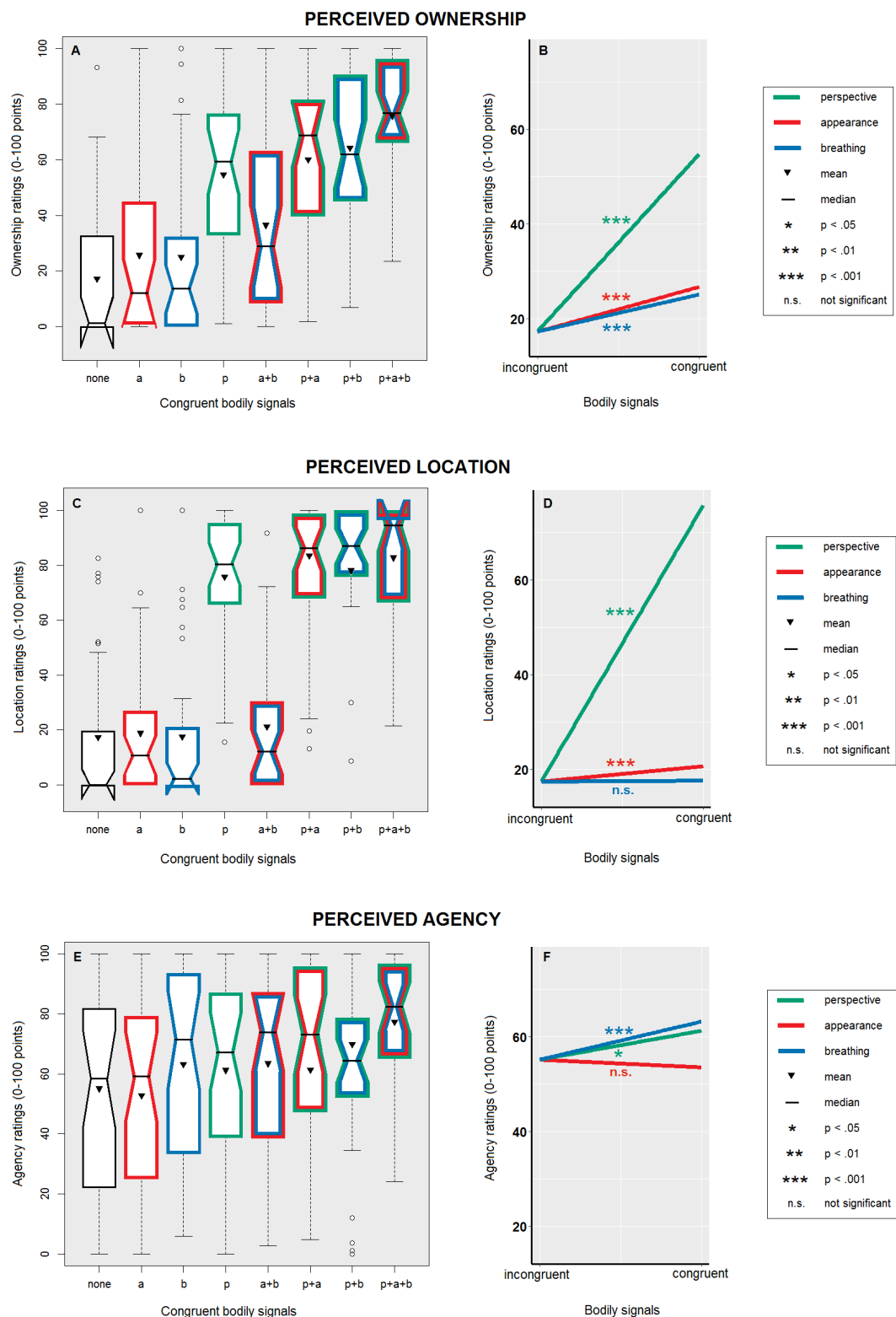


Figure 3.3. Congruency between real and virtual bodily signals impacts on feelings of body ownership (A-B), location (C-D) and agency (E-F). Left panels: boxplots of perceived ownership (A), location (C), and agency (E) ratings as a function of type of congruent bodily signals: appearance (a), breathing (b), perspective (p) and their combinations. Right panels: estimated effects of each bodily signal on the ratings of perceived ownership (B), location (D), and agency (F). Effects expressed as standardised regression coefficients (slopes) of the underlying linear mixed models. The steeper the slope, the greater the relative importance of a predictor (Darlington, 1990; cf. Johnson and LeBreton, 2004), i.e. the importance of a given bodily signal.

Perspective > appearance: the hierarchy of perceived location The multilevel mixed linear regression run on participants' subjective ratings of body location (see Section 3.2) revealed a main effect of appearance, $\chi^2(1, N = 255) = 12.42, p < .001$, which produced an estimated increase of 3.24 VAS points (SE = 2.58). However, a much greater contribution came from perspective, $\chi^2(1, N = 255) = 135.58, p < .001$, which increased location ratings by approximately 58.41 VAS points (SE = 5.66) (Figure 3.3D).

Furthermore, perspective interacted with the interoceptive sensibility index (i_{sen}), $\chi^2(1, N = 255) = 4.37, p = .036$: whenever i_{sen} values went down by 1-unit, the effect of perspective went up by 14.56 VAS points (SE = 9.43) (Figure 3.4B).

The model had a marginal R^2 of 0.64 and a conditional R^2 of 0.94.

Breathing > perspective: the hierarchy of perceived agency The multilevel mixed linear regression run on participants' subjective ratings of body agency (see Section 3.2) indicated a main effect of perspective, $\chi^2(1, N = 255) = 5.82, p = .016$, as congruency in perspective produced an increase by about 6.11 VAS points (SE = 5.36) in perceived body agency. This time, congruent breathing had a stronger main effect than perspective, $\chi^2(1, N = 255) = 13.63, p < .001$, since it boosted agency scores by about 8.05 points (SE = 4.93) (Figure 3.3F).

This main effect was qualified by an interaction with the interoceptive accuracy (i_{acc}) index, $\chi^2(1, N = 255) = 4.36, p = .037$: for each 1-unit decrease in i_{acc} , the effect of breathing increased by 15.62 VAS points (SE = 25.22) (Figure 3.4E).

The marginal R^2 of the model was 0.11, while the conditional R^2 of the model was 0.62.

Of note, there was no significant interaction ($p > .23$) between appearance, perspective, and breathing in any embodiment domain (perceived ownership, location and agency).

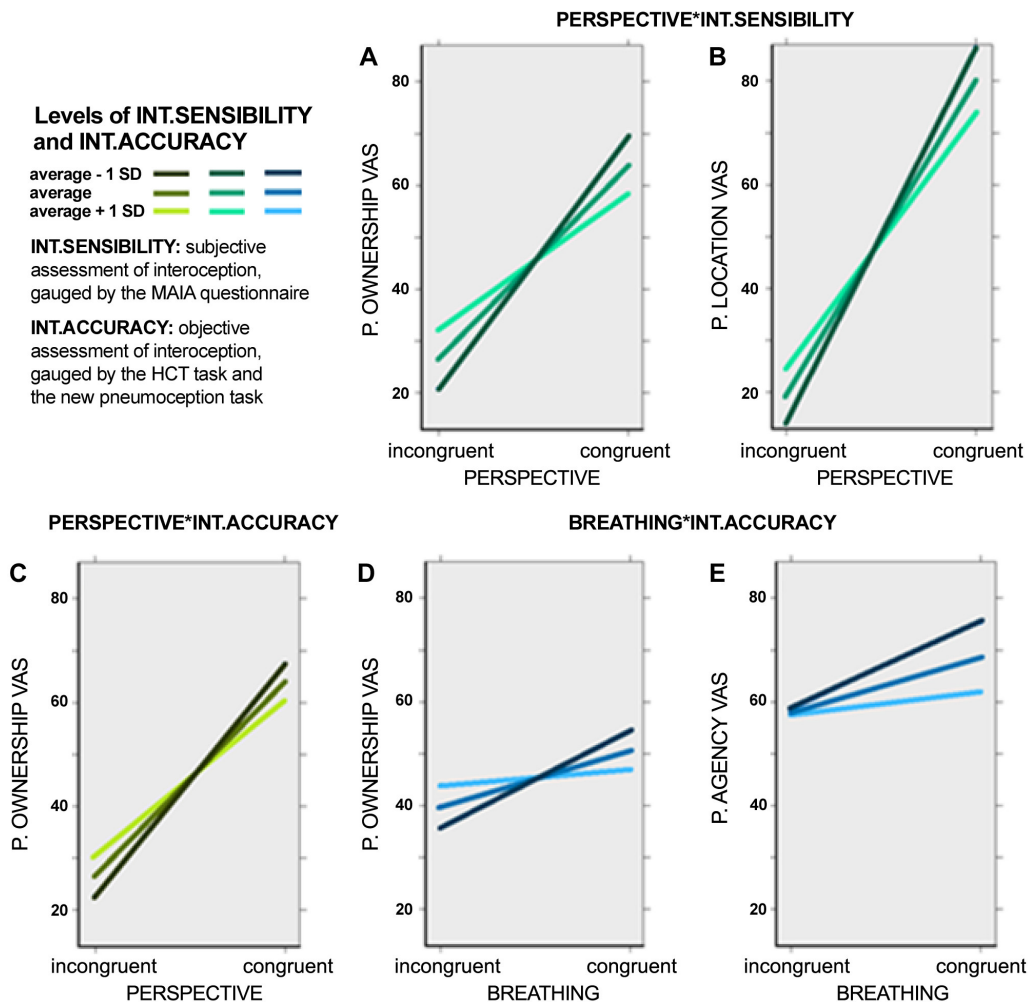


Figure 3.4. The effects of both visceral and non-visceral cues on corporeal awareness depend on the ability to perceive visceral signals, as measured through self-report questionnaires (interoceptive sensibility) and objective tests (interoceptive accuracy), including a new self-breathing discrimination test (pneumoception task). Interoceptive sensibility moderates the effects of perspective on ratings of perceived body ownership (A) and location (B). Interoceptive accuracy moderates the effects of perspective (C) and breathing (D) on perceived ownership, and the effect of breathing (E) on perceived agency. Overall, participants with lower interoception scores are more susceptible to the experimental manipulations. MAIA: Multidimensional Assessment of Interoceptive Awareness. HCT: Heartbeat Counting Task.

Congruency of bodily signals affects participants' breathing wave amplitude The multilevel mixed linear regression run on participants' breathing wave amplitude (see Section 3.2) showed a main effect of breathing, $\chi^2(1, N = 255) = 4.80, p = .028$: when the avatar breathed in phase with the real body, the amplitude of breathing waves had a 2.1 mm decrease (Figure 3.5B).

This latter main effect was moderated by visual appearance, which interacted with breathing, $\chi^2(1, N = 255) = 16.82, p < .001$: hence, the amplitude decreased by 1.7 mm when participants observed a 'wooden' in-phase avatar, and increased by 0.2 mm when the observed in-phase avatar had a 'human-like' appearance (Figure 3.5C). Furthermore, appearance interacted with perspective, $\chi^2(1, N = 255) = 9.16, p = .002$: thus, breathing amplitude decreased by 0.6 mm if there was a combination of congruent perspective and incongruent appearance, and increased by 0.7 mm if both appearance and perspective were congruent (Figure 3.5D).

Finally, there was a main effect of interoceptive accuracy, $\chi^2(1, N = 255) = 6.21, p = .013$: for each 1-point decrease in interoceptive accuracy, breathing wave amplitudes had an average 5.9 mm increase.

The model had a marginal R^2 of 0.15, while its conditional R^2 was 0.56.

Experimental controls Tests of statistical assumptions of linear mixed-effects models. For all linear mixed-effects models which were included in the final data analysis, visual inspection of residual plots did not reveal any obvious deviation from the standard assumptions of linearity, homoscedasticity, and normality of residuals. Condition indices of the matrix of the independent variables (Belsley et al., 1980) showed no collinearity problem (all indices < 30). DFBETAS values (Belsley et al., 1980; Nieuwenhuis et al., 2012) confirmed that there were no influential data points (all values < 2).

Specificity of experimental manipulations Figure 3.6 summarises the main descriptive statistics of VAS ratings for experimental and control questions. Since the notches of the boxes relative to the experimental questions never overlap with the

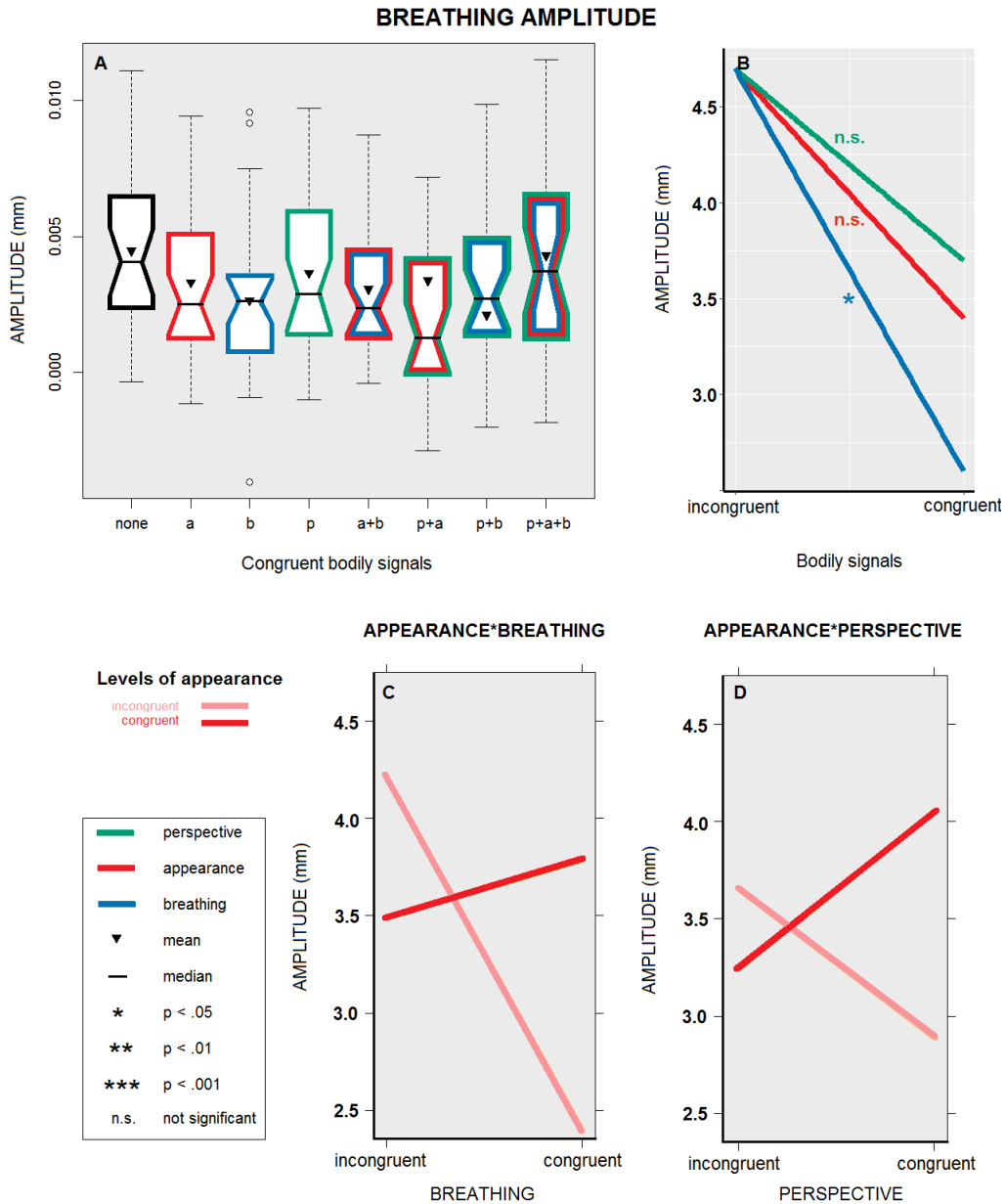


Figure 3.5. Boxplots representing the amplitude of participants' real breathing waves recorded in conditions 1-8 (A); estimated effect of perspective, appearance and breathing on the amplitude of participants' breathing waves (B); interaction plots showing how appearance (congruent vs incongruent) moderates the estimated effects of breathing (C) and perspective (D) on the amplitude of breathing waves.

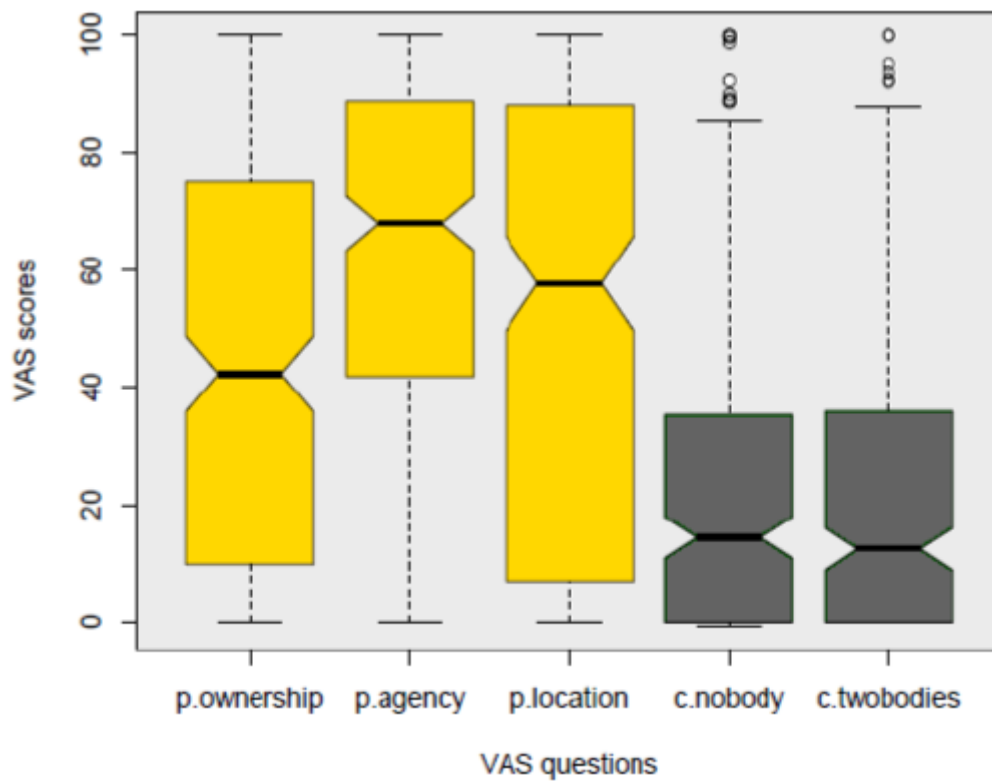


Figure 3.6. Boxplot of visual analogue scale (VAS) responses to experimental questions (yellow boxes) and control questions (grey boxes)

notches of the control questions boxes, there is strong evidence that the experimental medians differ from the control medians (McGill et al., 1978). Across conditions, the average perceived body ownership, agency, and location were 45.05 (SD = 34.44, range: 0-100), 63.13 (SD = 30.17, range: 0-100), and 49.54 (SD = 39.32, range: 0-100), respectively.

Interoception indices results *Multidimensional Assessment of Interoceptive Awareness (MAIA)*. The average scores of the three MAIA subscales of interest - noticing, attention regulation and body listening - were 3.12 (SD = 0.77, range: 1-4.75), 2.8 (SD = 0.75, range: 1.14-4), and 2.65 (SD = 0.9, range: 0.33-4.67), respectively.

Heartbeat counting task. The average interoceptive sensitivity (IS) score was 0.64 (SD = 0.16, range: 0.27-0.89). Metacognitive judgments of performance had a mean

condition	frequency		amplitude		correlation		
	mean	SD	mean	SD	r	df	p
<i>baseline</i>	16.34	3.29	4.67	2.7	-0.35	29	.048
1	-3.3	4.53	4.48	3.06	-0.53	26	.003
2	-3.1	3.72	2.64	2.83	-0.38	29	.037
3	-3.25	3.90	3.65	3.08	-0.45	27	.014
4	-2.86	4.49	2.13	2.68	-0.44	28	.016
5	-2.89	4.42	3.31	2.87	-0.48	28	.008
6	-2.8	4.00	3.07	2.43	-0.57	29	< .001
7	-3.89	4.24	3.38	2.79	-0.50	26	.007
8	-3.69	4.70	4.31	3.44	-0.60	28	< .001

Table 3.3. Respiratory rates, respiratory depths and their correlation at baseline and in each condition. Frequency: participants' respiratory rate (breaths per minute). Amplitude: participants' respiratory depth (millimetres). Correlation: Pearson's product-moment correlation (r) between respiratory rate and depth at baseline and in each condition.

value of 66.55 (SD = 18.89, range: 33.2-96.98). As expected, metacognition did not significantly correlate with IS, $r(30) = .04$, $p = .82$.

Interoceptive accuracy and sensibility scores. The average i_{acc} and i_{sen} scores were 0.58 (SD 176 = 0.21, range: 0.17-0.88) and 2.86 (SD = 0.64, range: 0.92-3.83), respectively.

Breathing sensor data Table 3.3 describes the respiratory rates and depths which were recorded at baseline and in each experimental condition; as expected, depths and rates were always egatively correlated, ($p < .05$ in all cases).

Data availability Data are available on the Open Science Framework at this link: https://osf.io/9k56a/?view_only=06dd2964c5bf4a109443708885c31930

3.4 Discussion

Recent theoretical models and experiments suggest that physiological signals are optimally mapped in the brain not only to maintain homeostasis (Barrett and Simmons, 2015; Iodice et al., 2019), but also to exert a multifaceted influence on

self-consciousness (Craig, 2002, 2009; Critchley and Harrison, 2013; Herbert and Pollatos, 2012; Park and Tallon-Baudry, 2014).

A few studies investigated whether participants were more likely to deem an image of a whole body or a body part as theirs when this image artificially flashed in sync with their heartbeat (Aspell et al., 2013; Porciello et al., 2016; Suzuki et al., 2013) or with their breathing (Adler et al., 2014; Allard et al., 2017). However, virtual body flashing may lack ecological validity, because such a condition never occurs in real life, and hence, strictly speaking, cannot reveal the proper contribute of physiological signals to corporeal awareness in ordinary circumstances (see Porciello et al., 2018). In addition to that, flashing whole-body images were always observed from a third-person perspective, making it impossible to assess if their effect holds also in a normal, first-person perspective. This can explain why breath-locked flashing does not consistently increase the perceived ownership of the flashing body silhouette (Adler et al., 2014; Allard et al., 2017).

Other studies used nose breathing (Watanabe et al., 2004) or a tension sensor (Czub and Kowal, 2019) to inflate and deflate avatars, but did not estimate the effect of breathing on corporeal awareness. Thus, to our knowledge, the present paradigm is the first to both manipulate a physiological signal in an ecological fashion and measure its impact on the sense of having a body, controlling its movements, and dwelling in it.

In contrast with classic embodiment and enfacement paradigms, breathing can be conceived as a form of continuous self-stimulation – a natural counterpart to the artificial kinds of transient visuo-tactile stimulation which have been employed so far. Breathing ceaselessly stimulates the body, producing both an inner sensation and a visible change such as an inflation of the trunk, driven by active contraction of inspiratory pump muscles, or a deflation of the trunk, due to a passive expiratory phase (Del Negro et al., 2018). By capitalising on this natural, continuous alignment of sensory cues, our embreathment bodily illusion reveals the unique contribution of breathing to corporeal awareness.

That congruent breathing increases the sensation of owning the virtual body fits well with theories which posit that physiological signals play a crucial role in giving rise to human self-consciousness (Craig, 2009; Critchley and Harrison, 2013; Herbert and Pollatos, 2012; Park and Tallon-Baudry, 2014). Furthermore, this finding confirms that congruency between expected and actual bodily signals is a general mechanism to ground the feeling that a body belongs to someone – a mechanism which applies not only to visual, tactile, and cardiac signals, but also to respiratory cues.

Congruent breathing also increased the sensation of controlling the movements of the avatar. The observed boost in agency ratings extends the finding that when the outcome of a voluntary, occasional action is consistent with expectations the sense of agency goes up (Sato and Yasuda, 2005; Villa et al., 2018). Here, we demonstrate that the same link between agency and outcome holds true even when dealing with a semi-voluntary, continuous action like breathing. If the belly inflates during inhalation and deflates during exhalation, expectations match with the outcomes, and agency ratings increase accordingly; whereas if breathing in yields the outcome one would expect when breathing out, and vice versa, the sense of agency declines – regardless of the fact that the participant is always the only effective cause of the movements of the avatar. Our data imply that spontaneous actions, which are under limited voluntary control and serve a built-in purpose, induce a strong feeling of agency if appropriately mapped onto a virtual body.

Based on the analysis of standardised regression coefficients (Darlington, 1990; Johnson and Lebreton, 2004), we also show that there is a hierarchy in the relative importance of body-related signals leading to corporeal awareness; moreover, the hierarchy changes according to the facet of corporeal awareness we take into consideration (i.e., feelings of ownership, agency and location of the body).

Our findings pave the way for a comprehensive model of corporeal awareness, complementing previous accounts which were concerned with a specific body part, a specific aspect of embodiment, or a specific set of sensory modalities (Blanke et

al., 2015; Pritchard et al., 2016; Seth, 2013; Tsakiris, 2010). On the one hand, we confirm on quantitative grounds the intuition lying behind some of those accounts, namely, that perspective is key to corporeal awareness (Maselli and Slater, 2013; Petkova et al., 2011), affecting all its facets. On the other hand, we reveal for the first time the true extent of the influence that breathing bears on embodiment: indeed, breathing contributes to the perceived body ownership nearly as much as the appearance of the body (figure 2B) and shapes the sense of bodily agency even more than perspective (figure 2F).

At the same time, contrary to what some neurocognitive models predict (Blanke et al., 2015; Tsakiris, 2010), visual appearance does not act as a major constraint on embodiment. Indeed, appearance ranks second as an ownership-inducing factor, has only a minor role in defining perceived location, and bears no influence on the sense of agency. This seems at odds with previous findings in a virtual rubber hand illusion paradigm, where the form of the hand was the leading force inducing hand embodiment across all domains and perspective changes affected only the perceived location (Pritchard et al., 2016). However, a local, transient feeling like the embodiment of a virtual hand is qualitatively distinct from a global, steady sensation of corporeal awareness, like the one induced by our embreathment illusion. As a consequence, body-part and whole-body embodiment likely rely on bodily signals combined according to different behavioural laws (David et al., 2014; Metzinger, 2004).

That appearance does not constrain embodiment is also underscored by the fact that there is no significant interaction between appearance, perspective, and breathing. This, in turn, entails that visual, spatial and respiratory signals have a purely additive effect on ratings of ownership, agency, and location – i.e. the combined effect of these signals is equal to the sum of their individual effects. As a consequence, perceived ownership is an additive combination of perspective, appearance, and breathing; perceived agency is an additive combination of breathing and perspective; and perceived location is an additive combination of perspective

and appearance.

This implies that corporeal awareness is based on a mild form of multisensory integration: had a strong integration obtained, the effect of a congruent sensory input should have been facilitated by the concurrent presence of another congruent sensory input – for example, the effect of seeing a body with congruent appearance should have been stronger when that body was seen from a first-person perspective. However, such cases never occur. Yet increasing the number of congruent sensory channels generally boosts feelings of ownership, agency, and (to a lesser extent) location, entailing that embodiment is higher when multiple senses are consistent with each other (figure 2A, 2C, 2E).

Of note, breathing itself is a multisensory process, since it provides the brain with exteroceptive, proprioceptive and interoceptive feedback. Indeed, breaths produce a visible deflation and inflation of the trunk, as well as a peculiar sound; at the same time, they can trigger a cascade of afferent cues (Davenport and Vovk, 2009; Del Negro et al., 2018) from respiratory tract/muscle mechanoreceptors (Adriaensen et al., 2003; Adrian, 1933; Brouns et al., 2006; Road, 1990; Widdicombe, 1982), carotid body chemoreceptors (de Castro, 1926; Heymans and Heymans, 1927; Kumar and Prabhakar, 2012), lung nociceptors (Adriaensen and Timmermans, 2011; Nassenstein et al., 2010; Yu et al., 2007) and nasal thermoreceptors (Sozansky and Houser, 2014; Zhao et al., 2011).

Since the embreathment illusion manipulates the live mapping of real breathing patterns onto a visible avatar, it chiefly taps into the (mis)alignment of the ‘exteroceptive’ and ‘proprioceptive’ components of breathing. However, the ‘interoceptive’ component of respiration also plays a key role. Although there is currently no consensus on the criteria that uniquely define ‘interoceptive’ signals (Ceunen et al., 2016; Craig, 2014; Critchley and Garfinkel, 2017; Sherrington, 1906), here, in keeping with the influential work of Craig (2002), we construe interoception as a broad feeling of the physiological condition of the body, implemented by small-diameter $A\delta$ and C primary afferents. In this sense, the embreathment illusion taps also

into the (mis)alignment between what is seen in the virtual world and what is felt through interoceptive small-fibre afferents, i.e. breath-related chemoreceptors and thermoreceptors.

The importance of interoception in the embreathment illusion is further underscored by the finding that interoceptive accuracy and sensibility moderate the impact of breathing and perspective on specific facets of corporeal awareness (figure 3). This suggests that someone who has a sharper sense of internal states also has a more stable corporeal awareness and thus becomes less susceptible to bodily illusions – extending previous findings limited to the rubber hand illusion and to cardiac interoception (Tsakiris et al., 2011).

Of note, we assessed interoceptive accuracy combining a standard heartbeat tracking measure (Schandry, 1981) with a new ‘pneumoception’ task which measures the ability to discriminate one’s own breathing from another’s (supplementary material, section 1B). Given that cardiac interoception alone does not predict performance across other interoceptive domains like breathing (Garfinkel et al., 2016), our new method provides a more comprehensive assessment of interoceptive accuracy.

Further studies may clarify whether breathing amplitude can be considered an implicit marker of embodiment, along with skin conductance (Armel and Ramachandran, 2003; Tieri et al., 2015), temperature (Moseley et al., 2008; Tieri et al., 2017 - but see de Haan et al., 2017) and histamine reactivity (Barnsley et al., 2011).

Indeed, we unexpectedly found that the participants’ real breathing amplitude was modulated by individual differences in interoceptive accuracy, as well as by our experimental manipulations of corporal awareness. Specifically, higher accuracy in perceiving breaths and heartbeats reduced the amplitude of real breaths, possibly because superior interoceptive abilities allow to fine-tune the respiratory cycle without resorting to deep inspiration. Likewise, congruent breathing and congruent perspective decreased the average breath amplitude, provided that the avatar had an incongruent appearance. In these cases, too, it was probably less useful to make

deep inhalations, because congruent breathing or perspective cues made it easier to regulate the respiratory cycle, and perhaps also because real breaths had an impact on a wooden virtual body, which was not strongly felt as one's own (as shown by subjective ratings).

Furthermore, an incongruent appearance elicits a higher autonomic arousal (Tieri et al., 2017), which in turn increases the respiratory frequency (Boiten et al., 1994) and thus makes it harder to breathe deeply. In contrast with that, when the avatar combined a human-like appearance with a congruent breathing or perspective, the average breath amplitude increased: we speculate that this implicitly reflects the explicit increase in perceived ownership triggered by (less arousing) congruent multisensory stimuli.

To sum up, thanks to our embreathment illusion, we discover that breathing significantly impacts on the feelings of body ownership and agency that are core to subjective experience of self-consciousness. Results also indicate that there is a hierarchy of sensations leading to corporeal awareness, and that the hierarchy changes according to the facet of corporeal awareness we take into consideration. Perspective plays a role in every aspect of corporeal awareness; appearance influences ownership and location; breathing is especially important for agency, but shapes also the perceived ownership of the body. Finally, thanks to the analysis of participants' performance on a new self-breathing discrimination test, we show that the effects of both visceral and non-visceral cues on embodiment depend on the ability to perceive visceral signals. These findings unveil the key role of breathing in embodiment and lay the groundwork for a comprehensive model of corporeal awareness.

Limitations and future directions Our bodily illusion mapped only the most prominent movements induced by breathing, namely, belly movements. However, inhalation and exhalation slightly stretch the upper trunk as well. Future improvements in our motion tracking system will allow researchers to map this upper trunk stretch onto the avatar, resulting in a more thorough illusion. A complete motion

tracking system would also make it possible to map limb movements (which were not reproduced in our virtual setting) thus increasing the sense of presence in the virtual environment. At the present stage, we cannot completely rule out that a fully moveable avatar would increase both body agency ratings and the goodness of fit of our model. Nevertheless, we note that our participants were simply required to observe an avatar while lying on a deck chair at rest.

In a similar vein, although our avatars came in twenty possible sizes, and each participant freely choose the avatar they deemed as fittest, the visual appearance of the virtual body did not perfectly match the real body. A full body scanner would help to overcome this issue, and assess the proper impact of appearance on corporeal awareness more precisely. A more accurate match between real and virtual appearance would also make it easier to include females in future samples, due to sex differences in body image.

The work of Garfinkel and colleagues (2015) that characterised the concepts of interoceptive accuracy and sensibility used objective performance in heartbeat detection/mental tracking tasks as a proxy for accuracy, and the ‘awareness’ subscale of the Body Perception Questionnaire (BPQ) or average confidence in detection performance as a proxy for sensibility. Here, we decided to gauge interoceptive accuracy combining the standard heartbeat counting accuracy scores with our new pneumoception task. We did so in order to obtain a computationally simple but far-reaching measure that could gauge multiple interoceptive channels at the same time, in keeping with the broad definition of interoceptive accuracy as “objective accuracy in detecting internal bodily sensations (Garfinkel et al., 2015)”.

This also enables a closer parallelism between accuracy and sensibility, since questionnaire measures of sensibility sample a multimodal spectrum of interoceptive sensations. Indeed, both the ‘awareness’ subscale of the BPQ and MAIA simultaneously take into account cardiac, respiratory, and other visceral sensations. Future studies may try to use separate accuracy and sensibility indices for each interoceptive modality, although this would pose a challenge in terms of computational and

theoretical complexity.

Finally, future research might also develop embreathment-based feedback protocols to improve interoception or normalise breathing in patients who suffer from panic disorder (Jerath et al. 2015), anxiety (Nardi et al., 2009, Neumann et al., 2006), depression (Neumann et al., 2006) or depersonalisation/derealisation (Michal et al., 2013). Since in all these conditions breaths are irregular, patients immersed in virtual reality could receive a negative feedback on their virtual body whenever they deviate from a canonical pattern of breathing and a positive feedback whenever their inspiration and expiration fall within a healthy range.

Chapter 4

Experiment II: gastric embodiment

4.1 Introduction

If the contribution of thoracic organs to corporeal awareness has been scarcely elucidated so far, the role of deep, sub-diaphragmatic organs is completely unknown. This is largely due to the fact that the study of organs located in the abdominal cavity, such as the stomach and the intestine, is ordinarily performed with invasive techniques - techniques that are more fittingly applied to patients than healthy people, as benefits outweigh costs only for those who suffer from gastrointestinal disorders.

Indeed, the standard repertoire of gastrointestinal tests ranges from gastroscopy to colonoscopy, colonic manometry, anthroduodenal manometry, breath tests based on carbon isotopes (Delbende et al., 2000; Szarka et al., 2008) or lactulose (Wilberg et al., 1990), radiopaque markers (Hinton et al., 1969) and scintigraphy (Abell et al., 2008). However, some of these methods are inaccurate; others are accurate but invasive and limited in scope, as they can be applied only to specific segments of the gastrointestinal tract; and others still are both reliable and wide-ranging in scope, but are based on radioactivity (Lee, Erdogan, & Rao, 2014; Saad, 2016).

However, the past few years have witnessed the resurgence of a non-invasive, relatively powerful if long neglected technique - electrogastrography (EGG). First discovered by Alvarez (1922), EGG records the electrophysiological activity of a selected cluster of cells at the junction of the enteric nervous system with the stomach - the so-called interstitial cells of Cajal (ICC; Cajal, 1911). ICC act as pacemakers of stomach contractions by generating and propagating electric slow waves which have a normal frequency of 0.05 Hz, i.e. 3 cycles/minute (Al-Shboul, 2013; Huizinga and Lammers, 2009). Although the slow wave electrical signal obtained from EGG is relatively weak, an appropriate placement of recording electrodes and a suitable filtering procedure can make it more salient (Koch and Stern, 2003; Rebollo et al., 2018; Yin and Chen, 2013).

The basic function of slow wave-induced stomach contractions is to facilitate the absorption of nutrients and the downstream movement of gastric chyme (Yin and Chen, 2008). This intrinsic, spontaneous activity is modulated by top-down control exerted by central and enteric neurons (Furness et al. 2014); in turn, contractions are sensed by stretch receptors and relayed to the central nervous system via vagal afferents (cf. Umans and Liberles, 2008). While this loop has the clear homeostatic purpose of regulating food intake, we hypothesised that the information about stomach contractions, once in the brain, may also influence a variety of higher-order processes, including corporeal awareness.

Stomach contractions per se are rarely attended to or perceived at the conscious level; nevertheless, it may well be the case that ongoing stomach activity provides the brain with the kind of internal information which it needs to give us the normal, everyday sensation that our body is not empty – an essential if overlooked feature of corporeal awareness, which becomes apparent only when it breaks down in neurological and psychiatric disorders, as the Cotard’s syndrome (Berrios and Luque, 1995).

Hence, we capitalised on a simplified version of the new embreathment illusion (see above, [Chapter 2](#)) and measured the EGG dominant frequency at baseline and

in two experimental conditions, in which participants embodied two avatars which had a higher or lower resemblance to a human-like body. We hypothesised that the electrogastrographic signals recorded during the experimental conditions would predict the subjective feelings of embodiment, as assessed through a visual analogue scale (VAS) questionnaire, and that the effect would be possibly moderated by the baseline frequency.

4.2 Materials and methods

Participants Thirty-one healthy male volunteers aged 18-35 took part in the study. None of them suffered from neurological, psychiatric, or gastrointestinal (GI) disorders; none took drugs which could alter GI physiology (antihistamines, antacids, prokinetics, antiemetics, anticholinergics, laxatives, antidiarrhoeals, analgesics, proton pump inhibitors, non-steroidal anti-inflammatory drugs); and none had metallic implants which could interfere with the recording procedure, as assessed through a screening procedure. The study was approved by the Santa Lucia research hospital ethical committee and performed according to its guidelines.

Experimental procedure Participants arrived in the lab after an overnight fast and ate a standardised 260 kcal breakfast meal (120 g egg whites, two slices of bread, 30 g jam and 120 ml water) to ensure that food intake was equalised across subjects and did not act as a confounding factor. For the same reason, participants were required to abstain from alcohol and tobacco 24 and 8 hours before the experiment, respectively.

After breakfast, participants were required to remove abdominal body hair with a razor and shaving foam. An experimenter then cleaned their skin with an alcoholic solution to further reduce impedance and placed three disposable, pre-gelled Ag/AgCl electrodes on their abdomen: the first electrode was located halfway between the xiphoid process and the umbilicus; the second was 5 cm up and 45deg to the participants' left; and the third (ground) electrode was on the left costal

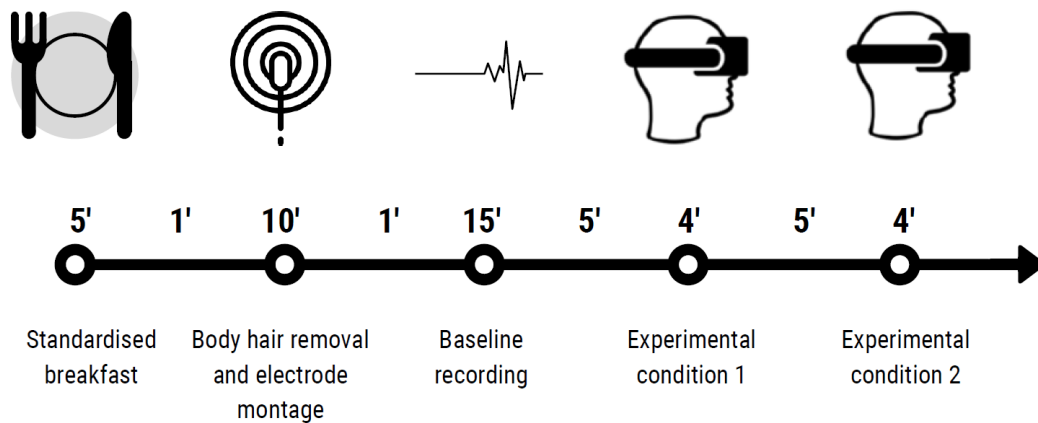


Figure 4.1. Timeline of experiment II.

margin horizontal to the first (Yin and Chen, 2013).

Electrical signals thus recorded were then relayed to an ADInstruments Power Lab data acquisition hardware (sampling frequency: 1000 Hz) in three different periods. First, subjects underwent an initial baseline phase (15') in which they lay at rest; then, they began the immersive virtual reality experience, which consisted of the experimental conditions 1 and 8 of the embreathment illusion described in [Chapter 2](#) – a ‘congruent’ first-person condition in which the participant saw an avatar which had a human-like appearance and breathed in phase with the real body and an ‘incongruent’ third-person condition in which the avatar was wooden and had an antiphase respiratory pattern. At the end of each condition, participants rated how much they felt embodied in the virtual avatar through a standard 5-item embodiment questionnaire (see above, Table 3.1) Conditions were counterbalanced across subjects and interspersed with 5' washout pauses to avoid carryover effects (Figure 4.1).

Data analysis The raw electrogastrographic recordings were visually inspected to remove artifacts due to body movements. A 0.016-0.15 Hz bandpass filter removed pink noise and unwanted higher frequencies that are ordinarily associated with cardiac, respiratory and small bowel activity (cf. Koch and Stern, 2003). The artifact-free tracings thus obtained (Figure 4.2) were then used to extract the EGG

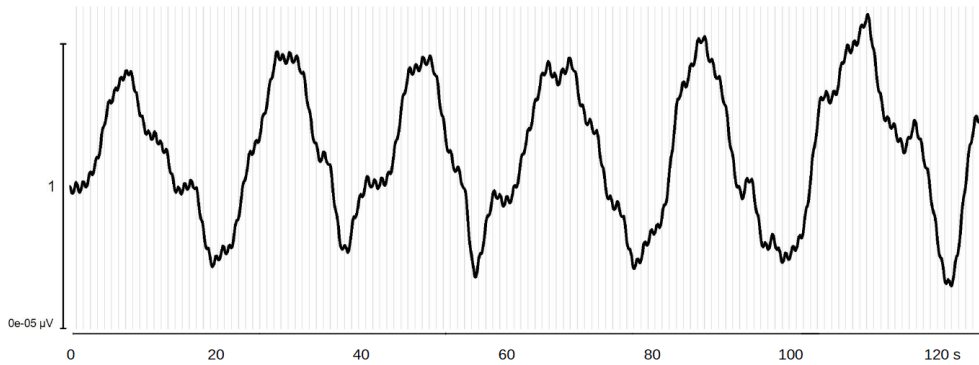


Figure 4.2. Example of an artifact-free, bandpass-filtered electrogastrographic recording on a 120 s period.

peak frequency for each subject and experimental condition. EGG spectral density was computed using Welch’s method (Welch, 1967) on 200 s time windows with 150 s overlap (Rebollo et al., 2018). EGG peak frequency (Figure 4.3) was defined as the maximum periodogram peak in the ‘normogastric’ range, i.e. the range of frequencies which is compatible with the number of stomach contractions in healthy individuals (0.033–0.066 Hz \sim 2-4 cycles per minute; cf. Rebollo et al. 2018). The whole EGG analysis procedure was performed with BrainVision Analyzer (Brain Products GmbH) and the MATLAB FieldTrip toolbox (Oostenveld et al. 2011).

As in Experiment I, the R software and the R lme4 package (Bates et al., 2015) were used to perform a linear mixed-effects analysis of the data. In particular, we modelled how much ratings of perceived body ownership, agency, and location changed depending on the experimental conditions as well as on the EGG values recorded at baseline and in each condition. The dependent variables were the VAS ratings of perceived body ownership, perceived body agency, and perceived body location, respectively. As fixed effects, all models had the experimental *condition*, i.e. human-avatar sensory congruency (two levels: congruent and incongruent), the baseline EGG peak frequency *EGGbase* (continuous) and the condition-specific EGG peak frequency *EGGcond* (continuous). These fixed effects were tested for interactions with each other. As random effects, the models included by-subject

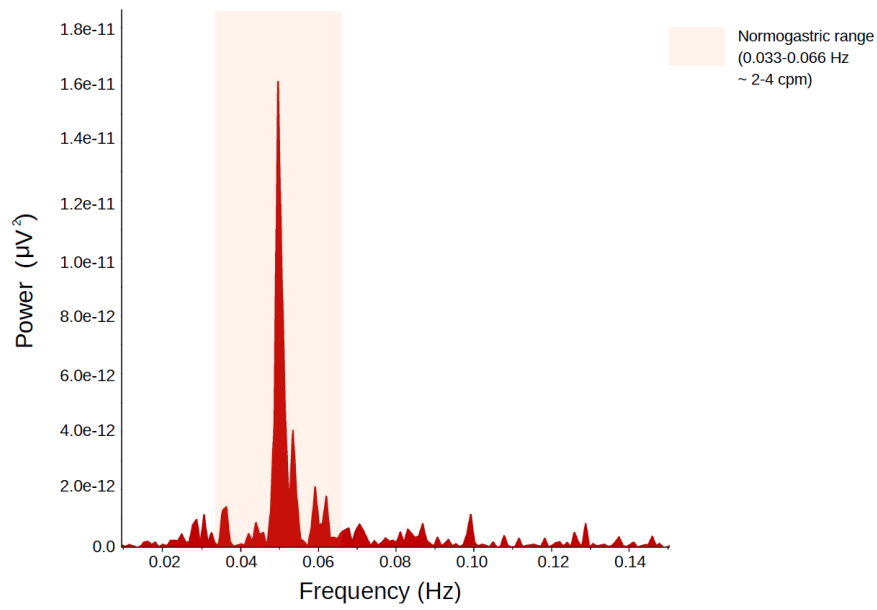


Figure 4.3. Example of spectral density estimate (periodogram) of an EGG signal with its peak frequency in the normogastric range.

intercepts. Hence, each mixed model was specified as follows:

$$p.ownership \sim EGGbase * EGGcond * condition + (1|subj)$$

$$p.agency \sim EGGbase * EGGcond * condition + (1|subj)$$

$$p.location \sim EGGbase * EGGcond * condition + (1|subj)$$

Finally, we tested whether the condition-specific EGG peak frequency changed as a function of each experimental condition and of the baseline frequency, adding by-subject intercepts as in the previous models:

$$EGGcond \sim EGGbase * condition + (1|subj)$$

As in Experiment I, we used the Anova function of the R car package (Fox and Weisberg, 2011) to compute p-values through Type II Wald chi-square tests.

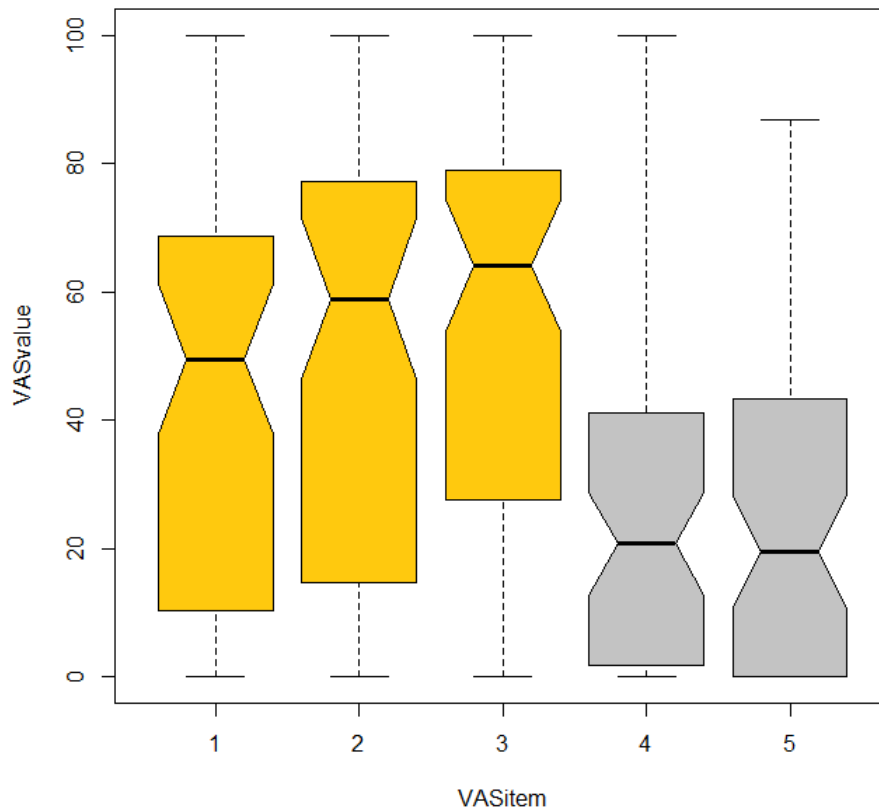


Figure 4.4. Median values for each item of the VAS embodiment questionnaire. Since the notches of the boxes of experimental items (yellow) do not overlap with the notches of the boxes of control items (grey), there is strong evidence that the median values are significantly different (Mc Gill et al., 1978; cf. Section 3.3). For numbers 1-5, cf. Table 3.1.

4.3 Results

Manipulation check and manipulation effects Median values of the experimental items in the VAS embodiment questionnaire were significantly higher than median values of control items, as shown by notched boxplots (Figure 4.4). For that reason, we did not further analyse control items and focused on the three experimental constructs, i.e. perceived body ownership, agency, and location.

The experimental manipulation proper, i.e. the change of degree in human-avatar sensory congruency, was successful, as shown by the multilevel linear mixed models

(see above, Section 4.2). On average, ratings of perceived body ownership were 48.95 ± 4.44 points higher on a 0-100 VAS scale in the congruent condition than in the incongruent condition, $\chi^2(1, N = 47) = 151.50, p < .001$. Likewise, in the congruent condition ratings of perceived body agency increased by 25.85 ± 6.99 points relative to the incongruent condition, $\chi^2(1, N = 47) = 21.89, p < .001$. Finally, also the perceived body location gauged in the congruent condition went up by 35.97 ± 6.49 points with respect to the incongruent condition, $\chi^2(1, N = 47) = 38.10, p < .001$.

Gastric effects on corporeal awareness The multilevel linear mixed model on perceived body ownership (see above, Section 4.2) indicated that the higher the EGG peak frequency recorded during the experimental manipulation, the stronger the sensation that the virtual body belongs to the participant. Specifically, every time the peak frequency increases by 0.01 Hz the rating of perceived body ownership increases by 5.5 ± 7.8 points, $\chi^2(1, N = 47) = 17.90, p < .001$ (Figure 4.5). The interaction between this effect and the effect of condition described in the previous paragraph did not reach the statistical significance threshold, $\chi^2(1, N = 47) = 3.04, p = .08131$.

EGG peak frequency specifically predicted ratings of perceived body ownership, as neither the sense of body agency nor the sense of body location were affected by gastric activity ($\chi^2(1, N = 47) = 0.60, p = .4395$ and $\chi^2(1, N = 47) = 0.61, p = .4342$, respectively).

Baseline EGG influences condition-specific EGG peak frequency The multilevel linear mixed model on condition-specific EGG peak frequencies (see above, Section 4.2) showed that the baseline peak value is related to values recorded during the experimental manipulation, as for each 0.1 Hz increase in the baseline peak there is a 0.056 Hz increase in the condition peak, $\chi^2(1, N = 47) = 5.23, p = .02215$. This main effect is generalised across conditions, as there is no *EGGbase : condition* interaction, $\chi^2(1, N = 47) = 0.50, p = .47828$.

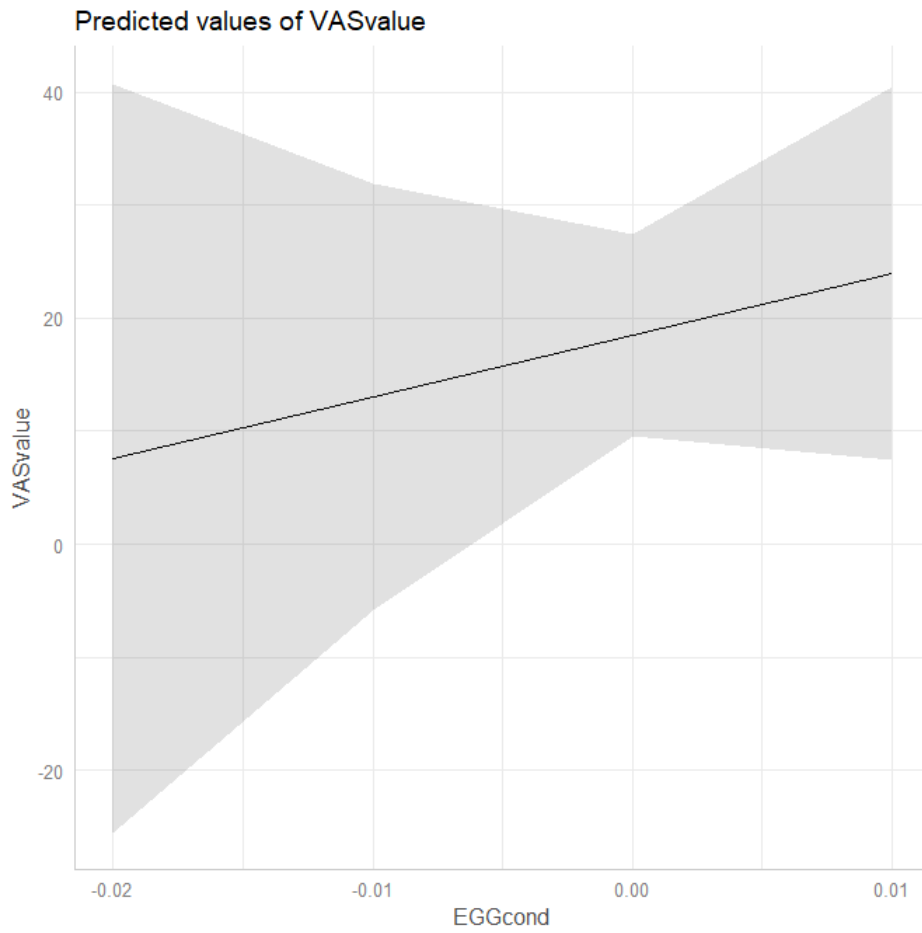


Figure 4.5. Predicted ratings of perceived body ownership as a function of electrogastrographic (EGG) peak frequency.

4.4 Discussion

Here, we report the first evidence of a role of gastric activity in corporeal awareness, as tested in a virtual reality paradigm that specifically manipulated embodiment in a controlled manner. In particular, the higher the EGG peak frequency, the more the experimental subjects felt that the virtual body belonged to them. The activity of the stomach, as mapped by EGG, had a selective effect on the sense of body ownership, while it did not influence the ratings of perceived body location and agency.

Our findings suggest that the central nervous system relies also on physiological information coming from the deep visceral periphery to tell us that our body is indeed ours. This implies that corporeal awareness is based upon multisensory integration processes whose scope is even wider than previously thought, gathering a wealth of sensory information from abdominal viscera as well as from thoracic organs and from skin receptors. Such a diverse range of sensory inputs probably helps the brain to maintain a ‘body template’ in a variety of circumstances, including those in which a particular sensory channel may be temporarily or permanently shut down, as in darkness, blindness or spinal cord injuries.

A remarkable feature of the gastric contribution to corporeal awareness is the fact that it follows the same pattern of other physiological signals which act as sources of embodiment, like skin conductance (Armel and Ramachandran, 2003; Tieri et al., 2015), medium-term temperature (Tieri et al., 2017), histamine reactivity (Barnsley et al. 2011) and, as we saw in Chapter 3, breathing amplitude: in all these cases, higher embodiment ratings are associated with an increased physiological activation. More studies are needed to further elucidate this general trend and clarify whether it is physiology to boost the sense of ownership originally induced by congruent visuo-tactile information, or vice versa.

A previous study by Rebollo and colleagues (2018) advanced the tantalising hypothesis that a resting-state ‘gastric network’ of cerebral areas phase-coupled

with the EGG slow gastric wave had the function of coordinating different ‘body-centered maps’ in the brain. This hypothesis entails that the insular cortex should be strongly involved in the network, since the insula receives direct input from the stomach and is thought to integrate visceral and non-visceral inputs to form a coherent representation of the whole body (Craig, 2009; Critchley and Harrison, 2013). However, contrary to this interpretation, Rebollo and coworkers found that the insula was only marginally synchronised to the rhythm of the stomach.

Thus, we have recently suggested that the gastric network may rather act as a homeostatic regulator of food intake (Porciello et al., 2018). Indeed, the network neatly overlaps with areas processing information from the face, mouth and hands, and with three brain regions activated by tongue- or hand-related actions (Amiez and Petrides, 2014). In order to clarify the exact function of the gastric network, it would be interesting to test whether our embodiment task activates the same nodes of the resting-state gastric network or a subset of the network, or even a superset including the insular cortex.

Chapter 5

Experiment III: gastric emotional awareness

5.1 Introduction

Corporeal awareness is often thought as a basic, minimal form of selfhood (Blanke and Metzinger, 2009), in contrast with the more complex and evolutionarily recent *emotional awareness*, i.e. the ability to recognise self- and other-generated emotions. However, visceral physiological signals may play a role in both forms of awareness. Historically, case studies of patients with gastric disorders, and gastric fistulas in particular, provided evidence on the link between gastric activity and emotions (Wolf, 1981). More recently, electrogastrographic (EGG) recordings obtained in healthy subjects showed that the stomach electrical slow wave indexes emotional arousal (Vianna and Tranel, 2006), is positively correlated with core disgust (Harrison et al., 2010) and negatively correlated with vivid emotion imagery (Vianna et al., 2009).

Here, we sought to determine whether the electrical activity of the stomach correlates with the conscious perception of discrete emotions, including not only disgust but also fear, sadness, and happiness. Thus, we used validated film clips to test whether the EGG baseline- and condition-specific peak frequency predicted explicit ratings of emotion intensity for one or more discrete emotions. While

we expected to find a high degree of correlation between EGG markers and the perception of disgust, as in previous studies, we also sought to determine whether the stomach plays a role also in other negative emotions, as fear and sadness.

5.2 Materials and methods

Participants The same thirty-one subjects who participated in experiment II took part also in this experiment. For further details, please see Section 4.2.

Experimental procedure After completing experiment II and having enjoyed a break, participants kept their abdominal EGG montage (see Section 4.2), lay supine on a deck chair and watched five sequences of short emotional video clips projected on a computer monitor in counterbalanced order. Four sequences consisted of 23 clips lasting 9 seconds each, designed to elicit a specific emotion (disgust, fear, happiness, sadness), while a fifth control sequence contained 23 emotionally neutral clips. All $23 \times 5 = 115$ videos were taken from a corpus of emotional stimuli which had been previously described and validated (Tettamanti et al., 2012). At the end of each sequence, subjects completed a 9-item questionnaire, indicating the intensity of the emotions and feelings they perceived while watching the clips on a visual analogue scale (VAS) ranging from ‘not at all’ (lowest possible intensity) to ‘very much’ (highest possible intensity). Sequences were separated by 2’ washout pauses. Table 5.1 lists the questionnaire items, while Figure 5.1 depicts the timeline of the experiment.

Data analysis As in experiments I and II, we relied on the R software and the R lme4 package (Bates et al., 2015) to perform a linear mixed-effects analysis of the data. Specifically, we modelled how much ratings of the perceived emotions and feelings listed in Table 5.1 changed depending on the experimental conditions as well as on the EGG values recorded at baseline and in each condition. The dependent variables were the VAS ratings of each emotion or feeling included in

it.	construct	question
1	<i>disgust</i>	How much disgust did you feel?
2	<i>happiness</i>	How much happiness did you feel?
3	<i>sadness</i>	How much sadness did you feel?
4	<i>fear</i>	How much fear did you feel?
5	<i>immorality</i>	How immoral did you deem the actions represented in the clips?
6	<i>arousal</i>	While you watched the clips you felt...(bored/aroused)
7	<i>gastric f.</i>	Did you feel nausea, stomach contractions, or other GI movements?
8	<i>resp f.</i>	Did you feel your breath changed?
9	<i>cardiac f.</i>	Did you feel your heartbeat changed?

Table 5.1. Visual analogue scale (VAS) questionnaire on emotions and feelings perceived in each sequence of video clips (abridged translation from Italian). Please note that questionnaire instructions specifically asked the participant to rate emotions and feelings that were aroused by that sequence in particular. it.: item. resp: respiratory. f.: feelings. GI: gastrointestinal.

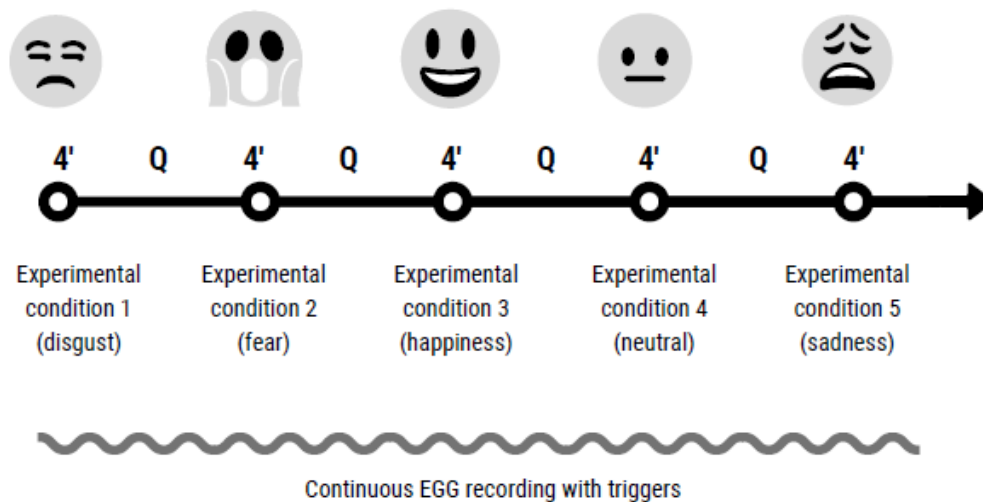


Figure 5.1. Timeline of experiment III. Q: inter-sequence intervals in which the VAS questionnaires relative to each preceding sequence were filled.

the questionnaire. As fixed effects, all models had the experimental *condition*, i.e. the type of video clips (five levels: disgusting, happy, fearful, sad, and neutral), the baseline EGG peak frequency *EGGbase* (continuous) and the condition-specific EGG peak frequency *EGGcond* (continuous). These fixed effects were tested for interactions with each other. As random effects, the models included by-subject intercepts. Hence, each mixed model was specified as follows:

$$\begin{aligned} \textit{disgust} &\sim \textit{EGGbase} * \textit{EGGcond} * \textit{condition} + (1|\textit{subj}) \\ \textit{happiness} &\sim \textit{EGGbase} * \textit{EGGcond} * \textit{condition} + (1|\textit{subj}) \\ \textit{sadness} &\sim \textit{EGGbase} * \textit{EGGcond} * \textit{condition} + (1|\textit{subj}) \\ \textit{fear} &\sim \textit{EGGbase} * \textit{EGGcond} * \textit{condition} + (1|\textit{subj}) \\ \textit{immorality} &\sim \textit{EGGbase} * \textit{EGGcond} * \textit{condition} + (1|\textit{subj}) \\ \textit{arousal} &\sim \textit{EGGbase} * \textit{EGGcond} * \textit{condition} + (1|\textit{subj}) \\ \textit{gastric} &\sim \textit{EGGbase} * \textit{EGGcond} * \textit{condition} + (1|\textit{subj}) \\ \textit{resp} &\sim \textit{EGGbase} * \textit{EGGcond} * \textit{condition} + (1|\textit{subj}) \\ \textit{cardiac} &\sim \textit{EGGbase} * \textit{EGGcond} * \textit{condition} + (1|\textit{subj}) \end{aligned}$$

Finally, we tested whether the condition-specific EGG peak frequency changed as a function of each experimental condition and of the baseline frequency, specifying by-subject intercepts as in the previous models:

$$\textit{EGGcond} \sim \textit{EGGbase} * \textit{condition} + (1|\textit{subj})$$

As in Experiment I, we used the Anova function of the R car package (Fox and Weisberg, 2011) to compute p-values through Type II Wald chi-square tests. Post-hoc tests were performed with the R package emmeans, using Tukey's method for comparing a family of 5 estimates.

5.3 Results

Manipulation check and condition effects The multilevel linear mixed-models analysis (see above) confirmed that the experimental manipulation managed to induce the desired emotions. There was a main effect of condition on VAS ratings of disgust ($\chi^2(1, N = 110) = 176.85, p < .001$), happiness ($\chi^2(1, N = 110) = 208.67, p < .001$), sadness ($\chi^2(1, N = 110) = 126.25, p < .001$), and fear ($\chi^2(1, N = 110) = 84.19, p < .001$). More specifically, subsequent post-hoc tests revealed that, on average, disgusting videos induced from 31.89 to 54.20 more VAS disgust points than all other clips (all $p < .001$, Figure 5.2). For their part, fearful videos induced from 12.19 to 30.47 more VAS fear points than all other clips (all $p < .001$ except the fear vs. disgust contrast, $p = .132$, figure 5.3), happy videos induced from 40.74 to 59.30 more VAS happiness points than all other clips (all $p < .001$, Figure 5.4) and sad videos induced from 30.82 to 47.88 more VAS sadness points than all other clips (all $p < .001$, Figure 5.5). As expected, neutral videos did not elicit any particular emotion, confirming their reliability as a control sequence (Figures 5.2-5.5, all panels).

Gastric effects on perceived disgust The two-way interaction between EGG baseline and condition-specific peak frequencies predicts the subjective ratings of disgust, $\chi^2(1, N = 110) = 5.77, p = .01628$: the higher the EGG frequency during the experimental manipulation, the higher the disgust felt by participants, provided that the EGG baseline frequency is either average or above average values (Figure 5.6).

Gastric effects on perceived sadness The three-way interaction between EGG baseline peak frequency, EGG condition-specific peak frequency and experimental condition predicts the subjective ratings of sadness, $\chi^2(1, N = 110) = 11.97, p = .01756$: the higher the peak frequency during the experiment, the lower the sadness that the participants felt while watching sad and disgusting videos, provided that

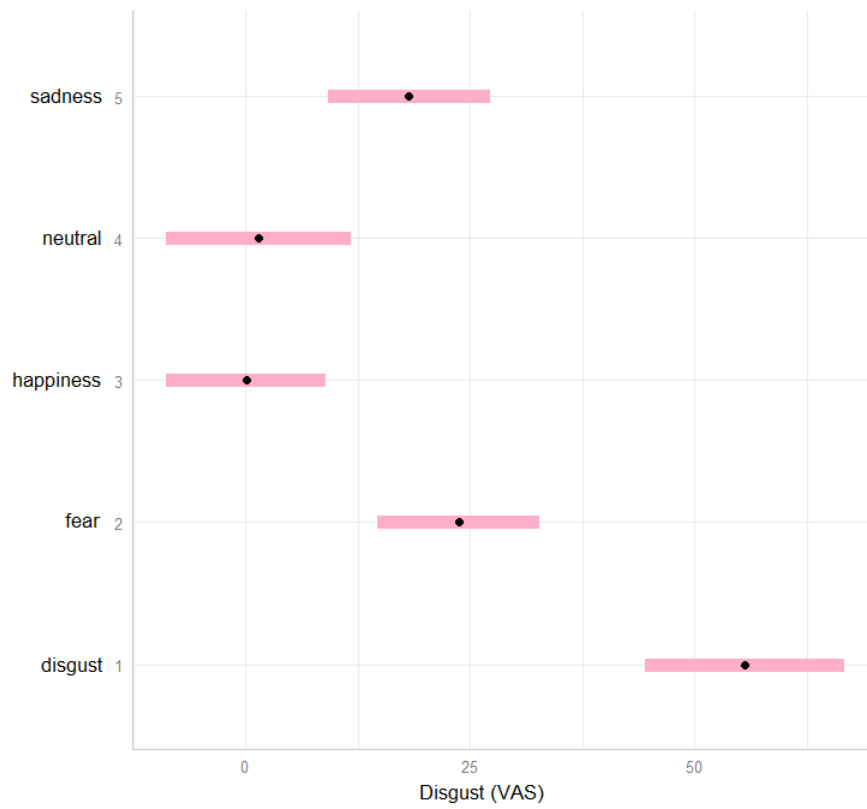


Figure 5.2. Estimated marginal means for disgust ratings in the five experimental conditions: disgust (1), fear (2), happiness (3), neutral (4) and sadness (5).

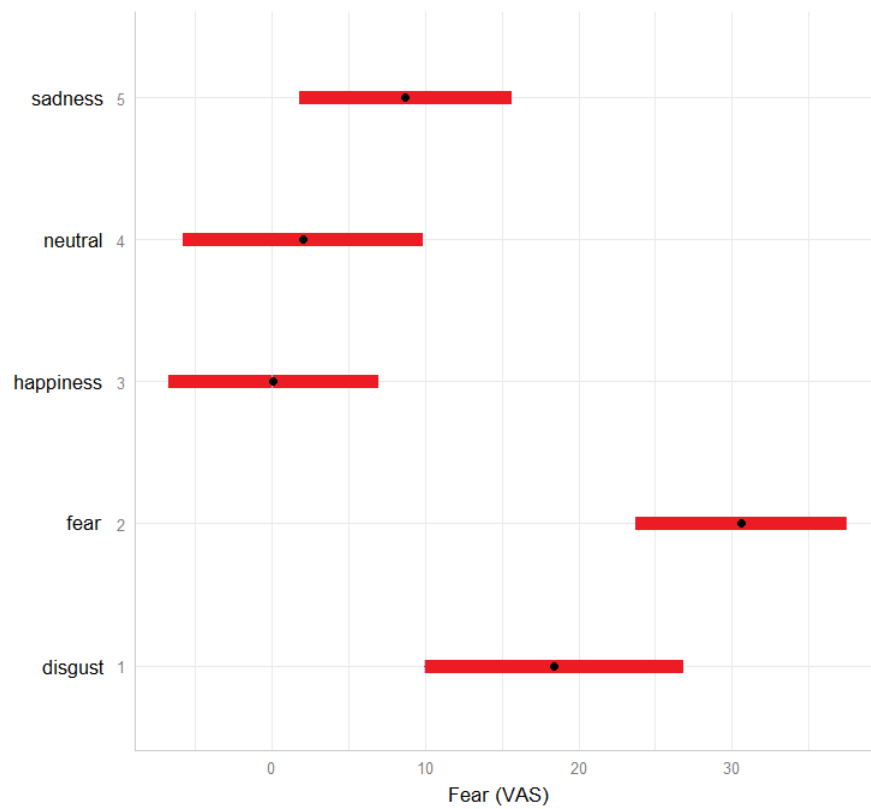


Figure 5.3. Estimated marginal means for fear ratings in the five experimental conditions: disgust (1), fear (2), happiness (3), neutral (4) and sadness (5).

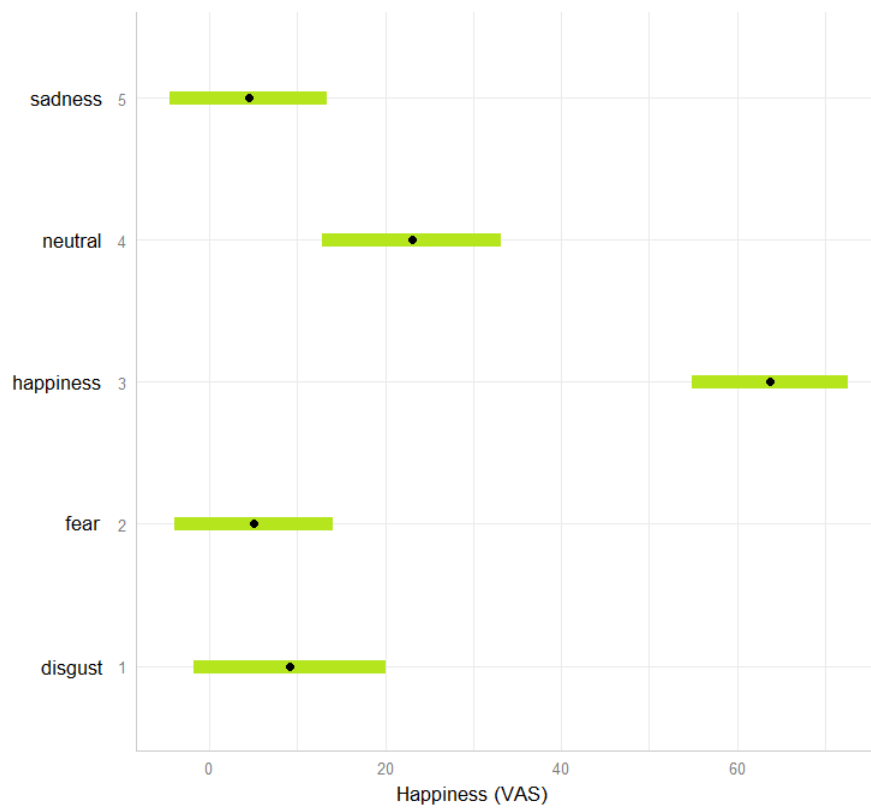


Figure 5.4. Estimated marginal means for happiness ratings in the five experimental conditions: disgust (1), fear (2), happiness (3), neutral (4) and sadness (5).

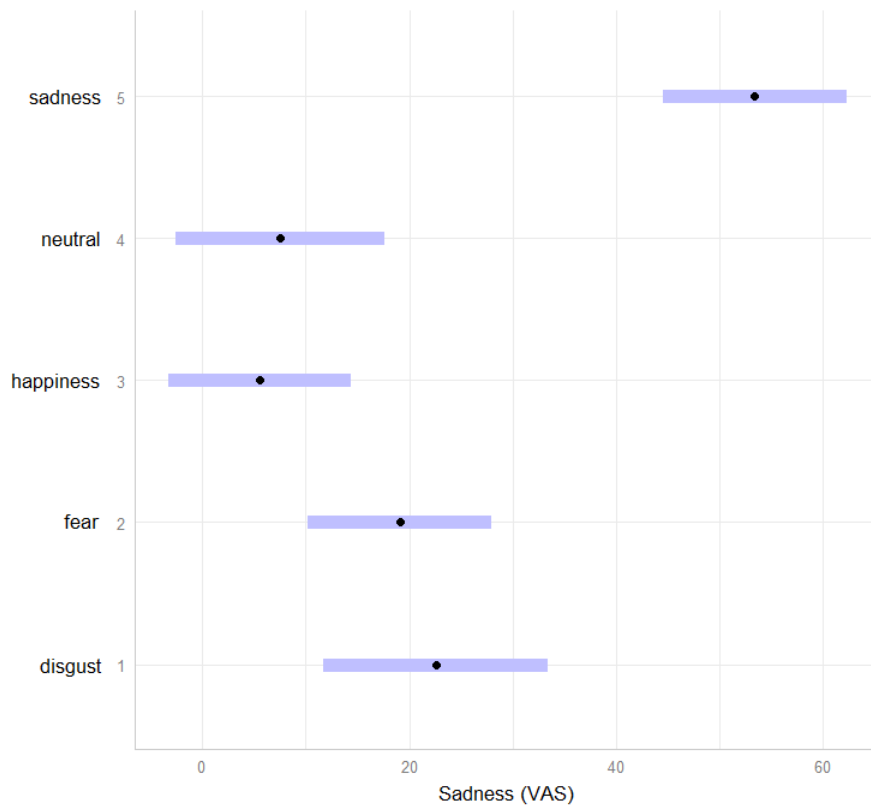


Figure 5.5. Estimated marginal means for sadness ratings in the five experimental conditions: disgust (1), fear (2), happiness (3), neutral (4) and sadness (5).

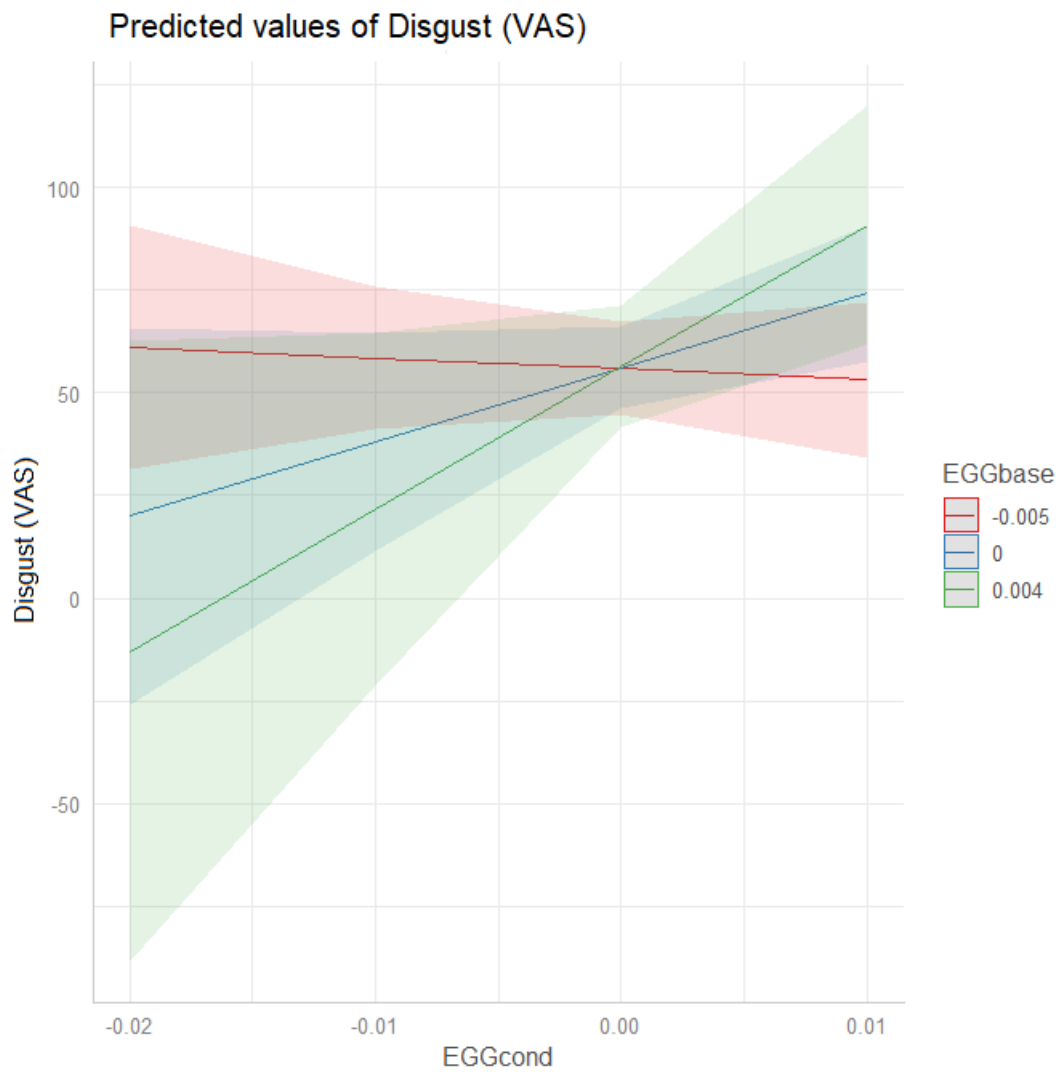


Figure 5.6. EGG baseline X condition interaction: marginal effect of condition-specific EGG peak frequency on VAS ratings of disgust at different EGG baseline levels.

the baseline peak frequency is either average or above average (Figure 5.7).

Gastric effects on perceived arousal The three-way interaction between EGG baseline peak frequency, EGG condition-specific peak frequency and experimental condition also predicts the subjective ratings of arousal, $\chi^2(1, N = 110) = 9.63, p = .047182$. In particular, as the condition-specific peak frequency increases, participants become less excited while watching sad clips and more excited while watching disgusting, fearful or happy clips, provided that the baseline EGG peak frequency is equal to or greater than average. Instead, if the baseline EGG peak frequency is below average, then the gastric-induced arousal effect on sad videos disappears and the analogous effect on happy videos is reversed, while all other effects are preserved (Figure 5.8).

Other results No gastric effect is observed for neutral video clips; electrogastric activity does not predict other sensations, although the interaction between baseline and condition-specific EGG values has an effect on ratings of consciously perceived gastric feelings which is near the statistical significance threshold, $\chi^2(1, N = 110) = 3.77, p = .0522097$.

5.4 Discussion

In this study, we show that gastric physiology, as indexed by electrogastric (EGG) peak frequency, contributes to the perception of disgust, sadness and arousal in healthy participants. In particular, for subjects with average or above-average baseline stomach contractions, high gastric activity is associated with high ratings of disgust, high disgust-triggered arousal and low ratings of sadness, while low gastric activity is linked to low ratings of disgust, high ratings of sadness and high sadness-triggered arousal. This suggests that the stomach maps the emotions of disgust and sadness with emotion-specific, opposing patterns of physiological activity. Thus, gastric physiology is directly involved in emotional awareness.

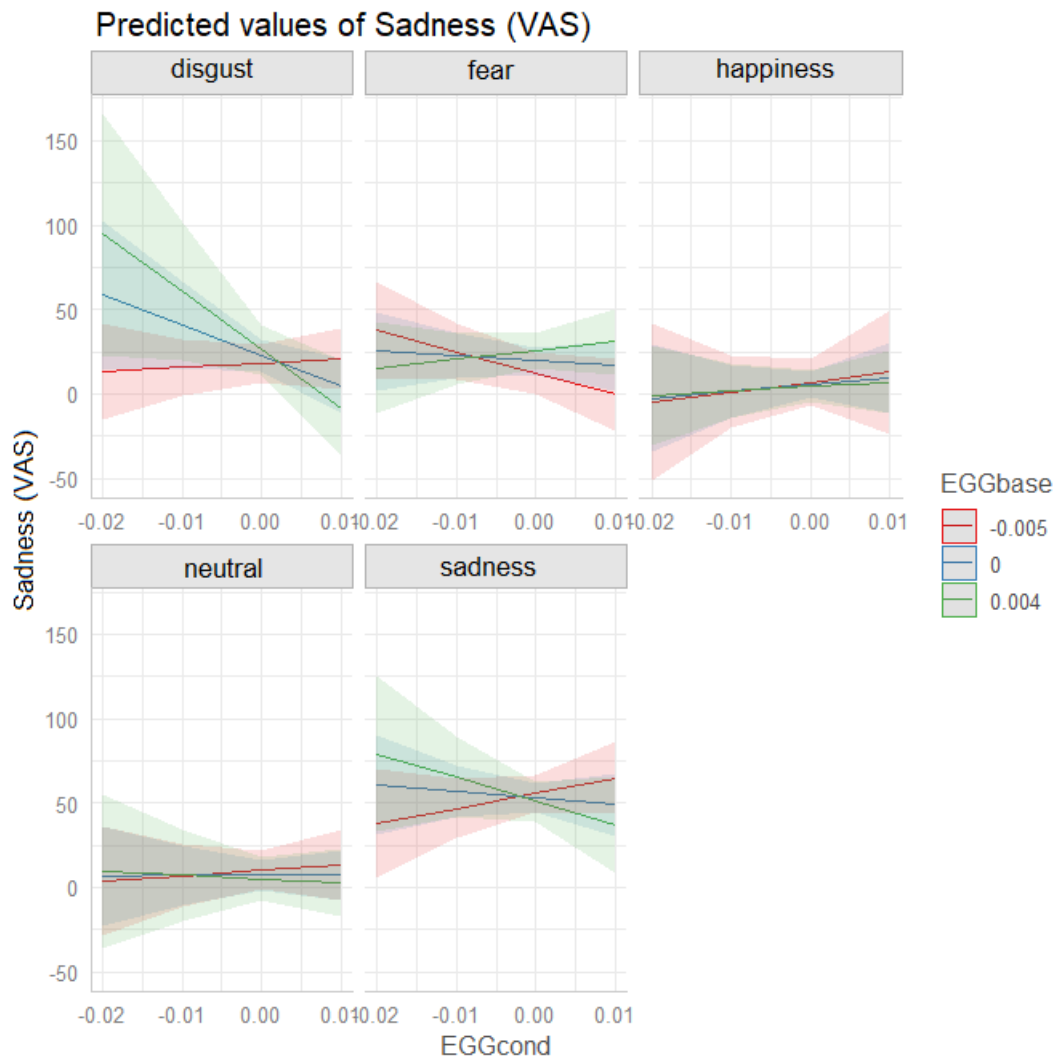


Figure 5.7. The three-way interaction between EGG baseline peak frequency, EGG condition-specific peak frequency and experimental condition predicts the subjective ratings of sadness.

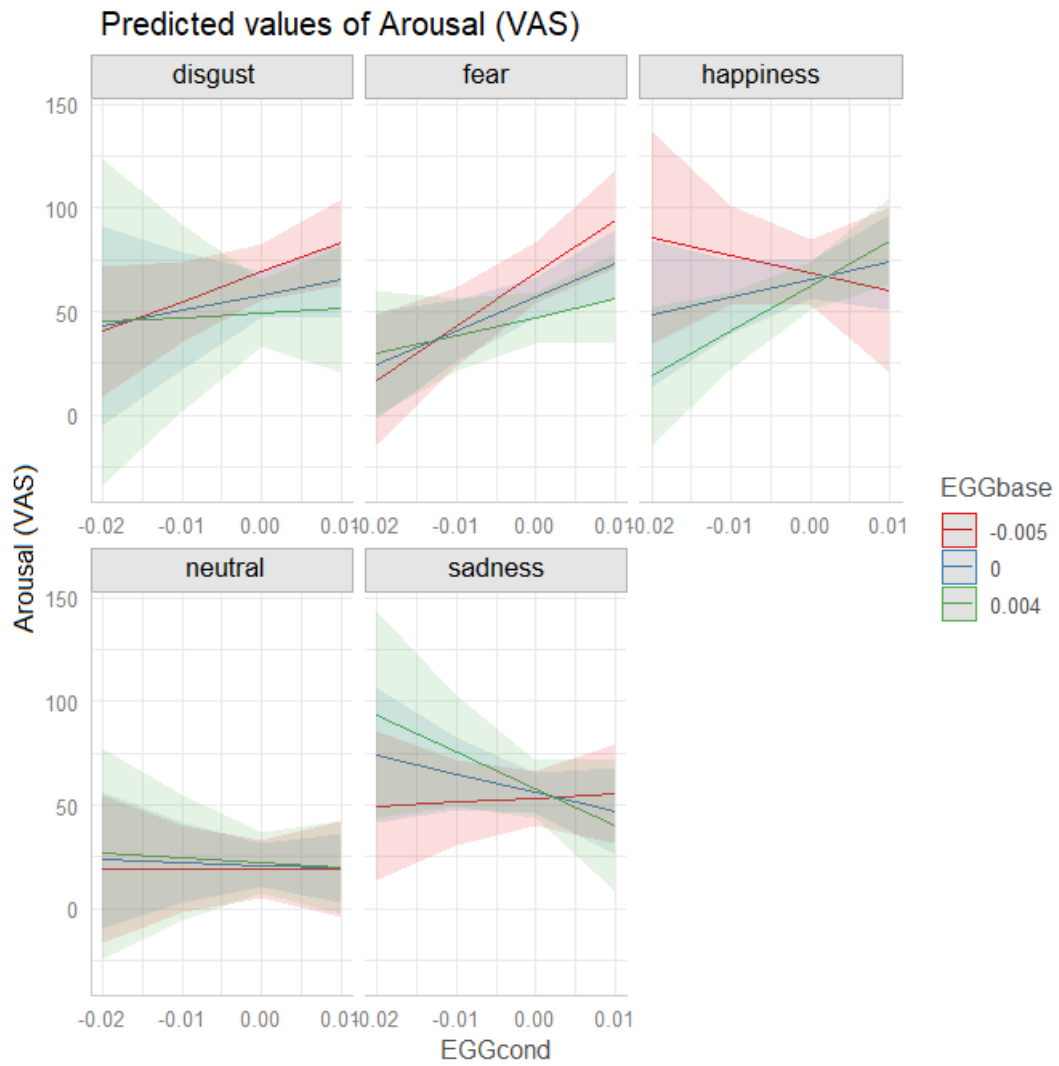


Figure 5.8. The three-way interaction between EGG baseline peak frequency, EGG condition-specific peak frequency and experimental condition predicts the subjective ratings of arousal.

A previous EGG study (Vianna & Tranel, 2006) used a dichotomous classification of emotions, based on valence and arousal and not on emotion-specific ratings of intensity. The results showed that EGG values correlated with arousal ratings, but not with valence. Instead, our study explicitly asked participants how much they were aware of each specific emotion, thus allowing to measure the link between discrete emotions and specific gastric physiological signals. Since we found that the gastric mapping of sadness and disgust is characterised by opposite patterns of activation, we speculate that grouping sadness and disgust in a single cluster of negative valence probably contributed to the null correlation between valence and EGG parameters in the study by Vianna and Tranel (2006). Hence, we believe that our results strengthen the case for a discrete taxonomy of emotions (cf. Kragel & LaBar, 2013).

Beyond its theoretical interest, the fact that the conscious perception of disgust, sadness and arousal is linked to specific electrogastric states could be exploited also for a variety of clinical applications, ranging from the treatment of psychological disorders associated with gastro-intestinal diseases (Shah et al., 2014) to the relationship between gastro-intestinal problems and deficits of emotional awareness in people within the autistic spectrum (Buie et al., 2010; Mulle, Sharp, & Cubells, 2013).

Chapter 6

Experiment IV: gastric moral awareness

6.1 Introduction

Besides having a corporeal and emotional awareness, healthy adult humans also display moral awareness: in other words, they are normally able to recognise and evaluate morality-driven behaviour both in themselves and in fellow human beings. This explains why in some circumstances they feel proud, while in some others they feel guilty or embarrassed, and in others still they become angry or disgusted towards someone who acted against their moral principles (Haidt, 2003; Rozin, Lowery, Imada, & Haidt, 1999).

Although the link between *exteroceptive* corporeal awareness and moral awareness has long been appreciated (Darwin, 1872; Lewis et al., 1989), to date a specific assessment of the relationship between the perception of *internal* bodily states, gastro-intestinal activity and morality is lacking. So far, even studies on moral disgust did not directly address the role of gastric physiology, as researchers either circumscribed their analysis to orofacial correlates of moral disgust (Chapman, Kim, Susskind, & Anderson, 2009; Eskine, Kacinik, & Prinz, 2011; Rozin, Haidt, & Fincher, 2009) or induced a sensation of disgust without examining the physical

effects of the induction procedure in the stomach (Schnall, Haidt, Clore, & Jordan, 2008; Wheatley & Haidt, 2005).

Hence, in this study we aimed at measuring how the gastric milieu changes when participants listen to short, vivid stories designed to trigger either physical or moral disgust, taking electrogastrographic (EGG) recordings as a proxy of gastric activity. Our hypothesis was twofold: on the one hand, we predicted that the slow electrical wave tracked by the EGG would show specific, distinct patterns of correlation with physical and moral disgust ratings; on the other hand, we expected that the role of gastric activity in moral disgust ratings would be particularly relevant when participants listened to stories that dealt with themselves, thus extending the link between the stomach and the corporeal self to the moral self.

6.2 Materials and methods

Participants A subset of seventeen subjects who had already participated in experiments II and III took part also in this experiment after providing the experimenter with a specific consent to listen to stories which could potentially cause distress or hurt their feelings. For further details, please see Section 4.2.

Experimental procedure At the end of experiment III (see Chapter 4), participants had a break and then were reconnected to the EGG apparatus which has been previously described (see Section 4.2). Then, they were requested to listen to six short (3') audio tracks and imagine the narrated scenes as vividly as possible, relying on all sensory modalities. In each audio track, a professional actor read a script in which the main character was either the participant himself (*first-person stories*) or a third party (*third-person stories*). Furthermore, the content of both first- and third-person stories was designed to be either emotionally neutral or physically disgusting or morally disgusting. The type and content of all stories is summarised in Table 6.1.

sc.	type	persp.	content
1	physical disgust	1PP	meeting an old, dirty, vomiting guest in a hospice
2	physical disgust	3PP	as in 1, but main character is a third party
3	moral disgust	1PP	incestuous intercourse with mother
4	moral disgust	3PP	as in 3, but main character is a third party
5	neutral	1PP	waking up and getting to university by train
6	neutral	3PP	as in 5, but main character is a third party

Table 6.1. Summary of scripts used as stimuli in experiment IV. 1PP: first-person perspective (the main character who acts throughout the script is the subject himself). sc.: script. persp.: perspective. 3PP: third-person perspective (the main character who acts throughout the script is a third party).

it.	construct	question
1	<i>immorality</i>	How immoral did you deem the actions narrated in the story?
2	<i>disgust</i>	How much disgust did you feel?
3	<i>anger</i>	How much anger did you feel?
4	<i>guilt</i>	How much guilt did you feel?
5	<i>arousal</i>	While hearing the story you felt...(bored/aroused)
5	<i>fear</i>	How much fear did you feel?
6	<i>gastric f.</i>	Did you feel nausea, stomach contractions, or other GI movements?
7	<i>resp f.</i>	Did you feel your breath changed?
8	<i>cardiac f.</i>	Did you feel your heartbeat changed?
9	<i>imageability</i>	Imagining the scene was...(extremely hard/easy)

Table 6.2. Visual analogue scale (VAS) questionnaire on emotions and feelings perceived while listening to each audio track (abridged translation from Italian). it.: item. resp: respiratory. f.: feelings. GI: gastrointestinal.

Two of the stories, i.e. the third-person physical and moral disgust stories, were adapted from a previous study (Ottaviani et al., 2013), while the other scripts were specifically written for this experiment. At the end of each sequence, subjects completed a 9-item questionnaire, indicating the intensity of the emotions and feelings they perceived while listening to the tracks on a visual analogue scale (VAS) ranging from ‘not at all’ (lowest possible intensity) to ‘very much’ (highest possible intensity). Audio tracks were counterbalanced and separated by 2’ washout pauses. Table 6.2 lists the questionnaire items, while Figure 6.1 depicts the timeline of the experiment.

Data analysis Like in the previous experiments, we used the R software and the R lme4 package (Bates et al., 2015) to perform a linear mixed-effects analysis of

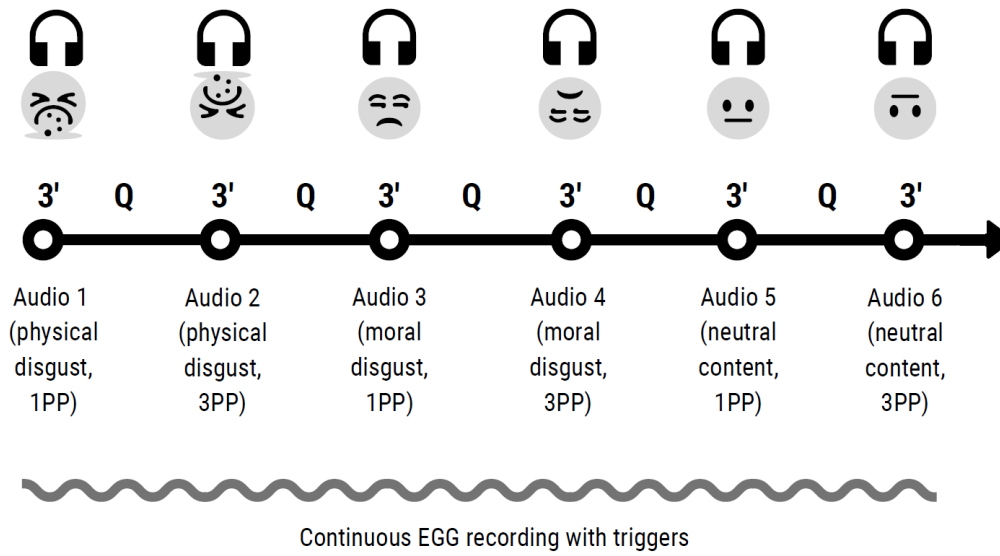


Figure 6.1. Timeline of experiment IV. Q: inter-sequence intervals in which the VAS questionnaires relative to each preceding audio track were filled.

the data. In particular, we modelled how much ratings of the perceived emotions and feelings listed in Table 6.2 changed depending on the experimental conditions as well as on the EGG values recorded at baseline and in each condition. The dependent variables were the VAS ratings of each emotion or feeling included in the questionnaire. As fixed effects, all models had the experimental *condition*, i.e. the type of audio clips (six levels: physical disgust 1PP, physical disgust 3PP, moral disgust 1PP, moral disgust 3PP, neutral 1PP, neutral 3PP), the baseline EGG peak frequency EGG_{base} (continuous) and the condition-specific EGG peak frequency EGG_{cond} (continuous). These fixed effects were tested for interactions with each other. As random effects, the models included by-subject intercepts. Hence, each mixed model was specified as follows:

$$immorality \sim EGG_{base} * EGG_{cond} * condition + (1|subj)$$

$$disgust \sim EGG_{base} * EGG_{cond} * condition + (1|subj)$$

$$anger \sim EGG_{base} * EGG_{cond} * condition + (1|subj)$$

$$guilt \sim EGG_{base} * EGG_{cond} * condition + (1|subj)$$

$$arousal \sim EGGbase * EGGcond * condition + (1|subj)$$

$$gastric \sim EGGbase * EGGcond * condition + (1|subj)$$

$$resp \sim EGGbase * EGGcond * condition + (1|subj)$$

$$cardiac \sim EGGbase * EGGcond * condition + (1|subj)$$

$$imageability \sim EGGbase * EGGcond * condition + (1|subj)$$

Finally, like in experiments II and III, we tested whether the condition-specific EGG peak frequency changed as a function of each experimental condition and of the baseline frequency, specifying by-subject intercepts as in the previous models:

$$EGGcond \sim EGGbase * condition + (1|subj)$$

As in experiments I-III, we used the Anova function of the R car package (Fox and Weisberg, 2011) to compute p-values through Type II Wald chi-square tests. Post-hoc tests were performed with the R package emmeans, using Tukey's method for comparing a family of 6 estimates.

6.3 Results

Manipulation check and condition effects The multilevel mixed effects analysis (see above) confirmed that the manipulation was effective, as indicated by the main effect of condition on VAS ratings of disgust ($\chi^2(1, N = 72) = 316.00, p < .001$), immorality ($\chi^2(1, N = 72) = 461.44, p < .001$), and guilt ($\chi^2(1, N = 72) = 54.78, p < .001$). Specifically, post-hoc tests revealed that both physical and moral disgust stories induce much more disgust than neutral stories (Figure 6.2); the actions described in moral disgust stories are deemed as significantly more immoral than the actions of any other story (Figure 6.3); and the first-person moral disgust story triggers more guilt than any other story (Figure 6.4).

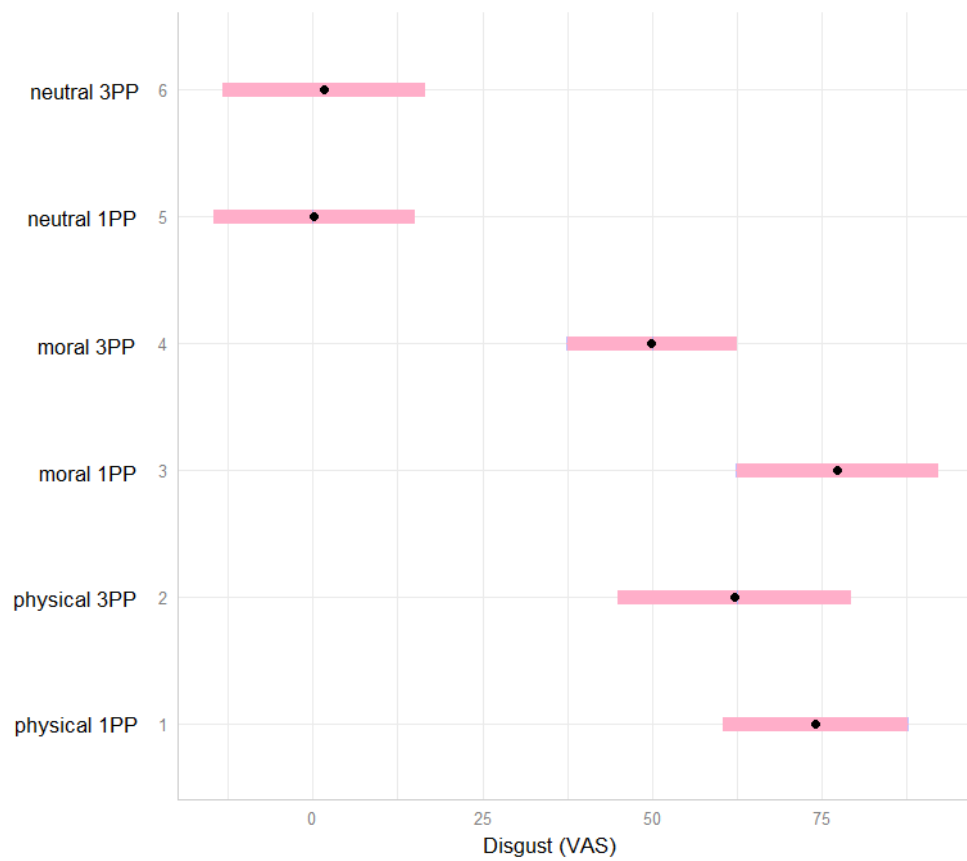


Figure 6.2. Estimated marginal means for disgust ratings in the six experimental conditions: first-person physical disgust (1), third-person physical disgust (2), first-person moral disgust (3), third-person moral disgust (4), first-person neutral (5) and third-person neutral (6)

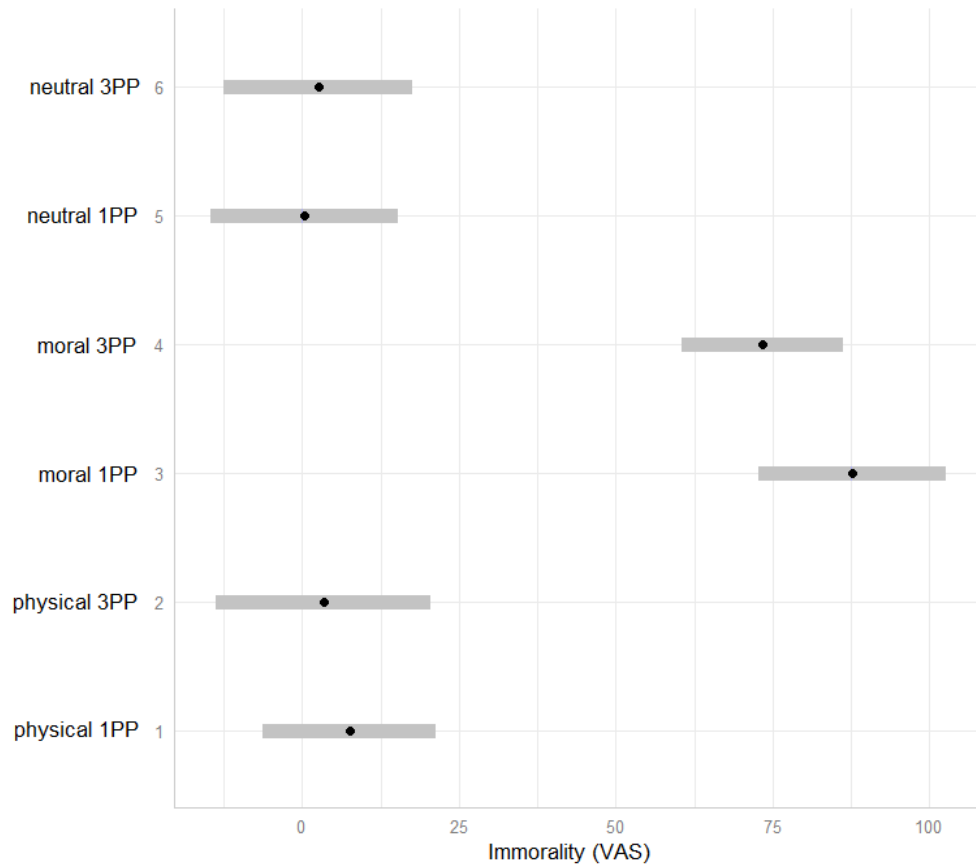


Figure 6.3. Estimated marginal means for immorality ratings in the six experimental conditions: first-person physical disgust (1), third-person physical disgust (2), first-person moral disgust (3), third-person moral disgust (4), first-person neutral (5) and third-person neutral (6)

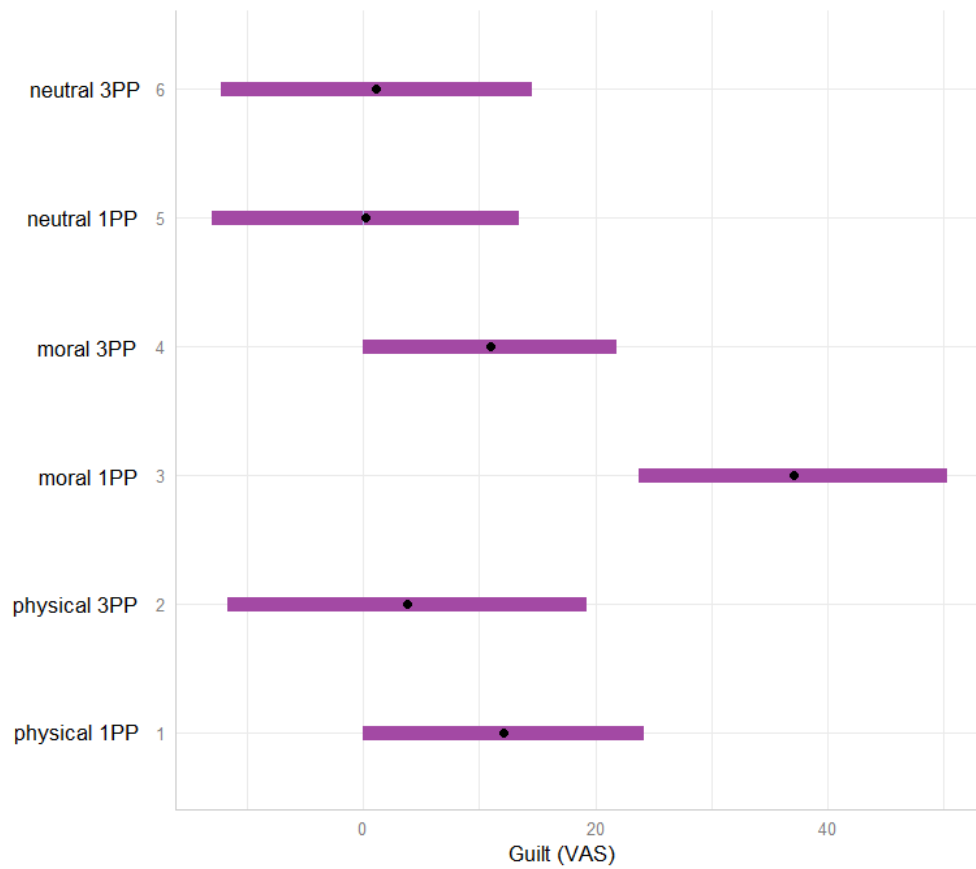


Figure 6.4. Estimated marginal means for guilt ratings in the six experimental conditions: first-person physical disgust (1), third-person physical disgust (2), first-person moral disgust (3), third-person moral disgust (4), first-person neutral (5) and third-person neutral (6)

Gastric effects on immorality ratings The three-way interaction between baseline EGG peak frequency, condition-specific EGG peak frequency and experimental condition predicts the judgement of immorality, $\chi^2(1, N = 72) = 11.97, p = .03522$. In the physical disgust first-person story and in both moral disgust stories, the lower the baseline and condition-specific peak frequencies, the higher is the immorality rating that participants assign to the actions described in the story. The effect holds also for the physical disgust third-person story provided that the baseline peak frequency is below average (Figure 6.5).

Gastric effects on disgust ratings The two-way interaction between baseline EGG peak frequency and experimental condition predicts subjective ratings of disgust, $\chi^2(1, N = 72) = 12.40, p = .02971$. In the first-person disgust stories (both physical and moral), the lower the baseline peak frequency, the higher the disgust felt and reported by the participants; the effect is reversed in the third-person moral disgust story (Figure 6.6).

Gastric effects on anger ratings The subjective perception of anger is predicted by a couple of interactions, namely, the two-way interaction between EGG peak frequency at baseline and experimental condition ($\chi^2(1, N = 72) = 21.72, p < .001$) and the two-way interaction between condition-specific EGG peak frequency and experimental condition ($\chi^2(1, N = 72) = 13.85, p = .01658$). In the moral disgust stories, particularly when there is a first-person perspective, the lower the baseline or condition-specific peak frequency, the higher the subjective feeling of anger (Figures 6.7-6.8).

Gastric effects on arousal The two-way interaction between baseline EGG peak frequency and experimental condition predicts participants' arousal ratings, $\chi^2(1, N = 72) = 12.96, p = .02372$. Both in physical and moral disgust stories, the lower the baseline peak frequency, the higher is the arousal reported by the participants; the effect is reversed for neutral stories (Figure 6.9).

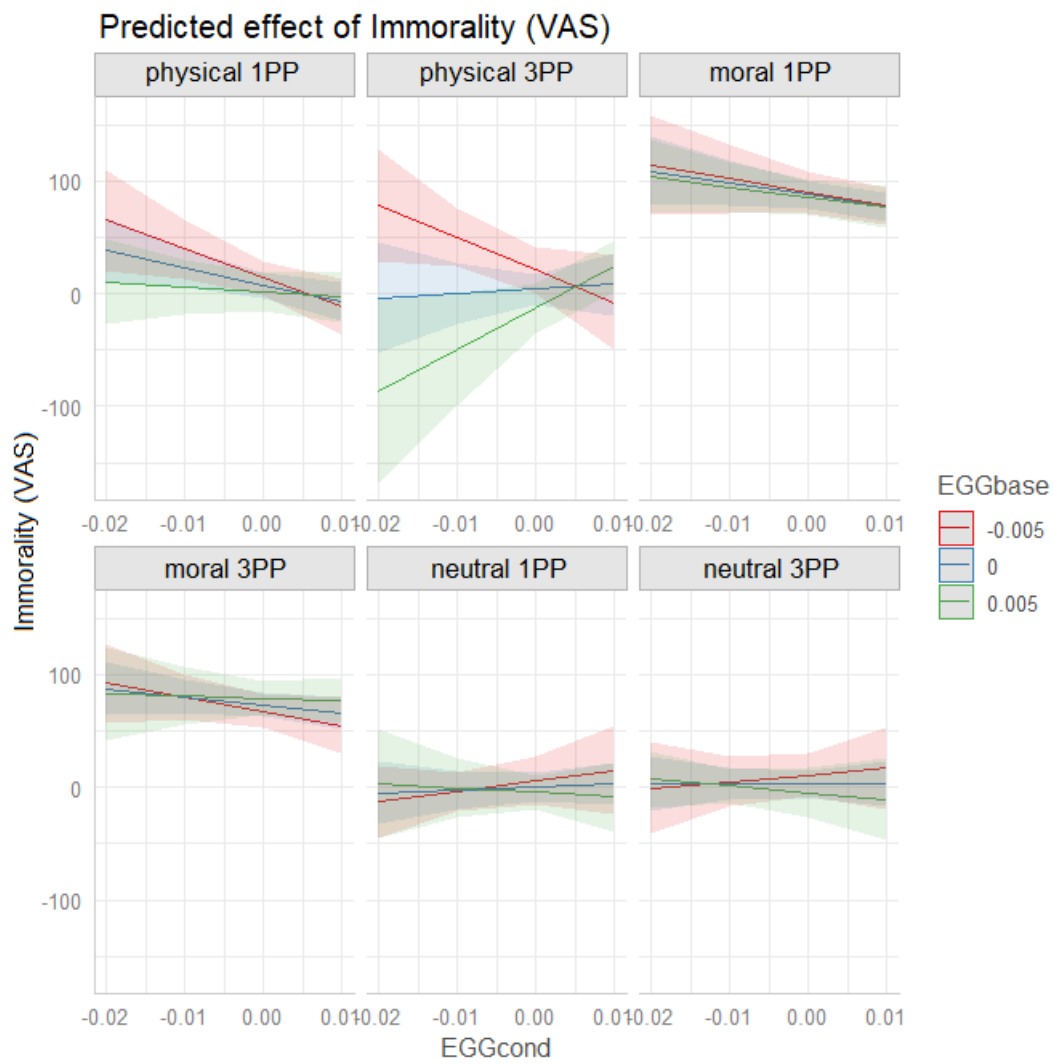


Figure 6.5. The three-way interaction between baseline EGG peak frequency, condition-specific EGG peak frequency and experimental condition predicts the judgement of immorality.

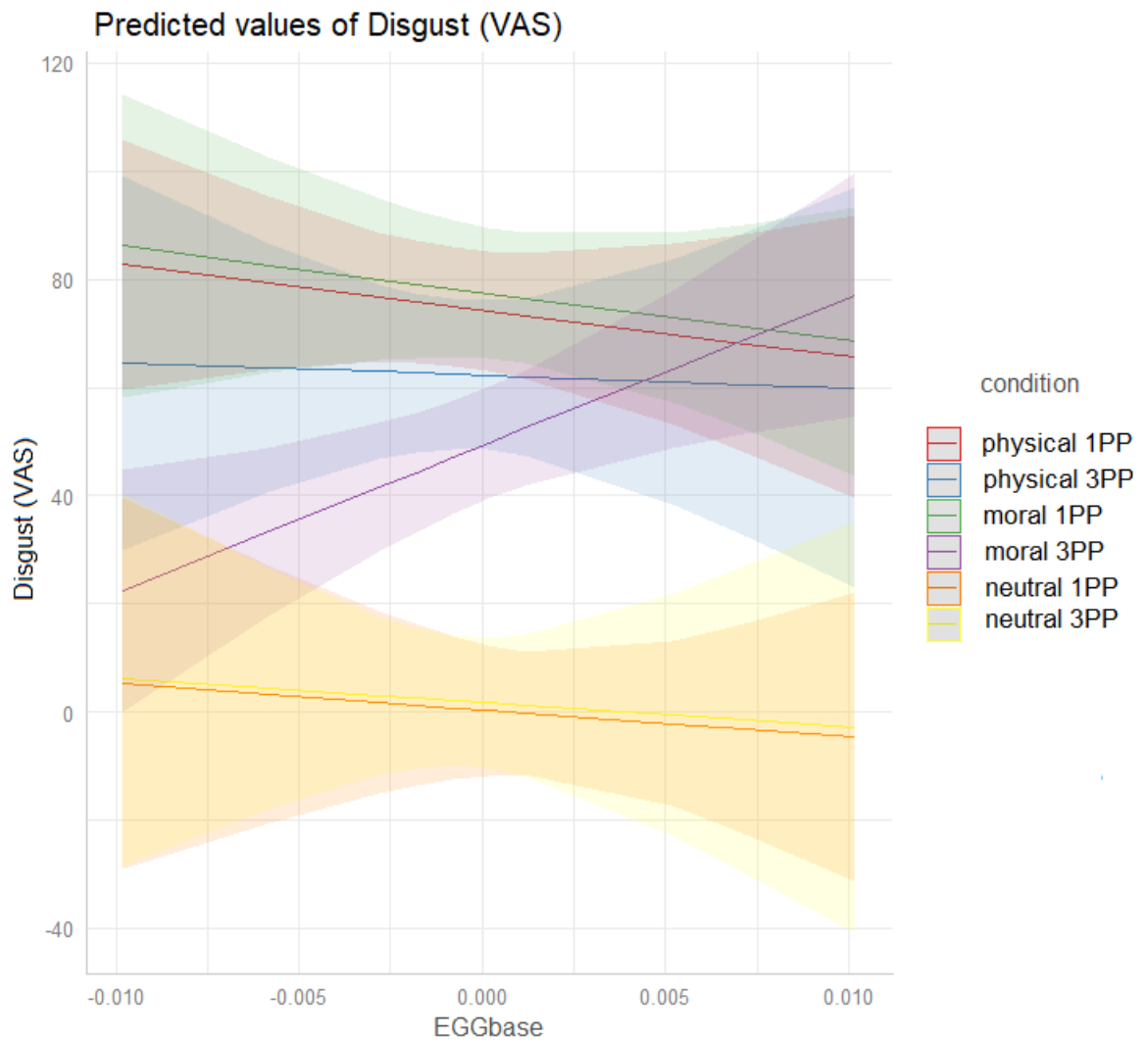


Figure 6.6. The two-way interaction between baseline EGG peak frequency and experimental condition predicts subjective ratings of disgust.

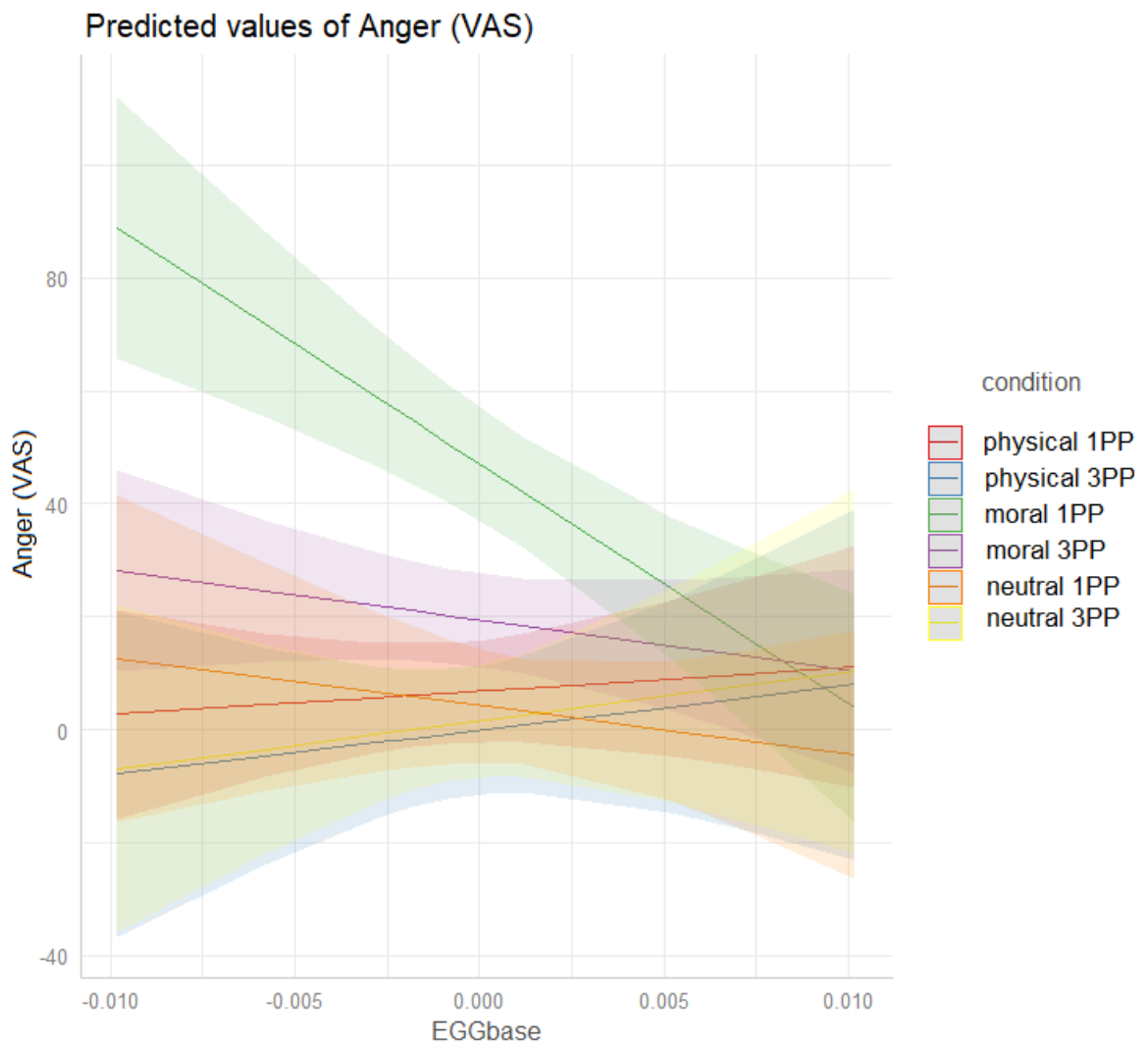


Figure 6.7. The two-way interaction between EGG peak frequency at baseline and experimental condition predicts subjective ratings of anger.

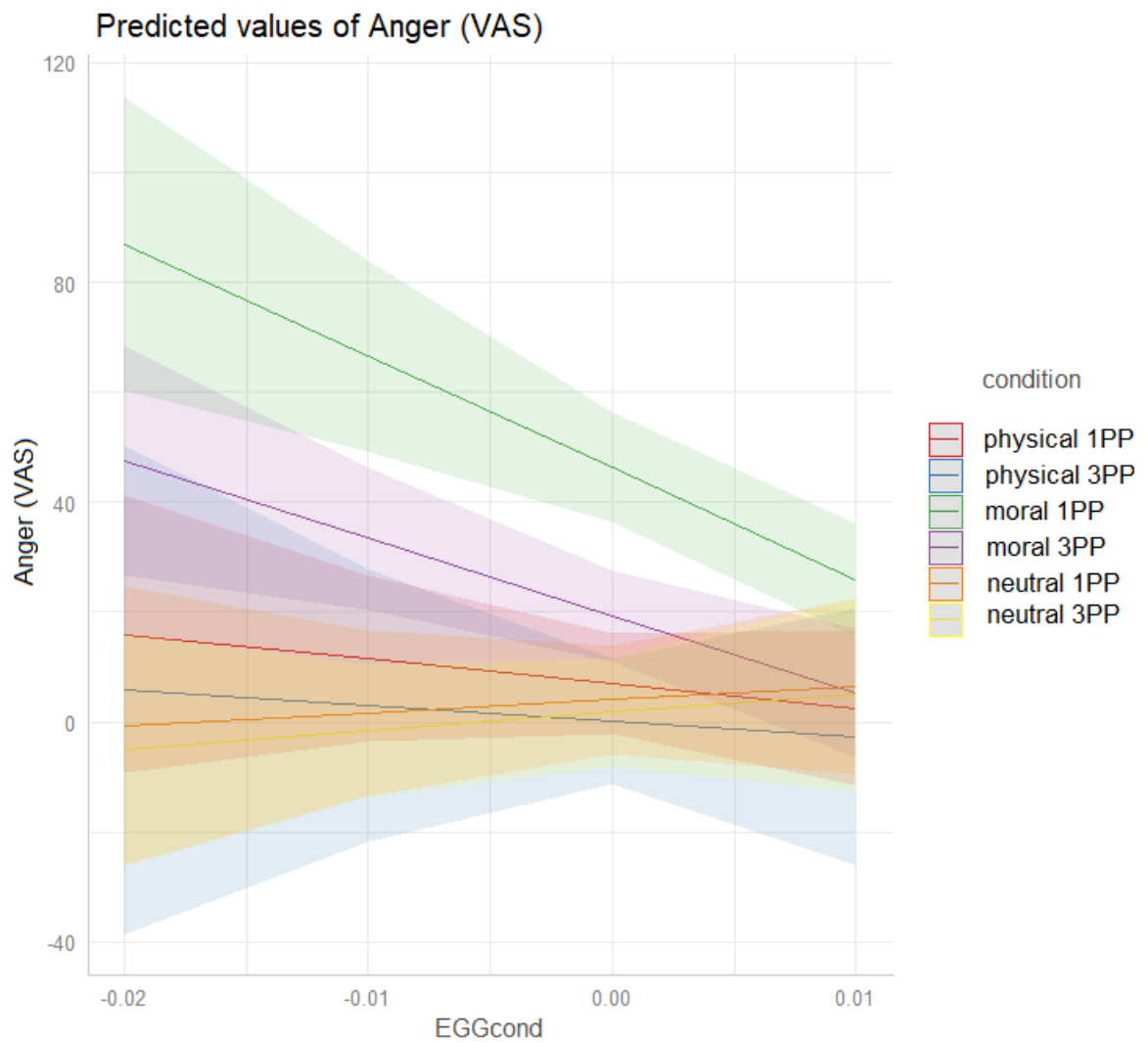


Figure 6.8. The two-way interaction between condition-specific EGG peak frequency and experimental condition predicts subjective ratings of anger.

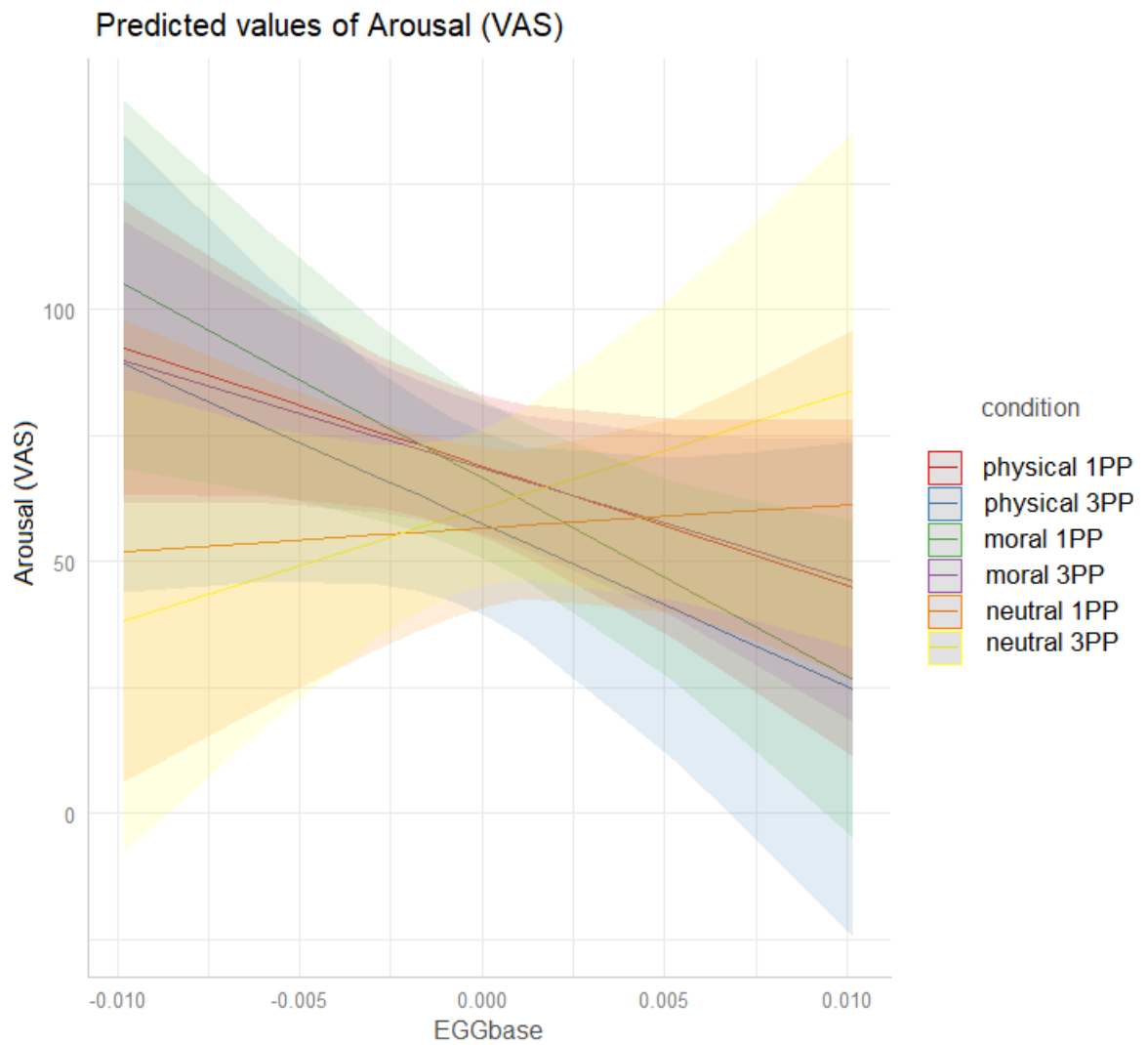


Figure 6.9. The two-way interaction between baseline EGG peak frequency and experimental condition predicts participants' arousal ratings.

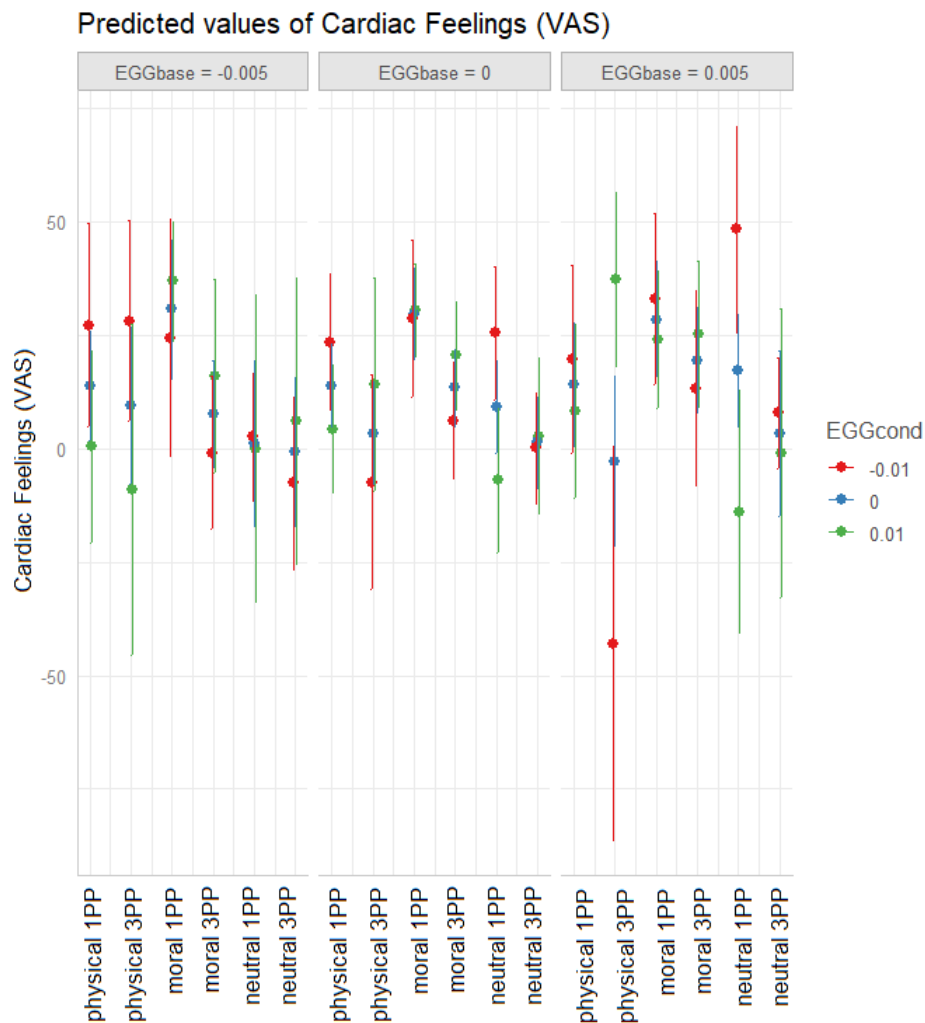


Figure 6.10. The three-way interaction between baseline EGG peak frequency, condition-specific EGG peak frequency and experimental condition predicts the conscious perception of cardiac activity.

Gastric effects on cardiac feelings The three-way interaction between baseline EGG peak frequency, condition-specific EGG peak frequency and experimental condition predicts the conscious perception of cardiac activity, ($\chi^2(1, N = 72) = 17.35, p = .003887$). More specifically, subjects with high baseline and condition-specific electrogastric peak frequencies display a heightened perception of cardiac activity in the third-person physical disgust story. Nevertheless, overall VAS ratings of cardiac feelings are quite low, with an average of ~ 12 VAS points (Figure 6.10).

Gastric effects on imageability The three-way interaction between baseline EGG peak frequency, condition-specific EGG peak frequency and experimental condition also predicts the self-reported ability of imagining the scenes described in the stories, $\chi^2(1, N = 72) = 11.54, p = .04166$. For participants who have a low baseline EGG frequency, the lower the condition-specific EGG peak frequency, the higher the imageability ratings of physical disgust and neutral stories; the effect is reversed in moral disgust stories. For participants who have a high baseline frequency, the higher the condition-specific EGG peak frequency, the higher the imageability ratings of third-person physical disgust and neutral stories; the effect is reversed in moral disgust stories and in the first-person neutral story. Overall, neutral stories are easier to imagine (Figure 6.11).

Condition-specific changes of EGG peak frequency Overall, there is a main effect of condition on the EGG peak frequency, $\chi^2(1, N = 72) = 13.46, p = .01944$, which reaches its maximum value in the first-person moral disgust story (Figure 6.12).

6.4 Discussion

In this first study on the relationship between electrical gastric activity and morality, we found that a low activity of the stomach predicts a harsher moral judgement from the participants, an increased arousal, and increased anger.

Furthermore, there are dissociable patterns of physiological activity depending on whether there is a first- or third-person perspective on the (im)moral actions that should be evaluated: when the ‘moral self’ is directly involved, there is an overall increase in stomach contractions and high disgust ratings are associated with a low stomach activity; when it is a third party who is at stake, high disgust ratings are linked to high stomach activity. Finally, the two constructs of core and moral disgust seem to be linked to different patterns of gastric physiology.

According to Russell and Giner-Sorolla (2013), anger should be more related to

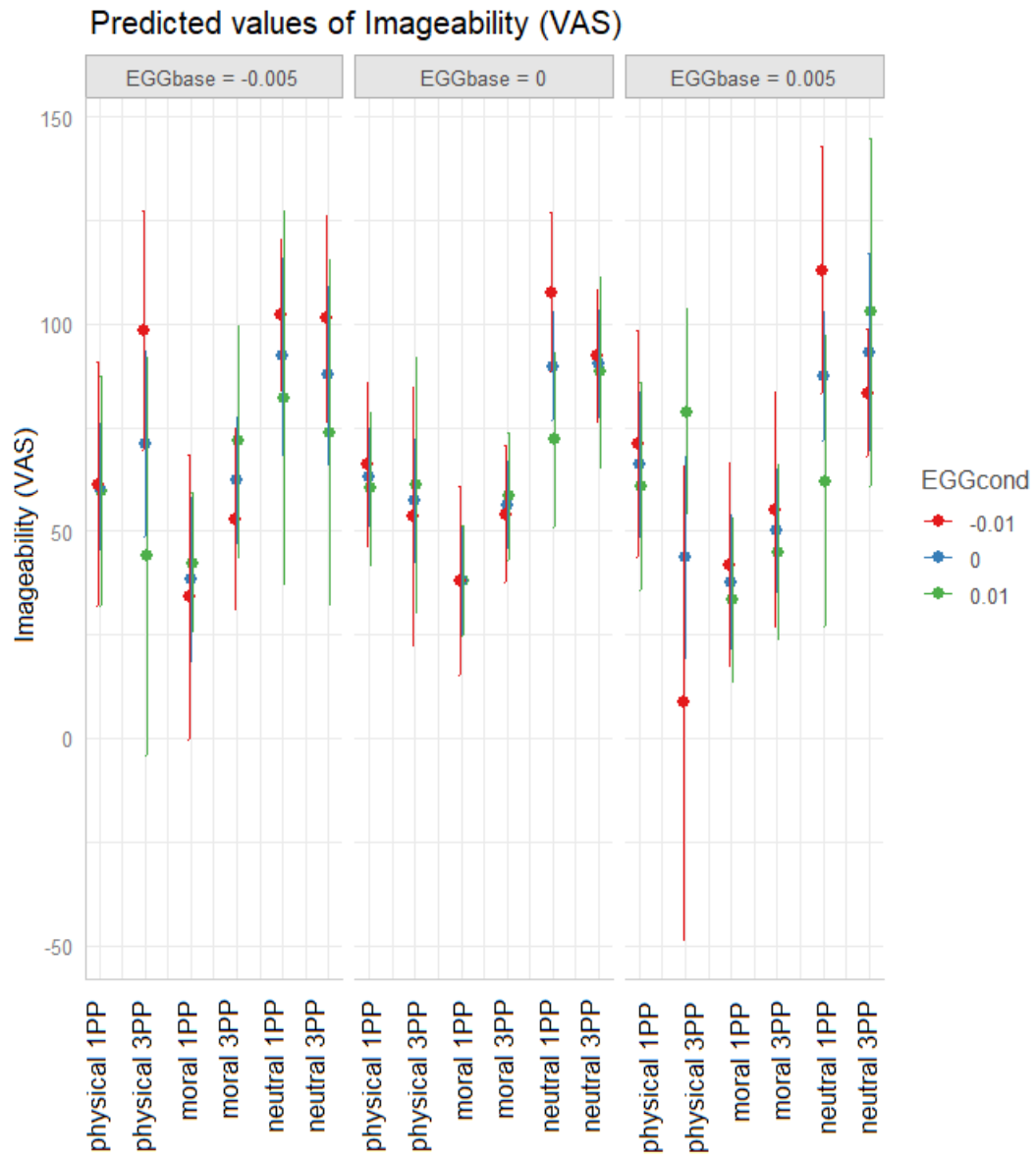


Figure 6.11. The three-way interaction between baseline EGG peak frequency, condition-specific EGG peak frequency and experimental condition predicts participants' imageability ratings.

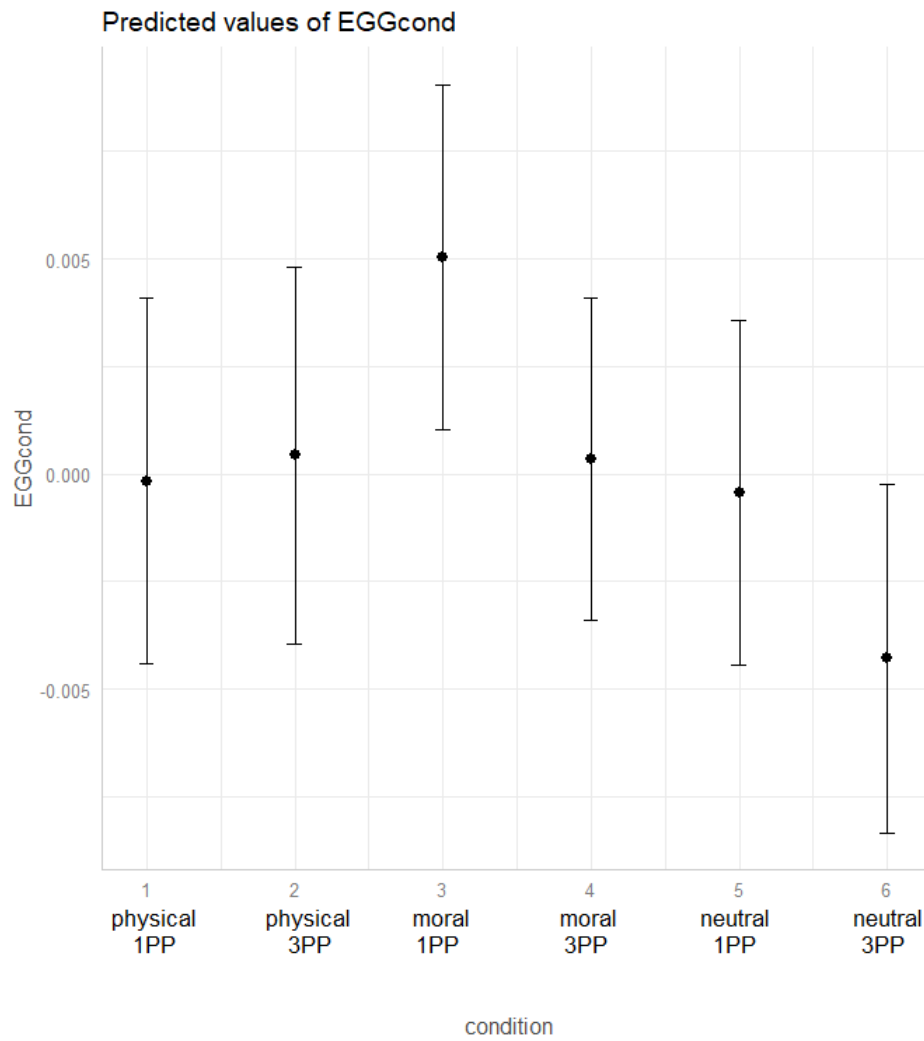


Figure 6.12. EGG peak frequency in the six experimental conditions: first-person physical disgust (1), third-person physical disgust (2), first-person moral disgust (3), third-person moral disgust (4), first-person neutral (5) and third-person neutral (6)

non-bodily moral violations and disgust to bodily moral violations. However, in our study we found a sharp increase of anger triggered by an extreme bodily moral violation (incest) committed by the moral self, suggesting that the anger/disgust dichotomy may be more appropriate to a ‘third-person morality’ than to a ‘first-person morality’.

Chapter 7

Experiment V: interoception in a PIEZO2 patient

7.1 Introduction

Experiments II-IV highlighted the role of gastric contractions in corporeal, emotional and moral awareness. These contractions are part of a wider family of mechanical bodily changes that take place inside us as well as on our skin, both on short and long timescales. Indeed, like many other physical entities, all vertebrate bodies are subject to ever-changing mechanical forces of tension and compression acting on their skin, muscles, bones, and hollow organs. Visceral organs, in particular, are regularly filled with air, water, nutrients and change their shape to accommodate, transform and expel these substances (Umans and Liberles, 2018).

To survive and thrive, vertebrates need to properly sense these forces of tension and compression and convert them into electrochemical signals. This process, known as mechanotransduction, relies on mechanically activated ion channels, whose key components have been recently identified with multipass transmembrane proteins PIEZO1 and PIEZO2 in a landmark paper by Coste and colleagues (2010).

Subsequent studies on animal models further highlighted that PIEZO2 in particular is key to Merkel-cells mechanosensitivity (Ikeda et al., 2014; Maksimovic et al.,

2014; Vásquez et al., 2014; Woo et al., 2014), innocuous touch in general (Ranade et al., 2014; Schneider et al., 2017), endothelium-dependent and bone marrow pain (Ferrari et al., 2015; Nencini and Ivanusic, 2017), proprioception (Florez-Paz et al., 2016; Woo et al., 2015) and many forms of visceral sensations (Umans and Liberles, 2018; Yang et al., 2016), from oral and gut mechanosensation (Alcaino et al., 2018; Bai et al., 2017; Moayedi et al., 2018) to airway stretch sensation, Hering-Breuer reflex (Nonomura et al., 2017) and baroreception (Zeng et al., 2018; but see Stocker et al., 2019).

In a similar vein, PIEZO2 underpins several varieties of human touch (García-Mesa et al., 2017; Schrenk-Siemens et al., 2015) and human proprioception, both of which become severely impaired in patients with PIEZO2 mutations (Alper, 2017; Chesler et al., 2016; Mahmud et al., 2017; Yamaguchi et al., 2019). However, to date, it is unknown whether human PIEZO2 also mediates the perception of visceral organs and, more generally, the broad interoceptive perception of the physiological state of the body, which in turn is key to corporeal, emotional and moral awareness, as shown by Experiments II-IV. Is PIEZO2 necessary for human interoception and embodiment?

To test this hypothesis, we studied a rare genetic condition which has been recently described in the clinical literature (Chesler et al., 2016). Patients who suffer from this yet unnamed disorder carry compound-inactivating variants in the PIEZO2 gene. As a result, they do not express the corresponding transmembrane protein. Hence, we performed a single case study and assessed how one of these patients differs from healthy controls in gastric interoception. In particular, we predicted that, relative to control participants, the patient would show a significantly lower interoceptive accuracy, as measured by the two-step Water Load Test (WLT-II).

7.2 Materials and methods

Participant Patient A, a 32-year old woman, took part in the study after giving informed consent. Since her childhood, she referred a series of unexplained medical symptoms including insensibility to innocuous tactile stimuli and a marked inability to localise body parts in space when her eyes are closed. In fact, she reports to “lose her body” when she closes her eyes. A neurologist referred her to the National Institutes of Health (NIH) in Bethesda, Maryland (USA) with a generic diagnosis of neuropathy. Subsequent genetic testing at NIH revealed that she carries a compound-inactivating variant of the *PIEZO2* gene. Her verbal and cognitive abilities are intact. The experiment took place at NIH and was performed in collaboration with the National Institute of Neurological Disorders and Stroke (NINDS).

Experimental procedure The patient underwent a two-step Water Load Test (WLT-II; van Dyck et al., 2016). As per standard guidelines, the patient came to the lab after fasting from food for 3 hours and from water for 2 hours, then filled a 7-item Likert questionnaire on gastric sensations (Table 7.1) and completed the two steps of the test. In step 1, she was instructed to drink as much plain water as she wanted until she reached the point of perceived satiation, i.e. the feeling that ordinarily signals to terminate a meal. At that point, she proceeded to step 2: she filled the same gastric questionnaire again and was told that she had to drink again until she perceived that her stomach was completely full. In order to prevent her from regulating the water intake based on external cues, she was not told in advance that she had to drink two times and she drank from an opaque bottle with a long straw. After completing the second drinking phase, she filled the gastric questionnaire for the third time. Figure 7.1 details the timeline of the experiment.

Data analysis Ingested water was measured with a standard beaker to calculate the four WLT-II indices (van Dyck et al., 2016): 1) water volume (ml) needed to induce satiation (sat_{ml}); 2) additional water volume required to induce maximum

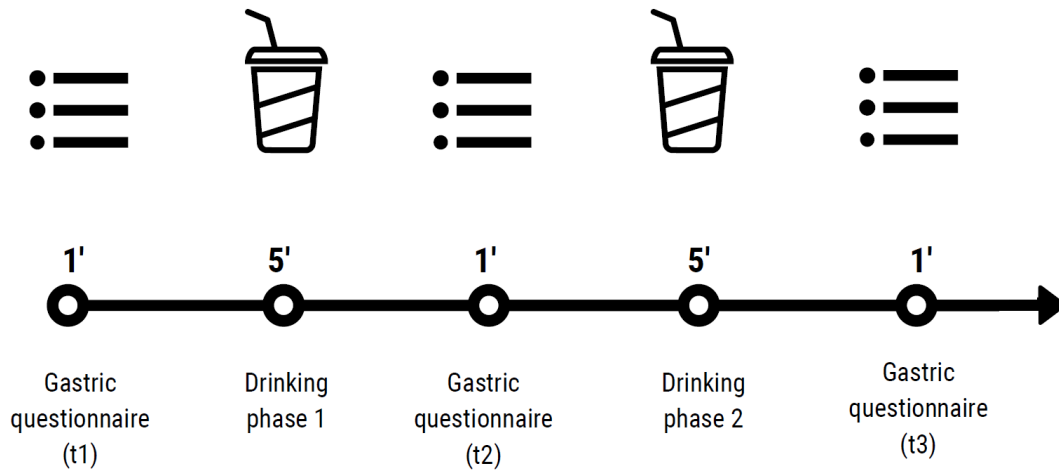


Figure 7.1. Timeline of experiment III.

item	construct	statement
1	<i>satiety</i>	How much satiety do you feel now?
2	<i>fullness</i>	How much fullness do you feel now?
3	<i>discomfort</i>	How much discomfort do you feel now?
4	<i>guilt</i>	How much guilt do you feel now?
5	<i>sluggishness</i>	How much sluggishness do you feel now?
6	<i>nausea</i>	How much nausea do you feel now?
7	<i>arousal</i>	How much arousal do you feel now?

Table 7.1. WLT-II questionnaire on gastric sensations. Responses were provided through a 7-point Likert scale ranging from 1 (not at all) to 7 (very much).

index	patient's value (ml)	control values (ml)
sat_{ml}	210	428.36 ± 242.48
$\Delta full_{ml}$	545	306 ± 171.10
$total_{ml}$	755	734.48 ± 316.80
$sat_{\%}$	27.81	57.82 ± 16.33

Table 7.2. WLT-II test data for patient A. vs the normative values measured in a healthy female sample (cf. van Dyck et al., 2016).

fullness ($\Delta full_{ml}$); (3) total water volume ($total_{ml}$), obtained adding $\Delta full_{ml}$ to sat_{ml} ; and (4) the satiation/total volume ratio ($sat_{\%}$), an adimensional index of the participant's gastric interoceptive accuracy which is not confounded with her stomach capacity. The index is calculated as follows:

$$sat_{\%} = 100 * \frac{sat_{ml}}{total_{ml}} = 100 * \frac{sat_{ml}}{sat_{ml} + \Delta full_{ml}}$$

Finally, the patient's gastric interoception score, $sat_{\%}$, was compared to the WLT-II normative values (van Dyck et al., 2016) using Crawford's modified t-test for single case studies (Crawford et al., 2010).

7.3 Results

Table 7.2 is a descriptive summary of the results of the WLT-II test, while Figure 7.2 depicts the results of the gastric questionnaire. Although in the first step the patient drank less than half the amount of water of healthy controls, her self-reported satiety was as high as controls' (Figure 7.2). The patient's gastric interoception index was 27.81, which is significantly lower than the average 57.82 ± 16.33 value of the normative sample, $t = -1.829$, $p = .03526$ (one-tailed).

7.4 Discussion

Our study presents the first evidence that PIEZO2 is necessary for normal interoception. It would be worth investigating if this impairment of interoception

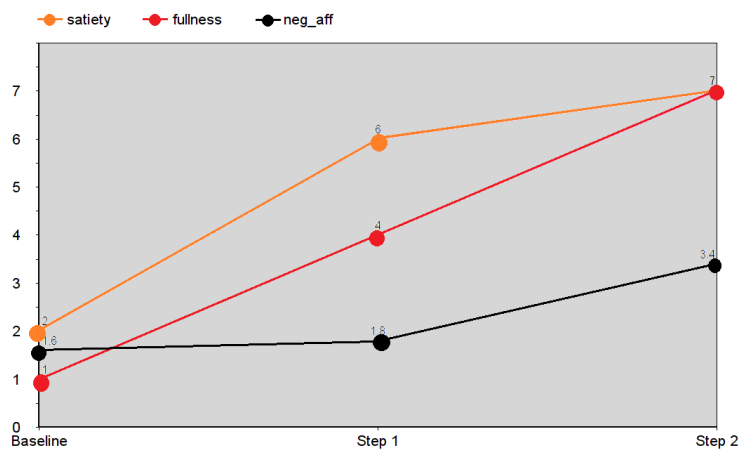


Figure 7.2. WLT-II questionnaire data for patient A.

also affects their corporeal awareness, increasing the uncertainty and plasticity of the mental representation of their body and thus making them more susceptible to bodily illusions. Given the increasingly recognized importance of interoception and corporeal awareness in decision making, emotion appraisal, and subjective experience (Craig, 2009; Park & Tallon-Baudry, 2014), a thorough investigation of these topics may help understand the symptoms of PIEZO2 patients, increase their quality of life, and shed light on the molecular and genetic underpinnings of bodily self-consciousness.

Chapter 8

General discussion and conclusions

8.1 Summary and discussion of key findings

Our body is the only object we sense from the inside; however, existing literature has largely left unanswered the question of how much inner physiology contributes to the global sensation of having a body and controlling it. The five experiments described in the previous chapters were planned and executed with the goal of filling this gap of knowledge and provide empirical insights into the visceral roots of corporeal awareness.

In fact, the goal was threefold: the whole research project aimed at improving methods to track interoceptive signals (objective 1), measure how each interoceptive modality contributes to corporeal awareness (objective 2), and gauge how corporal awareness changes when interoception is impaired (objective 3).

As far as **objective 1** is concerned, the project yielded a new method to record the respiratory interoceptive accuracy, i.e. pneumoception (Chapter 2). The task proved to be a quick and easy solution to gauge how much healthy people are aware of their normal, eupnoeic breathing. Hence, the pneumoception task provides the research community with a valuable complement to existing tests of dyspnoea,

allowing for the first time to quantitatively assess the whole spectrum of respiratory sensations and not just the most negative or uncommon respiratory feelings.

Experiments 1-4 dealt with **objective 2**. In particular, experiment 1 combined pneumoception with respiration recordings and immersive virtual reality to produce the new embreathment bodily illusion (Chapter 3). Results showed that making a virtual body breathe like the real body gives an illusory sense of ownership and agency over the avatar, elucidating the role of a key physiological process like breathing in corporeal awareness. The experiment also proved that individual differences in perceiving respiratory and cardiac signals matter for corporeal awareness, too. More precisely, individuals with a looser sense of their internal states, as gauged by pneumoception and heartbeat counting, are more sensitive to the embreathment illusion.

A simplified version of the embreathment illusion was then used to test the contribution of another key internal organ, the stomach, to bodily self-consciousness (experiment 2, Chapter 4). The experiment produced the first evidence of a role of gastric activity in corporeal awareness. Indeed, there was a direct correlation between the gastric peak frequency measured with an electrogastrogram (EGG) and subjective ratings of body ownership: the higher the EGG peak frequency, the more the participants reported that the virtual body belonged to them.

It has long been argued that the perception of one's own bodily states is involved also in higher forms of awareness, and particularly in emotional awareness (James, 1884; Damasio, 1999). Here, experiment 3 revealed that awareness of two emotions in particular, disgust and sadness, correlates with specific, opposing patterns of gastric physiological activity: a higher number of stomach contractions (as indexed by EGG) is linked to higher disgust and lower sadness, while a lower number of stomach contractions is associated with lower disgust and increased sadness (Chapter 5).

Experiment 4 further explored the contribution of gastric physiology to an even higher form of awareness, that is, moral awareness – the conscious perception of

disgust that is elicited by moral violations. Results suggested that reduced stomach activity predicts harsher moral judgments. Furthermore, gastric activity changes depending on whether these judgments involve a first- or third-person perspective (Chapter 6).

Finally, experiment 5 lay the groundwork for targeting **objective 3** by providing the first evidence that a specific gene, *PIEZO2*, is causally linked to interoceptive accuracy, as measured through a water load test in a single clinical case. Specifically, lack of *PIEZO2* expression severely impaired the perception of stomach fullness. It remains to be ascertained whether this interoceptive deficit extends beyond the gastric domain and is linked to anecdotal evidence on reduced corporeal awareness reported by the patient.

Overall, these results indicate that the contribution of inner physiological signals to corporeal, emotional and moral awareness is *substantive*, *specific*, and *subjective*.

- **Substantive:** breathing contributes to perceived body ownership almost as much as visual appearance (expt. 1), while stomach activity not only predicts body ownership (expt. 2) but also the conscious perception of disgust and sadness (expt. 3) and moral disgust (expt. 4).
- **Specific:** respiration impacts only on perceived body ownership and agency (expt. 1); the activity of the stomach, as mapped by EGG, had a selective effect on the sense of body ownership, while it did not influence the ratings of perceived body location and agency (expt. 2); the gastric effects on emotional awareness are specific for disgust and sadness (expt. 3), while the gastric signature of first-person moral judgments is different from that of third-person moral judgments (expt. 4).
- **Subjective:** individual levels of interoceptive accuracy and sensibility predict the strength of the embreathment illusion (expt. 1), while interoceptive deficits caused by individual features like the expression of a single gene (*PIEZO2*) seem to be associated with an impaired sense of one's own body (expt. 5).

These findings underscore that corporeal, emotional and moral awareness are veritable gut feelings, giving further strength to the ‘interoceptive turn’ that is increasingly dominating theories of embodied cognition (Arikha, 2019). Previous studies showed that the heart contributes to bodily self-consciousness; here, we find that the same holds true also for the stomach and the lungs. Past research showed that participants spontaneously and consistently map different emotions on different parts of a body template, including the stomach (Nummenmaa et al., 2013, 2018); here, we demonstrate that stomach contractions are actually linked to specific emotions. Existing literature provided evidence for the presence of orofacial correlates of disgust (Chapman, Kim, Susskind, & Anderson, 2009; Eskine, Kacinik, & Prinz, 2011; Rozin, Haidt, & Fincher, 2009); here, we show that the physiological correlates of moral disgust extend even deeper, in the stomach itself.

While existing models of corporeal and emotional awareness are increasingly underscoring the importance of interoceptive signals (Park & Tallon-Baudry, 2014; Seth, 2013), it must be noted that the current theoretical proposals are disproportionately based on the contribution of a single organ – the heart. Taken together with emerging studies on breath-based cognition (Varga & Heck, 2017; Zelano et al., 2016), the present findings suggest that the picture is broader, as there are also respiratory and gastric pathways to embodiment.

8.2 Future perspectives

Future studies may extend the present results in at least three directions. Given that the stomach contributes in a significant way to corporeal, emotional and moral awareness, it remains to be ascertained whether the same holds true also for the small and the large intestine. While the standard electrogastrographic setting can be twisted to capture also the electrical activity of the small intestine (Yin & Chen, 2013), ground-breaking methods should be employed for the colon. Likewise, the potential contribution of other organs, like the bladder, as well as the role of the

immune system (Damasio, 2003; Costantini, 2014) are still largely unexplored.

Even more importantly, new research is needed to assess how the physiological signals coming from peripheral organs and locally processed by the enteric and autonomic nervous system are further elaborated at the cortical level. In analogy with previous work on heartbeat-evoked potentials (Park & Blanke, 2019) and the resting-state gastric network (Rebollo et al., 2018), new experiments could investigate the potential links between corporeal awareness and respiratory-related evoked potentials (von Leupoldt et al., 2010), or explore how bodily self-consciousness covaries with breath-dependent fluctuations in the blood-oxygen-level-dependent (BOLD) signal.

Other studies may also record or stimulate the activity of specific cortical areas that are well known for their role in multisensory integration and corporeal/emotional awareness, from the insular cortex (Craig, 2009) to the extrastriate body area (EBA) and fusiform body area (FBA) (Berlucchi & Aglioti, 2010). Furthermore, it would be interesting to measure the extent to which information related to continuous homeostatic actions like breathing is processed separately and differently from information related to transient voluntary movements in areas involved in the construction of the body schema. This could be tested combining the existing embreathment setting with a full motion capture suit and a VR-compatible setup for electroencephalography or transcranial magnetic stimulation.

Finally, the paradigms developed in the present research project could be applied to a variety of clinical populations and particularly to patients affected by spinal cord injuries (SCI). Indeed, the scientific study of bodily awareness began in earnest with clinical observations on patients who suffered spinal cord lesions. Crucially, these lesions tend to spare interoceptive pathways. For this reason, it would be fascinating to probe how an almost intact processing of respiratory and gastric signals may continue to shape the feeling of one's own body when a human being is cut off from proprioceptive and tactile cues.

Bibliography

Abell, T. L., Camilleri, M., Donohoe, K., Hasler, W. L., Lin, H. C., Maurer, A. H., . . . Ziessman, H. A. (2008). Consensus Recommendations for Gastric Emptying Scintigraphy: A Joint Report of the American Neurogastroenterology and Motility Society and the Society of Nuclear Medicine. *Journal of Nuclear Medicine Technology*, 36(1), 44–54. <https://doi.org/10.2967/jnmt.107.048116>

Adler, D., Herbelin, B., Similowski, T., & Blanke, O. (2014). Breathing and sense of self: Visuo-respiratory conflicts alter body self-consciousness. *Respiratory Physiology & Neurobiology*, 203, 68–74. <https://doi.org/10.1016/j.resp.2014.08.003>

Adriaensen, D., Brouns, I., Genechten, J. V., & Timmermans, J.-P. (2003). Functional morphology of pulmonary neuroepithelial bodies: Extremely complex airway receptors. *The Anatomical Record Part A: Discoveries in Molecular, Cellular, and Evolutionary Biology*, 270A(1), 25–40. <https://doi.org/10.1002/ar.a.10007>

Adriaensen, D., & Timmermans, J.-P. (2011). Breath-taking complexity of vagal C-fibre nociceptors: Implications for inflammatory pulmonary disease, dyspnoea and cough. *The Journal of Physiology*, 589(Pt 1), 3–4. <https://doi.org/10.1113/jphysiol.2010.201434>

Adrian, E. D. (1933). Afferent impulses in the vagus and their effect on respiration. *The Journal of Physiology*, 79(3), 332–358. <https://doi.org/10.1113/jphysiol.1933.sp003053>

Alcaino, C., Knutson, K. R., Treichel, A. J., Yildiz, G., Strege, P. R., Linden, D. R., ... Beyder, A. (2018). A population of gut epithelial enterochromaffin cells is mechanosensitive and requires Piezo2 to convert force into serotonin release. *Proceedings of the National Academy of Sciences*, 115(32), E7632–E7641. <https://doi.org/10.1073/pnas.1804938115>

Allard, E., Canzoneri, E., Adler, D., Morélot-Panzini, C., Bello-Ruiz, J., Herbelin, B., ... Similowski, T. (2017). Interferences between breathing, experimental dyspnoea and bodily self-consciousness. *Scientific Reports*, 7(1), 9990. <https://doi.org/10.1038/s41598-017-11045-y>

Alper, S. L. (2017). Chapter Four—Genetic Diseases of PIEZO1 and PIEZO2 Dysfunction. In P. A. Gottlieb (Ed.), *Current Topics in Membranes* (pp. 97–134). <https://doi.org/10.1016/bs.ctm.2017.01.001>

Al-Shboul, O. A. (2013). The Importance of Interstitial Cells of Cajal in the Gastrointestinal Tract. *Saudi Journal of Gastroenterology: Official Journal of the Saudi Gastroenterology Association*, 19(1), 3–15. <https://doi.org/10.4103/1319-3767.105909>

Amiez, C., & Petrides, M. (2014). Neuroimaging Evidence of the Anatomic-Functional Organization of the Human Cingulate Motor Areas. *Cerebral Cortex*, 24(3), 563–578. <https://doi.org/10.1093/cercor/bhs329>

Armel, K. C., & Ramachandran, V. S. (2003). Projecting sensations to external objects: Evidence from skin conductance response. *Proceedings of the Royal Society B: Biological Sciences*, 270(1523), 1499–1506. <https://doi.org/10.1098/rspb.2003.2364>

Arikha, N. (2019, June 17). The interoceptive turn. Retrieved from aeon.co.

Aspell, J. E., Heydrich, L., Marillier, G., Lavanchy, T., Herbelin, B., & Blanke, O. (2013). Turning body and self inside out: Visualized heartbeats alter bodily self-consciousness and tactile perception. *Psychological Science*, 24(12), 2445–2453. <https://doi.org/10.1177/0956797613498395>

Azevedo, R. T., Aglioti, S. M., & Lenggenhager, B. (2016). Participants' above-chance recognition of own-heart sound combined with poor metacognitive awareness suggests implicit knowledge of own heart cardiodynamics. *Scientific Reports*, 6, 26545. <https://doi.org/10.1038/srep26545>

Bai, T., Li, Y., Xia, J., Jiang, Y., Zhang, L., Wang, H., ... Hou, X. (2017). Piezo2: A Candidate Biomarker for Visceral Hypersensitivity in Irritable Bowel Syndrome? *Journal of Neurogastroenterology and Motility*, 23(3), 453–463. <https://doi.org/10.5056/jnm16114>

Barnsley, N., McAuley, J. H., Mohan, R., Dey, A., Thomas, P., & Moseley, G. L. (2011). The rubber hand illusion increases histamine reactivity in the real arm. *Current Biology*, 21(23), R945–R946. <https://doi.org/10.1016/j.cub.2011.10.039>

Barrett, L. F., & Simmons, W. K. (2015). Interoceptive predictions in the brain. *Nature Reviews. Neuroscience*, 16(7), 419–429. <https://doi.org/10.1038/nrn3950>

Bates, D. M., Mächler, M., Bolker, B., & Walker, S. (2015). Fitting Linear Mixed-Effects Models Using lme4. *Journal of Statistical Software*, 67(1), 1–48. <https://doi.org/10.18637/jss.v067.i01>

Belsley, D. A., Kuh, E., & Welsch, R. E. (1980). Regression diagnostics: Identifying influential data and sources of collinearity. Retrieved from <http://adsabs.harvard.edu/abs/1980rdii.book.....B>

Berlucchi, G., & Aglioti, S. (1997). The body in the brain: Neural bases of corporeal awareness. *Trends in Neurosciences*, 20(12), 560–564. Berlucchi, G., & Aglioti, S. M. (2010). The body in the brain revisited. *Experimental Brain Research*, 200(1), 25–35. <https://doi.org/10.1007/s00221-009-1970-7>

Blanke, O., & Arzy, S. (2005). The Out-of-Body Experience: Disturbed Self-Processing at the Temporo-Parietal Junction. *The Neuroscientist*, 11(1), 16–24. <https://doi.org/10.1177/1073858404270885>

Blanke, O., Slater, M., & Serino, A. (2015). Behavioral, Neural, and Computational Principles of Bodily Self-Consciousness. *Neuron*, 88(1), 145–166. <https://doi.org/10.1016/j.neuron.2015.09.029>

Boiten, F. A., Frijda, N. H., & Wientjes, C. J. (1994). Emotions and respiratory patterns: Review and critical analysis. *International Journal of Psychophysiology: Official Journal of the International Organization of Psychophysiology*, 17(2), 103–128.

Boiten, Frans A. (1998). The effects of emotional behaviour on components of the respiratory cycle. *Biological Psychology*, 49(1), 29–51.

[https://doi.org/10.1016/S0301-0511\(98\)00025-8](https://doi.org/10.1016/S0301-0511(98)00025-8)

Botvinick, M., & Cohen, J. (1998). Rubber hands “feel” touch that eyes see. *Nature*, 391(6669), 756. <https://doi.org/10.1038/35784> Brainard, D. H. (1997). The Psychophysics Toolbox. *Spatial Vision*, 10(4), 433–436.

Brouns, I., Pintelon, I., De Proost, I., Alewaters, R., Timmermans, J.-P., & Adriaensen, D. (2006). Neurochemical characterisation of sensory receptors in airway smooth muscle: Comparison with pulmonary neuroepithelial bodies. *Histochemistry and Cell Biology*, 125(4), 351–367. <https://doi.org/10.1007/s00418-005-0078-9>

Buie, T., Campbell, D. B., Fuchs, G. J., Furuta, G. T., Levy, J., Vandewater, J., ... Winter, H. (2010). Evaluation, diagnosis, and treatment of gastrointestinal disorders in individuals with ASDs: A consensus report. *Pediatrics*, 125 Suppl 1, S1-18. <https://doi.org/10.1542/peds.2009-1878C>

Calì, G., Ambrosini, E., Picconi, L., Mehling, W. E., & Committeri, G. (2015). Investigating the relationship between interoceptive accuracy, interoceptive awareness, and emotional susceptibility. *Frontiers in Psychology*, 6, 1202. <https://doi.org/10.3389/fpsyg.2015.01202>

Ceunen, E., Vlaeyen, J. W. S., & Van Diest, I. (2016). On the Origin of Interoception. *Frontiers in Psychology*, 7. <https://doi.org/10.3389/fpsyg.2016.00743>

Chapman, H. A., Kim, D. A., Susskind, J. M., & Anderson, A. K. (2009). In Bad Taste: Evidence for the Oral Origins of Moral Disgust. *Science*, 323(5918), 1222–1226. <https://doi.org/10.1126/science.1165565>

Chesler, A. T., Szczot, M., Bharucha-Goebel, D., Čeko, M., Donker-voort, S., Laubacher, C., . . . Bönnemann, C. G. (2016). The Role of PIEZO2 in Human Mechanosensation. *The New England Journal of Medicine*, 375(14), 1355–1364. <https://doi.org/10.1056/NEJMoa1602812>

Coste, B., Mathur, J., Schmidt, M., Earley, T. J., Ranade, S., Petrus, M. J., . . . Patapoutian, A. (2010). Piezo1 and Piezo2 are essential components of distinct mechanically-activated cation channels. *Science (New York, N.Y.)*, 330(6000), 55–60. <https://doi.org/10.1126/science.1193270>

Craig, A. D. (2002). How do you feel? Interoception: the sense of the physiological condition of the body. *Nature Reviews Neuroscience*, 3(8), 655. <https://doi.org/10.1038/nrn894>

Craig, A. D. (2009). How do you feel — now? The anterior insula and human awareness. *Nature Reviews Neuroscience*, 10(1), 59–70. <https://doi.org/10.1038/nrn2555>

Craig, A. D. (Bud). (2014). *How Do You Feel?: An Interoceptive Moment with Your Neurobiological Self*. Princeton University Press.

Critchley, H. D., & Garfinkel, S. N. (2017). Interoception and emotion. *Current Opinion in Psychology*, 17, 7–14. <https://doi.org/10.1016/j.copsyc.2017.04.020>

Critchley, H. D., & Harrison, N. A. (2013). Visceral Influences on Brain and Behavior. *Neuron*, 77(4), 624–638. <https://doi.org/10.1016/j.neuron.2013.02.008>

Critchley, M. (1979). *The divine banquet of the brain and other essays*. Raven Press.

Crucianelli, L., Metcalf, N. K., Fotopoulou, A. K., & Jenkinson, P. M. (2013). Bodily pleasure matters: Velocity of touch modulates body ownership during the rubber hand illusion. *Frontiers in Psychology*, 4, 703. <https://doi.org/10.3389/fpsyg.2013.00703>

Costantini, M. (2014). Bodily self and immune self: is there a link? *Front. Hum. Neurosci.* 8, 138. <https://doi.org/10.3389/fnhum.2014.00138>

Czub, M., & Kowal, M. (2019). Respiration Entrainment in Virtual Reality by Using a Breathing Avatar. *Cyberpsychology, Behavior, and Social Networking*, 22(7), 494–499. <https://doi.org/10.1089/cyber.2018.0700>

Dale, A., & Anderson, D. (1978). Information Variables in Voluntary Control and Classical Conditioning of Heart Rate: Field Dependence and Heart-Rate Perception. *Perceptual and Motor Skills*, 47(1), 79–85. <https://doi.org/10.2466/pms.1978.47.1.79>

Damasio, A. (1999). *The feeling of what happens*. New York: Harcourt Brace & Company.

Damasio, A. (2003). Mental self: the person within. *Nature* 423:227. <https://doi.org/10.1038/423227a>

Darlington, R. B. (1990). *Regression and Linear Models*. McGraw-Hill.

Darwin, C. R. (1872). *The expression of the emotions in man and animals*. London: John Murray.

Daubenmier, J., Sze, J., Kerr, C. E., Kemeny, M. E., & Mehling, W. (2013). Follow your breath: Respiratory interoceptive accuracy in experienced meditators. *Psychophysiology*, 50(8), 777–789. <https://doi.org/10.1111/psyp.12057>

Davenport, P. W., Chan, P.-Y. S., Zhang, W., & Chou, Y.-L. (2007). Detection threshold for inspiratory resistive loads and respiratory-related evoked potentials. *Journal of Applied Physiology*, 102(1), 276–285. <https://doi.org/10.1152/jappphysiol.01436.2005>

Davenport, P. W., & Vovk, A. (2009). Cortical and subcortical central neural pathways in respiratory sensations. *Respiratory Physiology & Neurobiology*, 167(1), 72–86. <https://doi.org/10.1016/j.resp.2008.10.001>

David, N., Fiori, F., & Aglioti, S. M. (2014). Susceptibility to the rubber hand illusion does not tell the whole body-awareness story. *Cognitive, Affective, & Behavioral Neuroscience*, 14(1), 297–306. <https://doi.org/10.3758/s13415-013-0190-6>

de Haan, A. M., Van Stralen, H. E., Smit, M., Keizer, A., Van der Stigchel, S., & Dijkerman, H. C. (2017). No consistent cooling of the real hand in the rubber hand illusion. *Acta Psychologica*, 179, 68–77. <https://doi.org/10.1016/j.actpsy.2017.07.003>

Delbende, B., Perri, F., Couturier, O., Leodolter, A., Mauger, P., Bridgi, B., ... Galmiche, J. P. (2000). ¹³C-octanoic acid breath test for gastric emptying measurement. *European Journal of Gastroenterology & Hepatology*, 12(1), 85

Ehlers, A., Mayou, R. A., Sprigings, D. C., & Birkhead, J. (2000). Psychological and perceptual factors associated with arrhythmias and benign

palpitations. *Psychosomatic Medicine*, 62(5), 693–702.

Eskine, K. J., Kacinik, N. A., & Prinz, J. J. (2011). A bad taste in the mouth: Gustatory disgust influences moral judgment. *Psychological Science*, 22(3), 295–299. <https://doi.org/10.1177/0956797611398497>

Faull, O. K., Cox, P. J., & Pattinson, K. T. S. (2016). Psychophysical Differences in Ventilatory Awareness and Breathlessness between Athletes and Sedentary Individuals. *Frontiers in Physiology*, 7. <https://doi.org/10.3389/fphys.2016.00231>

Ferrari, L. F., Bogen, O., Green, P., & Levine, J. D. (2015). Contribution of Piezo2 to Endothelium-Dependent Pain. *Molecular Pain*, 11, s12990-015-0068-4. <https://doi.org/10.1186/s12990-015-0068-4>

Florez-Paz, D., Bali, K. K., Kuner, R., & Gomis, A. (2016). A critical role for Piezo2 channels in the mechanotransduction of mouse proprioceptive neurons. *Scientific Reports*, 6, 25923. <https://doi.org/10.1038/srep25923>

Fox, J., & Weisberg, S. (2011). *An R Companion to Applied Regression*. SAGE Publications.

Garfinkel, S. N., Seth, A. K., Barrett, A. B., Suzuki, K., & Critchley, H. D. (2015). Knowing your own heart: Distinguishing interoceptive accuracy from interoceptive awareness. *Biological Psychology*, 104, 65–74. <https://doi.org/10.1016/j.biopsycho.2014.11.004>

Geliebter, A. (1988). Gastric distension and gastric capacity in relation to food intake in humans. *Physiology & Behavior*, 44(4–5), 665–668.

Haidt, J. (2003). Moral emotions.

Hampel, F. R. (1974). The Influence Curve and its Role in Robust Estimation. *Journal of the American Statistical Association*, 69(346), 383–393. <https://doi.org/10.1080/01621459.1974.10482962>

Harrison, N. A., Gray, M. A., Gianaros, P. J., & Critchley, H. D. (2010). The Embodiment of Emotional Feelings in the Brain. *Journal of Neuroscience*, 30(38), 12878–12884. <https://doi.org/10.1523/JNEUROSCI.1725-10.2010>

Herbert, B. M., & Pollatos, O. (2012). The body in the mind: On the relationship between interoception and embodiment. *Topics in Cognitive Science*, 4(4), 692–704. <https://doi.org/10.1111/j.1756-8765.2012.01189.x>

Heydrich, L., & Blanke, O. (2013). Distinct illusory own-body perceptions caused by damage to posterior insula and extrastriate cortex. *Brain*, 136(3), 790–803. <https://doi.org/10.1093/brain/aws364>

Hinton, J. M., Lennard-Jones, J. E., & Young, A. C. (1969). A new method for studying gut transit times using radioopaque markers. *Gut*, 10(10), 842–847.

Huijbers, W., Pennartz, C. M. A., Beldzik, E., Domagalik, A., Vinck, M., Hofman, W. F., ... Daselaar, S. M. (2014). Respiration phase-locks to fast stimulus presentations: Implications for the interpretation of posterior midline “deactivations.” *Human Brain Mapping*, 35(9), 4932–4943. <https://doi.org/10.1002/hbm.22523>

Ikeda, R., Cha, M., Ling, J., Jia, Z., Coyle, D., & Gu, J. G. (2014).

Merkel Cells Transduce and Encode Tactile Stimuli to Drive A-Afferent Impulses. *Cell*, 157(3), 664–675. <https://doi.org/10.1016/j.cell.2014.02.026>

Iodice, P., Porciello, G., Bufalari, I., Barca, L., & Pezzulo, G. (2019). An interoceptive illusion of effort induced by false heart-rate feedback. *Proceedings of the National Academy of Sciences*, 116(28), 13897–13902. <https://doi.org/10.1073/pnas.1821032116>

James, W. (1884). What is an emotion? *Mind*, 9, 188–205.

Jerath, R., Crawford, M. W., Barnes, V. A., & Harden, K. (2015). Self-Regulation of Breathing as a Primary Treatment for Anxiety. *Applied Psychophysiology and Biofeedback*, 40(2), 107–115. <https://doi.org/10.1007/s10484-015-9279-8>

Johnson, J. W., & Lebreton, J. M. (2004). History and Use of Relative Importance Indices in Organizational Research. *Organizational Research Methods*, 7(3), 238–257. <https://doi.org/10.1177/1094428104266510>

Johnson, P. C. D. (2014). Extension of Nakagawa & Schielzeth's R2GLMM to random slopes models. *Methods in Ecology and Evolution*, 5(9), 944–946. <https://doi.org/10.1111/2041-210X.12225>

Kleiner, M., Brainard, D., Pelli, D., Ingling, A., Murray, R., & Broussard, C. (2007). What's new in psychtoolbox-3. *Perception*, 36(14), 1–16.

Kragel, P. A., & LaBar, K. S. (2013). Multivariate Pattern Classification Reveals Autonomic and Experiential Representations of Discrete Emotions. *Emotion (Washington, D.C.)*, 13(4), 681–690. <https://doi.org/10.1037/a0031820>

Kumar, P., & Prabhakar, N. R. (2012). Peripheral Chemoreceptors: Function and Plasticity of the Carotid Body. *Comprehensive Physiology*, 2(1), 141–219. <https://doi.org/10.1002/cphy.c100069>

Lee, Y. Y., Erdogan, A., & Rao, S. S. C. (2014). How to Assess Regional and Whole Gut Transit Time With Wireless Motility Capsule. *Journal of Neurogastroenterology and Motility*, 20(2), 265–270. <https://doi.org/10.5056/jnm.2014.20.2.265>

Lenggenhager, B., Tadi, T., Metzinger, T., & Blanke, O. (2007). Video ergo sum: Manipulating bodily self-consciousness. *Science*, 317(5841), 1096–1099. <https://doi.org/10.1126/science.1144876>

Lewis, M., Sullivan, M. W., Stanger, C., & Weiss, M. (1989). Self development and self-conscious emotions. *Child Development*, 60(1), 146–156.

Leys, C., Ley, C., Klein, O., Bernard, P., & Licata, L. (2013). Detecting outliers: Do not use standard deviation around the mean, use absolute deviation around the median. *Journal of Experimental Social Psychology*, 49(4), 764–766. <https://doi.org/10.1016/j.jesp.2013.03.013>

Lloyd, D. M., Gillis, V., Lewis, E., Farrell, M. J., & Morrison, I. (2013). Pleasant touch moderates the subjective but not objective aspects of body perception. *Frontiers in Behavioral Neuroscience*, 7, 207. <https://doi.org/10.3389/fnbeh.2013.00207>

Longo, M. R., Schüür, F., Kammers, M. P. M., Tsakiris, M., & Haggard, P. (2008). What is embodiment? A psychometric approach. *Cognition*,

107(3), 978–998. <https://doi.org/10.1016/j.cognition.2007.12.004>

Mahmud, A. a., Nahid, N. a., Nassif, C., Sayeed, M. s. b., Ahmed, M. u., Parveen, M., ... Michaud, J. l. (2017). Loss of the proprioception and touch sensation channel PIEZO2 in siblings with a progressive form of contractures. *Clinical Genetics*, 91(3), 470–475. <https://doi.org/10.1111/cge.12850>

Maksimovic, S., Nakatani, M., Baba, Y., Nelson, A. M., Marshall, K. L., Wellnitz, S. A., ... Lumpkin, E. A. (2014). Epidermal Merkel cells are mechanosensory cells that tune mammalian touch receptors. *Nature*, 509(7502), 617–621. <https://doi.org/10.1038/nature13250>

Maselli, A., & Slater, M. (2013). The building blocks of the full body ownership illusion. *Frontiers in Human Neuroscience*, 7. <https://doi.org/10.3389/fnhum.2013.00083>

McGill, R., Tukey, J. W., & Larsen, W. A. (1978). Variations of Box Plots. *The American Statistician*, 32(1), 12–16. <https://doi.org/10.2307/2683468> Mehling, W. E., Price, C., Daubemier, J. J., Acree, M., Bartmess, E., & Stewart, A. (2012). The Multidimensional Assessment of Interoceptive Awareness (MAIA). *PloS One*, 7(11), e48230. <https://doi.org/10.1371/journal.pone.0048230>

Metzinger, T. (2004). *Being No One: The Self-Model Theory of Subjectivity*. MIT Press.

Michal, M., Reuchlein, B., Adler, J., Reiner, I., Beutel, M. E., Vögele, C., ... Schulz, A. (2014). Striking Discrepancy of Anomalous Body Experiences with Normal Interoceptive Accuracy in Depersonalization-Derealization Disorder. *PLoS ONE*, 9(2), e89823. <https://doi.org/10.1371/journal.pone.0089823>

Moayedi, Y., Duenas-Bianchi, L. F., & Lumpkin, E. A. (2018). Somatosensory innervation of the oral mucosa of adult and aging mice. *Scientific Reports*, 8(1), 9975. <https://doi.org/10.1038/s41598-018-28195-2>

Moseley, G. L., Olthof, N., Venema, A., Don, S., Wijers, M., Gallace, A., & Spence, C. (2008). Psychologically induced cooling of a specific body part caused by the illusory ownership of an artificial counterpart. *Proceedings of the National Academy of Sciences*, 105(35), 13169–13173. <https://doi.org/10.1073/pnas.0803768105>

Mulle, J. G., Sharp, W. G., & Cubells, J. F. (2013). The Gut Microbiome: A New Frontier in Autism Research. *Current Psychiatry Reports*, 15(2), 337. <https://doi.org/10.1007/s11920-012-0337-0>

Nakagawa, S., & Schielzeth, H. (2013). A general and simple method for obtaining R² from generalized linear mixed-effects models. *Methods in Ecology and Evolution*, 4(2), 133–142. <https://doi.org/10.1111/j.2041-210x.2012.00261.x>

Nardi, A. E., Freire, R. C., & Zin, W. A. (2009). Panic disorder and control of breathing. *Respiratory Physiology & Neurobiology*, 167(1), 133–143. <https://doi.org/10.1016/j.resp.2008.07.011>

Nassenstein, C., Taylor-Clark, T. E., Myers, A. C., Ru, F., Nandigama, R., Bettner, W., & Udem, B. J. (2010). Phenotypic distinctions between neural crest and placodal derived vagal C-fibres in mouse lungs. *The Journal of Physiology*, 588(Pt 23), 4769–4783. <https://doi.org/10.1113/jphysiol.2010.195339>

Negro, C. A. D., Funk, G. D., & Feldman, J. L. (2018). Breathing matters. *Nature Reviews Neuroscience*, 19(6), 351–367. <https://doi.org/10.1038/s41583-018-0003-6>

Nencini, S., & Ivanusic, J. (2017). Mechanically sensitive A nociceptors that innervate bone marrow respond to changes in intra-osseous pressure. *The Journal of Physiology*, 595(13), 4399–4415. <https://doi.org/10.1113/JP273877>

Nieuwenhuis, R., te Grotenhuis, H. F., & Pelzer, B. J. (2012). Influence. ME: Tools for detecting influential data in mixed effects models.

Nonomura, K., Woo, S.-H., Chang, R. B., Gillich, A., Qiu, Z., Francisco, A. G., ... Patapoutian, A. (2017). Piezo2 senses airway stretch and mediates lung inflation-induced apnoea. *Nature*, 541(7636), 176–181. <https://doi.org/10.1038/nature20793>

Nummenmaa, L., Glerean, E., Hari, R., & Hietanen, J. K. (2013). Bodily maps of emotions. *Proceedings of the National Academy of Sciences*, 111 (2), 646–651. <https://doi.org/10.1073/pnas.1321664111>

Nummenmaa, L., Hari, R., Hietanen, J. K., & Glerean, E. (2018). Maps of subjective feelings. *Proceedings of the National Academy of Sciences*, 115 (37), 9198–9203; <https://doi.org/10.1073/pnas.1807390115>

Oostenveld, R., Fries, P., Maris, E., & Schoffelen, J.-M. (2011). Field-Trip: Open Source Software for Advanced Analysis of MEG, EEG, and Invasive Electrophysiological Data. *Computational Intelligence and Neuroscience*, 2011, 1–9. <https://doi.org/10.1155/2011/156869>

Ottaviani, C., Mancini, F., Petrocchi, N., Medea, B., & Couyoumdjian, A. (2013). Autonomic correlates of physical and moral disgust. *International Journal of Psychophysiology*, 89(1), 57–62. <https://doi.org/10.1016/j.ijpsycho.2013.05.003>

Park, H.-D., & Blanke, O. (2019). Heartbeat-evoked cortical responses: Underlying mechanisms, functional roles, and methodological considerations. *Neuroimage*, 197, 502-511. <https://doi.org/10.1016/j.neuroimage.2019.04.081>.

Park, H.-D., Bernasconi, F., Bello-Ruiz, J., Pfeiffer, C., Salomon, R., & Blanke, O. (2016). Transient Modulations of Neural Responses to Heartbeats Covary with Bodily Self-Consciousness. *Journal of Neuroscience*, 36(32), 8453–8460. <https://doi.org/10.1523/JNEUROSCI.0311-16.2016>

Park, H.-D., & Tallon-Baudry, C. (2014). The neural subjective frame: From bodily signals to perceptual consciousness. *Phil. Trans. R. Soc. B*, 369(1641), 20130208. <https://doi.org/10.1098/rstb.2013.0208>

Pelli, D. G. (1997). The VideoToolbox software for visual psychophysics: Transforming numbers into movies. *Spatial Vision*, 10(4), 437–442.

Perl, O., Ravia, A., Rubinson, M., Eisen, A., Soroka, T., Mor, N., ... Sobel, N. (2019). Human non-olfactory cognition phase-locked with inhalation. *Nature Human Behaviour*, 1. <https://doi.org/10.1038/s41562-019-0556-z>

Petkova, V. I., & Ehrsson, H. H. (2008). If I Were You: Perceptual Illusion of Body Swapping. *PLOS ONE*, 3(12), e3832. <https://doi.org/10.1371/journal.pone.0003832>

Petkova, V. I., Khoshnevis, M., & Ehrsson, H. H. (2011). The perspective matters! Multisensory integration in ego-centric reference frames determines full-body ownership. *Frontiers in Psychology*, 2, 35. <https://doi.org/10.3389/fpsyg.2011.00035>

Pollack, I., & Norman, D. A. (1964). A non-parametric analysis of recognition experiments. *Psychonomic Science*, 1(1–12), 125–126.

Pollatos, O., Kurz, A.-L., Albrecht, J., Schreder, T., Kleemann, A. M., Schöpf, V., ... Schandry, R. (2008). Reduced perception of bodily signals in anorexia nervosa. *Eating Behaviors*, 9(4), 381–388. <https://doi.org/10.1016/j.eatbeh.2008.02.001>

Porciello, G., Daum, M. M., Menghini, C., Brugger, P., & Lenggenhager, B. (2016). Not That Heart-Stopping After All: Visuo-Cardiac Synchrony Does Not Boost Self-Face Attribution. *PLOS ONE*, 11(8), e0160498. <https://doi.org/10.1371/journal.pone.0160498>

Porciello, G., Monti, A., & Aglioti, S. M. (2018). How the stomach and the brain work together at rest. *ELife*, 7, e37009. <https://doi.org/10.7554/eLife.37009>

Pritchard, S. C., Zopf, R., Polito, V., Kaplan, D. M., & Williams, M. A. (2016). Non-hierarchical Influence of Visual Form, Touch, and Position Cues on Embodiment, Agency, and Presence in Virtual Reality. *Frontiers in Psychology*, 7. <https://doi.org/10.3389/fpsyg.2016.01649>

Ranade, S. S., Woo, S.-H., Dubin, A. E., Moshourab, R. A., Wetzel, C., Petrus, M., ... Patapoutian, A. (2014). Piezo2 is the major transducer of mechanical forces for touch sensation in mice. *Nature*, 516(7529), 121–125.

<https://doi.org/10.1038/nature13980>

Rebollo, I., Devauchelle, A.-D., Béranger, B., & Tallon-Baudry, C. (2018). Stomach-brain synchrony reveals a novel, delayed-connectivity resting-state network in humans. *ELife*, 7, e33321. <https://doi.org/10.7554/eLife.33321>

Road, J. D. (1990). Chest Wall Afferent Output. *Chest*, 97, 40S-43S. <https://doi.org/10.1378/>

Rozin, P., Lowery, L., Imada, S., & Haidt, J. (1999). The CAD triad hypothesis: A mapping between three moral emotions (contempt, anger, disgust) and three moral codes (community, autonomy, divinity). *Journal of Personality and Social Psychology*, 76(4), 574–586.

Rozin, Paul, Haidt, J., & Fincher, K. (2009). From Oral to Moral. *Science*, 323(5918), 1179–1180. <https://doi.org/10.1126/science.1170492>

Russell, P. S., & Giner-Sorolla, R. (2013). Bodily moral disgust: What it is, how it is different from anger, and why it is an unreasoned emotion. *Psychological Bulletin*, 139(2), 328–351. <https://doi.org/10.1037/a0029319>

Saad, R. J. (2016). The Wireless Motility Capsule: A One-Stop Shop for the Evaluation of GI Motility Disorders. *Current Gastroenterology Reports*, 18(3). <https://doi.org/10.1007/s11894-016-0489-x>

Sato, A., & Yasuda, A. (2005). Illusion of sense of self-agency: Discrepancy between the predicted and actual sensory consequences of actions modulates the sense of self-agency, but not the sense of self-ownership. *Cognition*, 94(3), 241–255. <https://doi.org/10.1016/j.cognition.2004.04.003>

Schandry, R. (1981). Heart beat perception and emotional experience. *Psychophysiology*, 18(4), 483–488.

Schnall, S., Haidt, J., Clore, G. L., & Jordan, A. H. (2008). Disgust as Embodied Moral Judgment. *Personality & Social Psychology Bulletin*, 34(8), 1096–1109. <https://doi.org/10.1177/0146167208317771>

Schneider, E. R., Anderson, E. O., Mastrotto, M., Matson, J. D., Schulz, V. P., Gallagher, P. G., . . . Bagriantsev, S. N. (2017). Molecular basis of tactile specialization in the duck bill. *Proceedings of the National Academy of Sciences*, 114(49), 13036–13041. <https://doi.org/10.1073/pnas.1708793114>

Schrenk-Siemens, K., Wende, H., Prato, V., Song, K., Rostock, C., Loewer, A., . . . Siemens, J. (2015). PIEZO2 is required for mechanotransduction in human stem cell–derived touch receptors. *Nature Neuroscience*, 18(1), 10–16. <https://doi.org/10.1038/nn.3894>

Seth, A. K. (2013). Interoceptive inference, emotion, and the embodied self. *Trends in Cognitive Sciences*, 17(11), 565–573. <https://doi.org/10.1016/j.tics.2013.09.007>

Sforza, A., Bufalari, I., Haggard, P., & Aglioti, S. M. (2010). My face in yours: Visuo-tactile facial stimulation influences sense of identity. *Social Neuroscience*, 5(2), 148–162. <https://doi.org/10.1080/17470910903205503>

Shah, E., Rezaie, A., Riddle, M., & Pimentel, M. (2014). Psychological disorders in gastrointestinal disease: Epiphenomenon, cause or consequence? *Annals of Gastroenterology: Quarterly Publication of the Hellenic Society of*

Gastroenterology, 27(3), 224–230.

Sherrington, C. S. (1906). The integrative action of the nervous system. <https://doi.org/10.1037/13798-000>

Sozansky, J., & Houser, S. M. (2014). The physiological mechanism for sensing nasal airflow: A literature review. *International Forum of Allergy & Rhinology*, 4(10), 834–838. <https://doi.org/10.1002/alr.21368>

Stocker, S. D., Sved, A. F.,
Andresen, M. C. (2019). Missing Pieces of the Piezo1/Piezo2 Baroreceptor Hypothesis: An Autonomic Perspective. *Journal of Neurophysiology*. <https://doi.org/10.1152/jn.00315.2019>

Suzuki, K., Garfinkel, S. N., Critchley, H. D., & Seth, A. K. (2013). Multisensory integration across exteroceptive and interoceptive domains modulates self-experience in the rubber-hand illusion. *Neuropsychologia*, 51(13), 2909–2917. <https://doi.org/10.1016/j.neuropsychologia.2013.08.014>

Szarka, L. A., Camilleri, M., Vella, A., Burton, D., Baxter, K., Simonson, J., & Zinsmeister, A. R. (2008). A Stable Isotope Breath Test with a Standard Meal for Abnormal Gastric Emptying of Solids in the Clinic and in Research. *Clinical Gastroenterology and Hepatology: The Official Clinical Practice Journal of the American Gastroenterological Association*, 6(6), 635-643.e1. <https://doi.org/10.1016/j.cgh.2008.01.009>

Tettamanti, M., Rognoni, E., Cafiero, R., Costa, T., Galati, D., & Perani, D. (2012). Distinct pathways of neural coupling for different basic emotions. *NeuroImage*, 59(2), 1804–1817. <https://doi.org/10.1016/j.neuroimage.2011.08.018>

Tieri, G., Gioia, A., Scandola, M., Pavone, E. F., & Aglioti, S. M. (2017). Visual appearance of a virtual upper limb modulates the temperature of the real hand: A thermal imaging study in Immersive Virtual Reality. *European Journal of Neuroscience*, 45(9), 1141–1151. <https://doi.org/10.1111/ejn.13545>

Tieri, G., Tidoni, E., Pavone, E. F., & Aglioti, S. M. (2015). Body visual discontinuity affects feeling of ownership and skin conductance responses. *Scientific Reports*, 5. <https://doi.org/10.1038/srep17139>

Tsakiris, M., Jimenez, A. T., & Costantini, M. (2011). Just a heart-beat away from one's body: Interoceptive sensitivity predicts malleability of body-representations. *Proceedings of the Royal Society B: Biological Sciences*, 278(1717), 2470–2476. <https://doi.org/10.1098/rspb.2010.2547>

Tsakiris, M. (2010). My body in the brain: A neurocognitive model of body-ownership. *Neuropsychologia*, 48(3), 703–712.

Umans, B. D., & Liberles, S. D. (2018). Neural Sensing of Organ Volume. *Trends in Neurosciences*, 41(12), 911–924. <https://doi.org/10.1016/j.tins.2018.07.008>

van Dyck, Z., Vögele, C., Blechert, J., Lutz, A. P. C., Schulz, A., & Herbert, B. M. (2016). The Water Load Test As a Measure of Gastric Interoception: Development of a Two-Stage Protocol and Application to a Healthy Female Population. *PLoS ONE*, 11(9). <https://doi.org/10.1371/journal.pone.0163574>

van Stralen, H. E., van Zandvoort, M. J. E., Hoppenbrouwers, S. S., Vissers, L. M. G., Kappelle, L. J., & Dijkerman, H. C. (2014). Affective touch modulates the rubber hand illusion. *Cognition*, 131(1), 147–158.

<https://doi.org/10.1016/j.cognition.2013.11.020>

Varga, S., & Heck, D. H. (2017). Rhythms of the body, rhythms of the brain: Respiration, neural oscillations, and embodied cognition. *Conscious Cogn.* 56, 77-90. <https://doi.org/10.1016/j.concog.2017.09.008>.

Vianna, E. P. M., & Tranel, D. (2006). Gastric myoelectrical activity as an index of emotional arousal. *International Journal of Psychophysiology: Official Journal of the International Organization of Psychophysiology*, 61(1), 70–76. <https://doi.org/10.1016/j.ijpsycho.2005.10.019>

Vianna, E. P. M., Naqvi, N., Bechara, A., & Tranel, D. (2009). Does vivid emotional imagery depend on body signals? *International Journal of Psychophysiology: Official Journal of the International Organization of Psychophysiology*, 72(1), 46–50. <https://doi.org/10.1016/j.ijpsycho.2008.01.013>

Villa, R., Tidoni, E., Porciello, G., & Aglioti, S. M. (2018). Violation of expectations about movement and goal achievement leads to Sense of Agency reduction. *Experimental Brain Research*, 236, 2123–2135. <https://doi.org/10.1007/s00221-018-5286-3>

Vlemincx, E., Taelman, J., De Peuter, S., Van Diest, I., & Van Den Bergh, O. (2011). Sigh rate and respiratory variability during mental load and sustained attention: Sigh rate and respiratory variability. *Psychophysiology*, 48(1), 117–120. <https://doi.org/10.1111/j.1469-8986.2010.01043.x>

von Leupoldt, A., Keil, A., Chan, P.-Y. S., Bradley, M. M., Lang, P. J., & Davenport, P. W. (2010). Cortical sources of the respiratory-related evoked potential. *Respir. Physiol. Neurobiol.*, 170(2), 198-201.

<https://doi.org/10.1016/j.resp.2009.12.006>

Wang, G.-J., Tomasi, D., Backus, W., Wang, R., Telang, F., Geliebter, A., ... Volkow, N. D. (2008). Gastric distention activates satiety circuitry in the human brain. *NeuroImage*, 39(4), 1824–1831. <https://doi.org/10.1016/j.neuroimage.2007.11.008>

Watanabe, T., Ogikubo, M., & Ishii, Y. (2004). Visualization of Respiration in the Embodied Virtual Communication System and Its Evaluation. *International Journal of Human-Computer Interaction*, 17(1), 89–102. <https://doi.org/10.1207/>

Webster, K. E., & Colrain, I. M. (2000). The relationship between respiratory-related evoked potentials and the perception of inspiratory resistive loads. *Psychophysiology*, 37(6), 831–841.

Welch, P. (1967). The use of fast Fourier transform for the estimation of power spectra: A method based on time averaging over short, modified periodograms. *IEEE Transactions on Audio and Electroacoustics*, 15(2), 70–73. <https://doi.org/10.1109/TAU.1967.1161901>

Wheatley, T., & Haidt, J. (2005). Hypnotic Disgust Makes Moral Judgments More Severe. *Psychological Science*, 16(10), 780–784. <https://doi.org/10.1111/j.1467-9280.2005.01614.x>

Widdicombe, J. G. (1982). Pulmonary and respiratory tract receptors. *J Exp Biol*, 100, 41–57.

Wilberg, S., Pieramico, O., & Malfertheiner, P. (1990). [The H₂-lactulose

breath test in the diagnosis of intestinal transit time]. *Leber, Magen, Darm*, 20(3), 129–137.

Williams, E. J. (1949). Experimental Designs Balanced for the Estimation of Residual Effects of Treatments. *Australian Journal of Scientific Research A Physical Sciences*, 2, 149. <https://doi.org/10.1071/PH490149>

Woo, S.-H., Lukacs, V., de Nooij, J. C., Zaytseva, D., Criddle, C. R., Francisco, A., ... Patapoutian, A. (2015). Piezo2 is the principal mechanotransduction channel for proprioception. *Nature Neuroscience*, 18(12), 1756–1762. <https://doi.org/10.1038/nn.4162>

Woo, S.-H., Ranade, S., Weyer, A. D., Dubin, A. E., Baba, Y., Qiu, Z., ... Patapoutian, A. (2014). Piezo2 is required for Merkel-cell mechanotransduction. *Nature*, 509(7502), 622–626. <https://doi.org/10.1038/nature13251>

Yamaguchi, T., Takano, K., Inaba, Y., Morikawa, M., Motobayashi, M., Kawamura, R., ... Kosho, T. (2019). PIEZO2 deficiency is a recognizable arthrogryposis syndrome: A new case and literature review. *American Journal of Medical Genetics Part A*, 179(6), 948–957. <https://doi.org/10.1002/ajmg.a.61142>

Yang, L., Song, G., Ning, Y., & Poon, C.-S. (2016). A latent serotonin-1A receptor-gated spinal afferent pathway inhibiting breathing. *Brain Structure and Function*, 221(8), 4159–4168. <https://doi.org/10.1007/s00429-015-1155-z>

Yin, J., & Chen, J. D. Z. (2013). Electrogastrography: Methodology, Validation and Applications. *Journal of Neurogastroenterology and Motility*, 19(1), 5–17. <https://doi.org/10.5056/jnm.2013.19.1.5>

Yu, J., Lin, S., Zhang, J., Otmishi, P., & Guardiola, J. J. (2007). Airway nociceptors activated by pro-inflammatory cytokines. *Respiratory Physiology & Neurobiology*, 156(2), 116–119. <https://doi.org/10.1016/j.resp.2006.11.005>

Zelano, C., Jiang, H., Zhou, G., Arora, N., Schuele, S., Rosenow, J., & Gottfried, J. A. (2016). Nasal Respiration Entrain Human Limbic Oscillations and Modulates Cognitive Function. *Journal of Neuroscience*, 36(49), 12448–12467. <https://doi.org/10.1523/JNEUROSCI.2586-16.2016>

Zeng, W.-Z., Marshall, K. L., Min, S., Daou, I., Chapleau, M. W., Abboud, F. M., . . . Patapoutian, A. (2018). PIEZOs mediate neuronal sensing of blood pressure and the baroreceptor reflex. *Science*, 362(6413), 464–467. <https://doi.org/10.1126/science.aau6324>

Zhang, J., & Mueller, S. T. (2005). A note on ROC analysis and non-parametric estimate of sensitivity. *Psychometrika*, 70(1), 203–212. <https://doi.org/10.1007/s11336-003-1119-8>

Zhao, K., Blacker, K., Luo, Y., Bryant, B., & Jiang, J. (2011). Perceiving Nasal Patency through Mucosal Cooling Rather than Air Temperature or Nasal Resistance. *PLoS ONE*, 6(10). <https://doi.org/10.1371/journal.pone.0024618>

Zhao, W., Martin, A. D., & Davenport, P. W. (2002). Detection of inspiratory resistive loads in double-lung transplant recipients. *Journal of Applied Physiology*, 93(5), 1779–1785. <https://doi.org/10.1152/jappphysiol.00210.2002>